NEW DIMENSIONS OF ANEMIA IN PALEOPATHOLOGY

NEW DIMENSIONS OF ANEMIA IN PALEOPATHOLOGY:

DEVELOPMENT AND APPLICATION OF NOVEL METHODS FOR ANEMIA DIAGNOSIS IN SKELETAL REMAINS

By BRIANNE MORGAN, MSc, BSc (Hons)

A Thesis Submitted to the School of Graduate Studies in Partial Fulfillment of the Requirements for the Doctoral Degree

McMaster University DOCTOR OF PHILOSOPHY (2024)
Hamilton, Ontario (Anthropology)

TITLE: New Dimensions of Anemia in Paleopathology

AUTHOR: Brianne Morgan, M.Sc. (Bournemouth University), B.Sc. (Trent University)
SUPERVISOR: Dr. Megan Brickley

NUMBER OF PAGES: xii, 121

LAY ABSTRACT

Anemia is a condition that has severely affected vulnerable groups in the past, but diagnosing it using skeletal remains can be challenging. Few studies have used bone measurements to investigate anemia or integrated data from known cases of anemia into archaeological analysis. In this thesis, I investigated metric aspects of the sternum and skull, and found that there were differences associated with anemia. I used these metric differences to propose a framework for diagnosing anemia in the skeleton, and then applied this framework to a sample from 18th-19th century Quebec to investigate co-occurrence of anemia and scurvy/vitamin C deficiency, which is clinically common. I found that the prevalence of anemia and scurvy were high in this context, which demonstrates the significant amount of stress that communities in Quebec experienced. My research has demonstrated that improving skeletal anemia diagnosis leads to greater confidence in interpretations of how anemia affected past health.

ABSTRACT

In modern populations, anemia is highly prevalent and can have a significant effect on health at the individual and population level. The condition is likely to have been as important for past communities, but research on the subject is challenging due to the limitations of paleopathological anemia diagnosis, which typically relies on assessment of porosity. This research explores the utility of quantitative methods for anemia diagnosis in skeletal remains, and uses these novel methods to investigate the co-occurrence of anemia and scurvy in three communities from 18th-19th century Quebec.

To investigate metric changes associated with anemia, hematological and sternal imaging data from a modern cohort of individuals was assessed for changes associated with anemia/marrow hyperplasia. Additionally, sixty-eight orbits from archaeological individuals underwent micro-CT analysis, and were also evaluated for metric differences related to marrow hyperplasia. Results demonstrated that there are changes in bone microarchitecture associated with anemia, and that these changes are identifiable through visual and metric assessment.

Based on these principles, a framework for anemia diagnosis was developed, and used to explore how anemia may have interacted with scurvy to affect children in Colonial Quebec. Prevalence of both conditions was high, and patterns of metabolic disease at urban and rural sites were similar, suggesting that children across different sites were at risk for developing scurvy and anemia.

This research highlights the importance of looking beyond porosity for anemia assessment in skeletal remains. It demonstrates the utility of visualizing and assessing the internal marrow space for anemia assessment, and demonstrates that metric data has a place in analyses of anemia in archaeological contexts. It also shows that investigating co-occurrence and clustering can be a valuable source of information on past health, and demonstrates the utility of methods that allow us to do so.

LAND ACKNOWLEDGEMENT

McMaster University is located on the traditional territories of the Haudenosaunee confederacy and Anishinabe nations. This land is protected by the "Dish with One Spoon" wampum agreement, which describes how the land of the Great Lakes region should be shared between peoples and lived on peacefully. That wampum uses the symbolism of a dish to represent the territory, and one spoon to represent that the people are to share the resources of the land and only take what they need.

I live on the traditional territory of the Chonnonton, Huron-Wendat, Haudenosaunee Confederacy, and the Mississaugas of the Credit First Nation. This land is also protected by the Dish with One Spoon Wampum, as well as the 1764 Treaty of Niagara, the Silver Covenant Chain of Friendship, and Treaty No. 3 (1792).

I am grateful to live and work on these territories, and recognize my responsibility to respect and honour the intimate relationship Indigenous peoples have to these lands.

ACKNOWLEDGEMENTS

First and foremost, I would like to extend my deepest thanks and appreciation to my committee for their advice, honest feedback, and encouragement. I am incredibly grateful to Dr. Megan Brickley, my thesis supervisor, for her guidance through the world of metabolic bone disease and for offering me so many valuable opportunities during my time at McMaster, to Dr. Michelle Zeller, who provided much-appreciated clinical perspectives, and to Dr. Tina Moffat, for her insightful questions and comments throughout the entirety of this process. My sincere thanks also to my external examiner, Dr. Darlene Weston, for her valuable feedback and thorough comments.

I would also like to thank all of my collaborators and coauthors, including Dr. Isabelle Ribot at the University of Montreal for hosting me during my fieldwork and providing access to collections, Kayla Lucier and Maryam Akbari-Moghaddam at the Michael G. DeGroote Centre for Transfusion Research for facilitating clinical data access and collection, Julie Nguyen and Meghan Langlois at McMaster University for co-analyzing osteological data, Dr. Rachael Schats at Leiden University and Dr. Alie van der Merwe at the University of Amsterdam for providing valuable feedback and access to osteological data, and to Dr. Andrea Waters-Rist and Dr. Andrew Nelson at Western University for collection access and facilitating micro-CT analysis respectively.

This research was made possible due to the support of various funding sources, including: the Social Science and Humanities Research Council (SSHRC) Joseph-Armand Bombardier Canada Graduate Scholarship, the McMaster University Shelley Saunders/Koloshuk Family Scholarship, a SSHRC Insight Grant (File Number: 435-2021-0665), the Canadian Association for Biological Anthropology Shelley R. Saunders Thesis Research Grant, and the McMaster School of Graduate Studies.

Thank you to the Department of Anthropology staff, including Delia Hutchinson, Marcia Furtado, Katie Miller, and John Silva for your support in managing the bureaucratic aspect of doctoral research. Thanks also to my peers and colleagues throughout the department, and especially to those in our lab group; I appreciate the new perspectives and valuable insight that each of you has brought.

I would also like to thank my friends and family, especially my parents, for your endless support and for always at least pretending to be interested when I talked about my research. Thank you especially to Akacia Propst, Dana Thacher, and Marie-Hélène B-Hardy for your friendship, laughter, and creative business ideas. Finally, to my partner Michael Prysiazny and our dog Nutmeg: Michael, thank you for always having confidence in me, especially when I didn’t, and for being my best friend throughout everything. Nutmeg, thank you for making me laugh, and teaching me that the only things in life worth truly stressing over are thunderstorms, fireworks, and trucks with trailers.

TABLE OF CONTENTS

LIST OF FIGURES

LIST OF TABLES

ABBREVIATIONS

RBCs ..... Red blood cells

PH ..... Porotic hyperostosis

CO ..... Cribra orbitalia

CT ..... Computed tomography

TbSp ..... Average trabecular separation

CtThOL ..... Average cortical thickness of the orbital lamina

TbTh ..... Average trabecular thickness

TbSpTh ..... Trabecular space thickness

DECLARATION OF ACADEMIC ACHIEVEMENT

I declare that I am the main contributor to the three articles that make up this thesis. Chapter two, titled “Evaluating skeletal manifestations of anemia in the sternum using a modern clinical sample” is a co-authored paper in the Journal of Archaeological Sciences. Chapter three, titled " A framework for anemia diagnosis in paleopathology using metric methods” is a co-authored paper that has been submitted to the American Journal of Biological Anthropology. Chapter four, titled “Co-occurrence of anemia and scurvy in nonadults from 18th-19th century Quebec”, is a co-authored paper that has been prepared for submission to PLOS ONE. I am the first author on all papers. My contribution was to collect and analyze osteological data, perform micro-CT imaging and analysis, collect, analyze clinical imaging and hematological data, and prepare first drafts for all three papers, including Figures and Tables. I worked with co-authors on revisions and edits.

CHAPTER 1: INTRODUCTION AND BACKGROUND

Anemia is a condition characterized by deficiency in red blood cells (RBCs) or hemoglobin that impedes the delivery of oxygen throughout the body (WHO, 2011). Globally, it currently affects approximately 1.8 billion people, the majority of whom are women and children (WHO, 2023). The risk factors that contribute to high anemia prevalence, such as micronutrient deficiencies, social exclusion and poverty, and poor maternal health (WHO, 2023) would have also significantly affected vulnerable groups in the past. Consequently, anemia has been studied in past populations across a wide variety of archaeological contexts and communities (e.g. Angel, 1966; Scaffidi, 2020; Sullivan, 2005; Wapler et al., 2004). External visualization of porotic lesions in the cranial vault and orbital roof, known as *porotic hyperostosis* and *cribra orbitalia* respectively, has typically been the most common method of evaluating anemia in skeletal remains (Brickley, 2024; Grauer, 2019), but as understanding of the varied etiologies of porous lesions has grown, this approach has fallen under criticism (Anderson, 2023; Brickley, 2024; Grauer, 2019). The lack of consensus on diagnosis in skeletal remains has likely limited research on other aspects of anemia in archaeological contexts, such as its co-occurrence with other conditions. New approaches to this old problem are needed.

My doctoral research seeks to address this issue by exploring new aspects of anemia in skeletal remains. I seek to investigate and test novel methods of anemia diagnosis, and to apply these techniques using archaeological skeletal collections from 18th-19th century Quebec. This research is centered around two core questions:

1. How can metric changes in bone be leveraged for anemia diagnosis, and how does this change how we study anemia in archaeological contexts?
2. How prevalent are scurvy, anemia, and scurvy/anemia co-occurrence within this context, and what factors influence their development and clustering?

Each of the three papers included in this thesis contribute to answering these questions. Chapter 2 ("Evaluating skeletal manifestations of anemia in the sternum using a modern clinical sample") presents a novel method of anemia diagnosis using relative cortical bone ratios in the sternum. This research used imaging data from individuals clinically diagnosed with anemia using World Health Organization standards (WHO, 2011), and then applies these metric parameters to archaeological individuals. This paper has been published in the *Journal of Archaeological Sciences.* Chapter 3 ("A framework for anemia diagnosis in paleopathology using metric methods") has been submitted to the *American Journal of Biological Anthropology*, and explores cranial changes related to anemia in nonadults, and presents a general framework for how these data can be used as part of diagnosis. Chapter 4 ("Co-occurrence of anemia and scurvy in nonadults from 18th-19th century Quebec") uses these diagnoses and previously published standards for scurvy diagnosis to understand the prevalence and pathways of anemia/scurvy co-occurrence and clustering in historic Quebec. Age-at-death data were used to understand the effects of co-occurrence on mortality. This paper is prepared for submission to *PLOS ONE.*

My contribution to these papers involved a senior role in recording osteological data from the Montreal collections, accessed with permission from Dr. Isabelle Ribot. Julie Nguyen also contributed to this data collection process. I conducted micro-CT scanning of the archaeological samples, with training from Dr. Andrew Nelson. I analyzed the Montreal micro-CT reconstructions and developed rubrics and methods for this analysis. I trained Meghan Langlois in the use of these protocols, and she did the visual analysis of the orbits from the Dutch collections (access with permission from Dr. Rachel Schats, Dr. Alie van der Merwe, and Dr. Andrea Waters-Rist) using these methods. I did the micro-CT measurements from the Montreal manubria, Montreal and Dutch orbits, and measured frontal ratios from the Montreal collections, while Meghan Langlois collected the Dutch frontal ratios. I performed all statistical tests and analysis myself. For the clinical data, I obtained ethics approval in conjunction with Dr. Michelle Zeller, Kayla Lucier and Maryam Akbari-Moghaddam, who also provided guidance on clinical data collection. I collected sternal measurements and haematological data from this sample, and did the data analysis, with input on methods from Maryam Akbari-Moghaddam. I wrote all first drafts, and revisions were made based on feedback from co-authors.

This thesis includes the three articles described above, as well as this introductory chapter and a concluding chapter. The introduction provides background information on the relationship between anemia and bone, and the history of anemia diagnosis in paleopathology to situate the reader in the broader context of anemia diagnosis in skeletal remains. It also discusses the individual and population-level burden of anemia, to illustrate why the study of anemia is important for understanding overall health and well-being. These topics are broadly covered in all three papers (Chapters 2-4), but this general information provides a more detailed overview. The biocultural aspects of anemia and scurvy co-occurrence and clustering are also discussed, to provide a background to the work presented in Chapter 4. The final chapter describes how the three papers contribute to meeting the overall objectives of the thesis, and suggests ways in which this work can be used in the future for continued study of anemia in the past.

1.1 Anemia Development and Global Burden

There are three main pathways that anemia develops: excessive blood loss, increased destruction of RBCs (hemolysis), or impaired RBC production or formation. These mechanisms can overlap, and determining the exact cause is often challenging or impossible, even in clinical settings (WHO, 2023). Anemia can be inherited/genetic, such as sickle cell anemia or thalassemia, or can be acquired through nutritional deficiencies, trauma and injury, or chronic health conditions like kidney disease or gastrointestinal conditions (Kassebaum, 2016).

In clinical settings, anemia diagnosis is done through a complete blood count, which measures parameters such as hemoglobin level, hematocrit value, and RBC count (Cascio & DeLoughery, 2017). Other diagnostic tests may be performed to investigate blood cell shape and size, or marrow health. Moderate anemia is typically diagnosed when hemoglobin concentrations are below 110 g/L (WHO, 2011), and severe anemia is classified as concentrations below 80 g/L. These values can vary based on age, sex, and pregnancy status. For example, the non-anemia hemoglobin value for pregnant people is a hemoglobin concentration over 110 g/L, but this value

is over 130 g/L for men over age 15 years (WHO, 2011). To establish the clinical cohort in Chapter 2, individuals in the non-anemic sample needed to have a hemoglobin level of over 130 g/L, and the anemic sample used a maximum hemoglobin level of 110 g/L. Pregnancy was not used as an exclusion criterion, but due to the cutoff values used for both groups, differences in diagnostic parameters for different demographics should not have affected the cohort composition. Individuals diagnosed with genetic anemias were excluded; currently, non-genetic forms of anemia are most common globally (WHO, 2023), and this is expected to be the same for past contexts. While genetic anemias do produce marked skeletal changes, and these lesions can assist in a diagnosis, genetic anemias are unlikely to represent the majority of cases in most paleopathological research contexts. Individuals diagnosed with osteoporosis or with an osteoporotic fracture were also excluded, to eliminate any issues differentiating between the source of observed changes. Both osteoporosis and skeletal manifestations of anemia can result in changes to bone quantity (see section 1.2) and so differentiating between these two potential causes of skeletal changes was important. Additionally, only individuals 45 years old or younger were included in the sample, as osteoporosis and age-related bone loss tends to affect individuals over 50 years (Clynes et al., 2020).

Individual consequences of anemia are related to oxygen deficiency, which leads to generalized fatigue, and has a significant impact on an individual's ability to exert themselves and perform physical activities (Kassebaum, 2016; Ludwig & Strasser, 2001). Cognition may also be affected, and these effects in combination can have a negative effect on quality of life (Lucca et al., 2008; WHO, 2023). Children and women of reproductive age are most vulnerable to anemia and its associated negative consequences; in part, this is due to high physiological demand for micronutrients during pregnancy, growth, and development (Sifakis & Pharmakides, 2000). Anemia is associated with increased mortality and fragility within vulnerable groups, and can exacerbate the risk of complications during pregnancy, contracting an infectious disease, and of heart failure (Kassebaum, 2016; Sifakis & Pharmakides, 2000; WHO, 2023). However, anemia risk is not only a result of biological and physiological mechanisms. Determinants of anemia can also include environmental (e.g. proximity to malaria hotspots), structural (e.g. access to health services), and cultural (e.g. birth spacing practices) variables that operate on individual and community-based scales, and can vary from context to context, even within individual households (Balarajan et al., 2011; Kassebaum, 2016; Piperata et al., 2014; WHO, 2023) (Figure 1-1). At the population level, anemia is associated with risk factors such as higher infectious disease burden, food insecurity and reduced micronutrient availability, poor maternal healthcare, conflict, poverty, and poor sanitary infrastructure (Balarajan et al., 2011; Fischer et al., 2014; Kassebaum, 2016; WHO, 2023). High anemia prevalence can have significant economic consequences due to lowered productivity and diminished work capacity, often leading to economic disadvantage and resulting in a negative feedback loop that further exacerbates anemia risk (Balarajan et al., 2011; WHO, 2023).

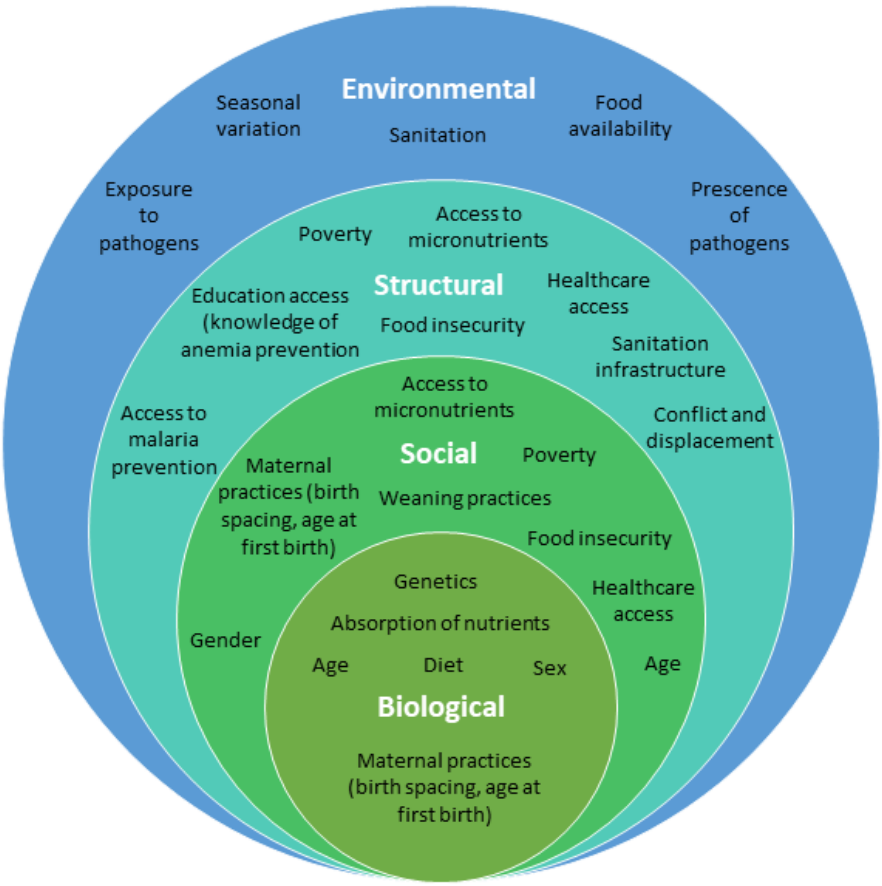

Figure 1-1: Examples of anemia risk factors on biological, social, structural, and environmental levels. Data from Balarajan et al., 2011; Hoffbrand & Steensma, 2019; Kassebaum, 2016; WHO, 2023. Figure design adapted from Perry & Gowland, 2022. Some factors can be classified under more than one broad category, and are included in multiple sections to reflect this.

1.2 Anemia and Bone

Skeletal changes caused by anemia are due to the process of marrow hyperplasia, where bone marrow expands past its usual boundaries in response to an increased demand for RBC production (erythropoiesis) (Hoffbrand & Steensma, 2019). Red blood cell formation is stimulated by the protein erythropoietin, which is upregulated during periods of anemia (Erslev, 1991). In conjunction with increasing RBC production, erythropoietin also stimulates osteoclast (bone-resorbing cells) development, thereby promoting bone resorption (Hiram-Bab et al., 2015; Shiozawa et al., 2010;). Ultimately, the pressure of expanded bone marrow and increased osteoclast activity can lead to thinning of the cortical bone, which causes porosity in locations where the bone is already thin (Wapler et al., 2004). This enhanced pressure may result in trabeculae that are oriented perpendicularly to the cranial vault and can perforate the outer table, leading to "hair-on-end" radiographic appearance of the cranium (Hollar, 2001). Resorption of the cortical bone also causes a relative increase in trabecular space thickness (Reynolds, 1962, 1965). Other aspects of bone microarchitecture can also be affected by marrow hyperplasia; increased intertrabecular separation and trabecular thinning are also expected (Agarwal et al.,

1970; Hoffbrand & Steensma, 2019; Jaffe, 1972). These aspects of how skeletal manifestations of anemia develop are further explored in Chapters 2 and 3.

Skeletal manifestations of marrow hyperplasia can only develop in locations where bone marrow is active, and capable of producing more RBCs (Brickley, 2018). Distribution of active bone marrow throughout the body is highly age-dependant. In those under one year old, active marrow is found throughout the entire skeleton, but with age, marrow converts to an inactive stage, and its hematopoietic potential decreases (Brickley, 2018; Burkhardt et al., 1987). After 25 years of age, the vertebrae, sacrum, pelvis, thorax, and long bone metaphyses contain the highest percentage of active marrow (Brickley, 2018; Burkhardt et al., 1987; Guillerman, 2013). Over the age of 40 years, the hematopoietic potential of the marrow further decreases, which subsequently affects the likelihood of developing skeletal manifestations of anemia initiated after this age. For context, red marrow typically contains a minimum of 60% hematopoietic cells by volume (Blebea et al., 2007), and only the lumbar vertebrae maintain a volume of over 50% by age 40 years (Burkhardt et al., 1987). Additionally, marrow has the capacity to reconvert to the active state, as long as it has not fully transitioned to inactivity (Brickley, 2018; Guillerman, 2013). If reconversion meets the demand for erythropoiesis during anemia, skeletal manifestations of marrow hyperplasia would not develop, as the bone marrow does not need to expand (Brickley, 2018; Yildirim et al., 2005).

Differentiating between skeletal manifestations of marrow hyperplasia and other lesion etiologies is a key issue when associating porous lesions with anemia, but few studies have attempted to do so by visualizing the internal marrow space (exceptions include Morgan, 2014; Naveed et al., 2012; Saint-Martin et al., 2015; Wapler et al., 2004). Other etiologies of skeletal porosity include taphonomy, scurvy, rickets, infection/inflammation, and normal growth and development (Brickley & Morgan, 2022) (see Section 1.4). Differentiating between lesion etiologies requires assessing the underlying biological mechanisms that could have contributed to observed skeletal changes (Klaus, 2017; Mays, 2018). This approach, termed the biological approach, requires consideration of anatomy and physiology, in conjunction with clinical observations (Mays, 2018). In cases of anemia, it is expected that porous lesions will be accompanied by underlying signs of marrow hyperplasia, which are difficult to assess through external examination alone.

1.3 Anemia Diagnosis in Paleopathology

The link between porous cranial lesions and anemia was established using radiographic and macroscopic observations of skeletal changes that occurred in genetic anemia (Angel 1966; Hooten, 1930; Williams, 1929). Early researchers, such as Moseley (1965) and Angel (1966), emphasize widening of the diploic space in conjunction with porous lesions as a key feature linking these skeletal changes to anemia. Angel also highlighted the importance of considering other possible lesion etiologies, and evaluating postcranial skeletal elements for ensuring that differential diagnosis could be as thorough as possible (Buikstra & Prevedorou, 2012). Initial research on porous lesions and anemia focused on genetic anemias, but the relationship between skeletal changes and anemia was also documented in other forms of anemia, notably iron

deficiency anemia (Britton et al., 1960; Moseley, 1965; Shahidi et al., 1960). Researchers used this information to expand their studies of anemia in archaeological contexts to include other forms of anemia as well.

Porous cranial lesions were used as evidence for anemia, especially iron deficiency anemia, in archaeological contexts. Lesions helped to identify contexts where malnutrition and dietary deficiencies may have affected past communities, and explore dietary differences between groups (e.g. El-Najjar et al., 1976; Von Endt & Ortner, 1982). Other studies hypothesized that infections and early childhood stress were a potential cause of iron deficiency anemia (e.g. Mensforth et al., 1978), and some proposed multiple interacting pathways that led to the development of anemia and subsequent lesions (e.g. Palkovich, 1987). Consequently, the terms porotic hyperostosis (PH) and cribra orbitalia (CO), used to describe these lesions, became a regular part of the paleopathological lexicon.

Although initial work emphasized importance of observing evidence of marrow hyperplasia, the terms PH and CO became synonymous with anemia over time (Brickley, 2024; Grauer, 2019). Grauer (2019) hypothesizes that this shift occurred inadvertently due to the extensive use of Buikstra and Ubelaker's *Standards for Data Collection from Human Skeletal Remains* (1994), which used PH and CO as descriptive terms for the purposes of recording pathology, and led to "researchers conflating description with diagnosis" (Grauer, 2019: 515). This shift meant that diagnosis of anemia did not always consider whether lesions were related to skeletal manifestations of marrow hyperplasia, and that Angel's early recommendations on evaluating lesions were not necessarily followed (Brickley, 2024). Many studies calculated anemia prevalence using only the presence of PH and CO, without full consideration of the underlying processes that may have caused the lesions. By the early 2000s, researchers began to articulate the limitations of this method of anemia diagnosis (e.g. Wapler et al., 2004), and recognized the wide variety of underlying etiologies that could contribute to PH and CO, leading to greater caution in paleopathological anemia research overall (Brickley, 2024). Interpretation of porous lesions as non-specific stress indicators tied to poor population health, instead of anemia specifically, became more common (e.g. Yaussy et al., 2016). Currently, researchers tend to be much more cautious in ascribing porous lesions directly to anemia.

Beyond diagnosis, other challenges and debates on anemia in past contexts have developed throughout time. Walker and colleagues (2009) suggested that porous cranial lesions were more likely linked to megaloblastic anemia (due to B12 and/or folate deficiency) rather than iron deficiency anemia, although McIlvaine (2015) and Oxenham and Cavill (2010) have disputed this idea. This debate highlights the complexity of anemia as a condition; in clinical settings, multiple forms of anemia can develop in the same person, and it is not always possible to determine one specific etiology (Chapparro & Suchdev, 2019). This means that when evaluating anemia in bone, it may be challenging or even impossible to determine an exact etiology, especially as a range of anemias, beyond just iron deficiency or megaloblastic anemia, can result in marrow hyperplasia and potential skeletal changes (Oxenham & Cavill, 2010). Other questions have centered on the etiological relationship between CO and PH (Rivera & Lahr, 2017; Stuart-Macadam, 1989), interobserver error when scoring lesions (Anderson, 2023;

Santos et al., 2023), and timing of lesion development (Brickley, 2018; Stuart-Macadam, 1985). These questions and debates highlight many of the issues with overreliance on lesions for anemia diagnosis.

As awareness of the issues surrounding anemia diagnosis in paleopathology rises, solutions to these challenges have been proposed. Radiography has a long history of being used to visualize the internal marrow space (e.g. Moseley, 1965; Reynolds, 1962, 1965), but improved skeletal imaging methods, such as computed tomography (CT) and micro-CT analysis, are gaining prominence (e.g. O'Donnell et al., 2023; Panzer et al., 2023), and provide improved resolution that allows for visualization of bone microarchitecture (e.g. Naveed et al., 2012; Saint-Martin et al., 2015). In their pivotal study of porous lesion etiology, Wapler and colleagues (2004) used destructive sampling to expose a single sagittal plane of the eye orbit, but non-destructive imaging can now achieve visualization of the entire orbit, and the changes that develop throughout (e.g. Morgan, 2014). Visualization of the internal marrow space also allows for quantitative analysis, and Brickley (2024) suggests reframing how we think about anemia diagnosis in the skeleton using metric analysis, which can be thought of as "direct measure[s] of a diagnostic parameter" (Mays, 2018: 13). Skeletal manifestations of marrow hyperplasia can affect the relative amount of bone present (Reynolds, 1962, 1965; Sebes & Diggs, 1979), and developing baselines for bone measurements in individuals without anemia can be used to identify variation that may be indicative of changes related to marrow hyperplasia. My research is situated within this paradigm shift, and seeks to explore how such quantitative methods can be used to improve anemia diagnosis using non-destructive imaging methods.

The World Health Organization defines anemia prevalence of 40% or higher as severely significant to public health in a given context (WHO, 2011). Reported prevalences of porotic lesions in archaeological contexts can vary widely, but can reach this level in certain contexts and age groups (e.g. Pechenkina & Delgado, 2006). Studies have attributed high prevalence of CO and/or PH to factors such as diet and micronutrient availability (e.g. Fairgrieve, & Molto, 2000), parasitic infection (e.g. Godde & Hens, 2021), lower socioeconomic status and presence of chronic disease (e.g. Sullivan, 2005). However, it is important to note that crude prevalence of porous lesions, including PH and CO, cannot be directly correlated to the prevalence of anemia, due to the varied etiologies of porous cranial lesions, as discussed above. Instead, my research aims to specifically diagnose and evaluate anemia, and develop improved approaches to diagnosis, so that the documented burden that anemia can have on population and individual health (see Section 1.1) can be better assessed. Determinants of anemia will not operate in the same way across different contexts, and to understand how the intersection of local risk factors contributes to anemia in specific communities and samples, we must first be able to have greater certainty and consistency in anemia diagnosis in skeletal remains.

1.4 Anemia and Scurvy Co-Occurrence

Greater confidence in anemia diagnosis allows us to investigate different aspects of the condition in archaeological contexts. Anemia commonly co-occurs with other conditions (Chaparro & Suchdev, 2019; Trapani et al., 2022; WHO, 2023), and while co-occurrence of

porotic lesions with other skeletal indicators of disease are common (e.g. Yaussy et al., 2016), studies in paleopathology that specifically examine the clustering of anemia and other conditions are limited. My research focuses specifically on co-occurrence with scurvy (caused by vitamin C deficiency), which often co-occur in clinical settings (Trapani et al., 2022). To date, however, work on anemia and scurvy co-occurrence in archaeological collections has identified individual cases of co-occurrence (e.g. Lovasz et al., 2013; Ortner et al., 2001), rather than examining these conditions on a wider scale, or has focused on methods of differentiating between the conditions skeletally (e.g. Zuckerman et al., 2014), rather than considering how co-occurrence may have affected skeletal manifestations of either condition.

Scurvy and anemia share a biological/physiological relationship that makes them likely to co-occur. Vitamin C facilitates iron absorption and maintains folate levels, meaning that either iron deficiency anemia or megaloblastic anemia can occur during scurvy (Golding, 2018; Trapani et al., 2022). It also plays a role in tissue repair through collagen production, and the significant haemorrhaging and blood loss during scurvy, especially in later stages, can also lead to a form of acquired anemia (Schlueter & Johnston, 2011; Trapani et al., 2022). Scurvy and anemia also share structural, environmental, and social risk factors, such as access to micronutrients, food insecurity, displacement, and poverty, further enhancing the likelihood that they will co-occur, particularly in vulnerable populations (Rowe & Carr, 2008; WHO, 1999). Figure 2-2 shows the

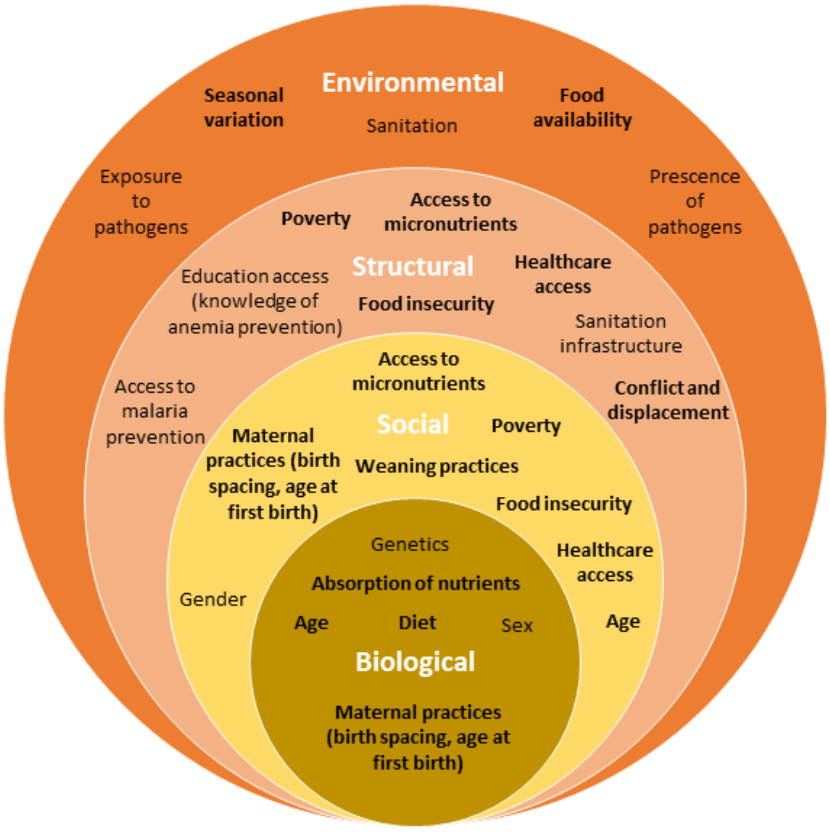

Figure 1-2: Repeated version of Figure 1-1 to highlight the similarities in risk factors between anemia and scurvy. Examples of scurvy and anemia risk factors are bolded. Data from; Balarajan et al., 2011; Hoffbrand & Steensma, 2019; Kassebaum, 2016; Schlueter & Johnston, 2011; Trapani et al., 2022; WHO, 1999; WHO, 2023.

same examples of anemia risk factors as Figure 1, but risk factors common to both anemia and scurvy are bolded, demonstrating the wide degree of overlap between the risk factors for both conditions. Factors such as exposure to pathogens and sanitation were not bolded, but are still tangentially related to scurvy, as vitamin C requirements tend to increase due to infectious disease (WHO, 1999).

Scurvy and anemia both have a negative effect on the immune system, and exploring multimorbidity with other diseases helps to further evaluate the factors that contributed to mortality risk and susceptibility to disease. Understanding the co-occurrence of various health conditions is vital for recognizing patterns and identifying potential adverse health outcomes stemming from their interaction. This approach falls under the umbrella of syndemics, a theory first proposed by Singer (1994) to describe the phenomenon of two or more diseases or conditions that synergistically interact to negatively affect health within a given sociocultural context (Singer et al., 2017). Syndemic theory helps to explore the pathways that affect disease clustering, and explains why these pathways can differ depending on local factors (Mendenhall et al., 2017). Syndemic theory explicitly emphasizes that biological interaction and synergism is essential for recognizing a syndemic, not just co-occurrence of multiple conditions (Mendenhall, 2017; Tsai, 2018). Using mortality data is one way to study syndemic interaction in archaeological contexts; disproportionate mortality rates amongst certain groups, or younger age-at-death can be a proxy for worse health outcomes (Perry & Gowland, 2022). This is the approach used in Chapter 4 to investigate scurvy and anemia in 18th-19th century Quebec.

Co-occurrence can cause complications for assessing skeletal changes related to anemia as other conditions may also affect bone quantity or quality. For example, other metabolic bone diseases, such as scurvy and rickets, can result in generalized osteopenia and loss of bone mass (Brickley & Morgan, 2023), similar to the reduction in cortical/trabecular thickness expected for skeletal manifestations of marrow hyperplasia. Changes to bone microarchitecture, particularly cortical thinning, may enhance the porosity that develops in scurvy. Differentiating between skeletal changes caused by different metabolic conditions, therefore, requires thorough consideration of the entire skeleton, including factors such as age, lesion appearance, and lesion distribution. Changes that can be attributed to multiple conditions (i.e. those that fall under the 'consistent with' category of diagnostic certainty as described by Appleby et al. (2015)) will mean that high levels of diagnostic certainty may not be achievable for that case. Chapter 3 briefly explores how co-occurrence may affect anemia diagnosis, and Chapter 4 elaborates on how co-occurrence with scurvy is expected to affect the diagnostic guidelines presented in Chapter 3.

CHAPTER 2: SKELETAL MANIFESTATIONS OF ANEMIA IN THE STERNUM IN A MODERN CLINICAL SAMPLE: AN INITIAL INVESTIGATION

Title: Skeletal Manifestations of Anemia in the Sternum in a Modern Clinical Sample: An Initial Investigation

Brianne Morgan [a], Michelle Zeller [bc], Isabelle Ribot [d], & Megan B. Brickley [a]

[a] Department of Anthropology, McMaster University, Hamilton, Ontario, Canada, L8S 4L9
morgab5@mcmaster.ca, brickley@mcmaster.ca

[b] Michael G. DeGroote Centre for Transfusion Research and Division of Hematology and Thromboembolism, Department of Medicine, McMaster University, Hamilton, Ontario, Canada, L8S 4L9
zeller@mcmaster.ca

[c] Canadian Blood Services, Ottawa, Ontario, Canada, *K1G 4J5*

[d] Department of Anthropology, University of Montréal, Montréal, Québec, Canada, QCH3T 1N8
i.ribot@umontreal.ca

Accepted (January 29 2024) for publication in the Journal of Archaeological Science.
DOI: 10.1016/j.jas.2024.105942

Abstract
Anemia is a globally significant condition, both today and throughout history. Studying how it affected past communities contributes to understanding its impact on vulnerable groups. However, anemia diagnosis in skeletal remains is challenging, and improving methods for diagnosis is necessary for moving forward. In current clinical practice, sternal bone marrow undergoes anemia-related changes, which could affect underlying bone structure, but the sternum has never been investigated as a skeletal marker of anemia. We used a cohort of individuals with known hematological data (N=23) to investigate whether there are quantitative bone changes in the sternum of individuals clinically diagnosed with anemia. Sternal bone features were measured using CT imaging to calculate a ratio of the relative cortical bone to trabecular space. The sample was separated into non-anemic and anemic cohorts based on World Health Organization diagnostic parameters. We found significant differences in ratios between those with and without anemia, suggesting that sternal bone ratio measurements could be used as a diagnostic parameter. In individuals without clinically-diagnosed anemia, ratios never exceeded 3.6 in the manubrium and 2.3 in the sternal body. We repeated these ratio measurements using micro-CT analysis on a sample of archaeological sternums and found that the ratio diagnostic parameter could also be used in this sample to identify those who could have experienced anemia. These results demonstrate the utility of quantitative methods for diagnosing anemia in skeletal remains and suggest that sternal ratio measurements can be used as part of anemia diagnosis in past contexts.

Keywords: marrow hyperplasia, porous lesions, micro-CT, hemoglobin, hematopoiesis

1.0 Introduction

Anemia is a condition characterized by a reduction of the body's ability to transport and supply oxygen to its tissues, generally due to a deficiency in the oxygen-carrying capacity of red blood cells (RBCs) (Lopez, 2016; WHO, 2011). Bioarchaeologists have long been interested in studying anemia (e.g. Angel, 1966; El Najjar et al., 1976), both on a diagnostic level (e.g. Stuart-Macadam, 1987; Anderson et al., 2021) and as an indicator of overall poor health and nutrition amongst vulnerable groups (e.g. Sullivan, 2005). However, diagnosing anemia in human remains is challenging, partly due to the disconnect between typical clinical methods of anemia diagnosis and the types of data available to those diagnosing disease in bone (Brickley, 2024).

Assessments of anemia in bone tend to rely on evaluating porosity, which has a variety of causes (Brickley, 2024). There is a lack of current research that investigates the skeletal manifestations of anemia using known clinical cases, although researchers have recognized the necessity of this work. Specifically, Grauer (2019) suggests investigating the potential correlations between clinical measures of anemia (e.g., hemoglobin concentration, serum ferritin level, transferrin saturation, etc.), length of illness, and skeletal lesions to understand better the factors contributing to lesion manifestation/appearance. To improve the diagnosis of anemia in archaeological settings, there is a broader need to work collaboratively with clinicians to develop new methods, and investigate and understand the marrow space changes that occur in individuals clinically diagnosed with anemia. This research builds on these suggestions, and is the first study to incorporate both paleopathological and hematological data into its research design.

Skeletal manifestations of anemia are due to the interaction of red blood cells (RBCs), bone marrow, and bone microarchitecture. Red blood cells are produced in the bone marrow, and increased RBC production to address the oxygen deficiency can result in expansion of bone marrow -a process called marrow erythroid hyperplasia (Hoffbrand & Steensma, 2019). When the marrow exceeds its regularly occupied space, marrow hyperplasia can cause skeletal changes such as thinning of the trabecular bone and widening of intertrabecular separation, as well as resorption/thinning of the cortical bone that can lead to porous lesions (Agarwal et al., 1970; Jaffe, 1972). In the cranium, porous lesions such as cribra orbitalia, and/or porotic hyperostosis are typically used as part of anemia diagnosis in archaeological skeletal remains (Brickley, 2024), and anemia has been proposed as a potential etiology of post-cranial lesions such as cribra femora or cribra humeri (e.g. Smith-Guzmán, 2015). However, since other processes can also cause cortical porosity (e.g. taphonomy, incomplete mineralization, vascularization), a biological approach is necessary for evaluating the etiology of porous lesions (Wapler et al., 2004; Mays, 2018; Brickley et al., 2020). Alternative methods of evaluating these lesions and any underlying evidence of marrow hyperplasia, such as imaging and/or metrics, have been proposed or used, and may be a way to improve the accuracy of anemia diagnosis in archaeological remains (Morgan, 2014; Rivera & Lahr, 2017; Anderson et al., 2020; O'Donnell et al., 2020; O'Donnell et al., 2023; Panzer et al., 2023; Brickley, 2024).

The clinical data on skeletal changes associated with marrow hyperplasia and anemia comes from physicians using radiographs (e.g. Reynolds, 1962,1965; Moseley, 1965; Agarwal et al., 1970). These publications focus on cranial manifestations of anemia, likely because these

changes are more extreme (e.g. the hair-on-end appearance of the cranial vault), although the involvement of long bones has also been considered in some cases (e.g. Agarwal et al., 1970). Many of these studies involve observational data; however, Reynolds (1962, 1965) and Sebes & Diggs (1979) also incorporate quantitative approaches to evaluating marrow space changes. Using radiographs, Reynolds (1962) measured the parietal bones of 12 patients with known sickle cell anemia and calculated the ratio of diploic thickness to total cortical bone. A "comparable group of normal subjects" was also measured. Their ratios never exceeded 2.3 (Reynolds, 1965: 72). Based on this finding, Sebes & Diggs (1979) also measured frontal ratios, and considered the diploe of their clinical subjects to be abnormally expanded when diploic thickness was at least 2.5 times greater than cortical thickness (measurements shown in Panzer et al., 2023, Figure 1).

These early clinical studies (e.g. Reynolds, 1962, 1965) demonstrate the utility of quantitative methods for assessing marrow hyperplasia. However, current literature on metric assessment and anemia is limited to the cranium, and postcranial elements have not been investigated to the same extent, meaning that archaeological individuals with poorly preserved or absent crania cannot be evaluated. The location of marrow space changes is important for anemia, and is age-dependent, as only active "red" bone marrow or mixed marrow that contains some active marrow can produce RBCs (Brickley, 2018). With age, hematopoietic cells in red marrow are replaced with fatty/yellow cells, and its capacity for producing RBCs significantly decreases (Brickley, 2018). When demand for RBCs is especially high, reconversion of mixed marrow can also occur, which increases the proportion of red marrow, meaning that more RBCs can be produced without the possibility of marrow expansion. The red-yellow marrow conversion process happens at different times in different skeletal elements; in children, active marrow is found in high concentrations in the cranium (see Brickley, 2018, Figure 1). Cranial manifestations of marrow hyperplasia that are used for anemia diagnosis in skeletal remains can therefore be linked to episodes of anemia initiated in childhood (McFadden & Oxenham, 2020; O'Donnell et al., 2023). Alternative locations of skeletal changes related to marrow hyperplasia are much less understood, and the potential for postcranial changes that represent episodes of anemia occurring at older ages has not been investigated.

The sternum is one potential area where active marrow persists at older ages, and could show skeletal manifestations of marrow hyperplasia (Chirsty, 1981; Burkhardt et al., 1987; Brickley, 2018). Burkhardt et al. (1987) found that the sternum, on average, contains a higher volume percentage of hematopoietic tissue compared to other common sites of RBC production in individuals aged 20-39 years (e.g. the iliac crest and the lumbar vertebrae). Although the iliac crest is the most-used site for taking marrow samples in anemic patients, aspiration of the sternum is also used for adults if the iliac crest is inaccessible (Riley et al., 2004). Porous "lattice" lesions on the posterior manubrium are common in archaeological material, and it has been suggested that they could be related to various forms of anemia (Mann & Tuamsuk, 2005; Lagia et al., 2007; Sanchez, 2014). Based on these factors, we hypothesize that there is potential for relative changes in cortical thickness and trabecular space in the sternum to be a marker of anemia.

This exploratory study aims to investigate this hypothesis by using imaging data from modern individuals clinically diagnosed with anemia. The study aims to determine if there are quantitative differences in cortical thickness and trabecular space in the sternums of these individuals and establish whether such differences can also be observed in archeological bone. Furthermore, we seek to evaluate whether manubrium porosity and other visual skeletal changes are associated with any observed metric differences.

2.0 Materials

2.1 Clinical sample

The Hamilton Integrated Research Ethics Board approved data collection and study methods. The clinical cohort was comprised of 23 individuals from Hamilton Health Sciences' Transfusion Research Utilization, Surveillance, and Tracking (TRUST) database who met the selection criteria listed in Table 2-1. Anemia diagnosis in this study was based on established hemoglobin thresholds for anemia (WHO, 2011) and supplemented by specific ICD-10 code diagnoses (see Supplemental Table 2-S1). From the total cohort, 15 manubria and 22 sternal bodies were measured, and both the manubrium and sternal body were measured from 14 individuals. The non-anemic sample consisted of individuals with a complete blood count performed but who were not clinically diagnosed with anemia in the three years before undergoing CT imaging (n=11 for the manubrium; n=16 for the sternal body). The anemic sample consisted of individuals who had experienced a form of non-genetic anemia in the three years before their CT imaging (n=4 for the manubrium; n=6 for the sternal body) (Table 2-2). Length of anemia before imaging ranged from one month to 2.5 years. To mitigate the effects of age-related bone loss on ratio measurements, individuals ≤ age 45 years at the time of imaging were prioritized, as risk of osteoporosis increases past age 50 (Clynes et al., 2020). Individuals diagnosed with osteoporosis or an osteoporosis-related fracture were excluded (Supplemental Table 2-S1).

Table 2-1: General clinical sample selection criteria.

Criteria	Anemic Sample	Non-Anemic Sample
Age (years)	18-45 years	18-45 years
Hemoglobin Level (g/L)	≤110	>130
CT Imaging	Sternum visible	Sternum visible
Other Criteria	Includes: • Acquired anemias Excludes: • Genetic anemias • Osteoporosis	Excludes: • Any form of anemia • Osteoporosis

* Exact criteria for data extraction are presented in Supplemental Table 2-S1

Clinical	Number of individuals	23	12	11	7	16
	Mean age at time of imaging (years)	33	33	33	36	33
	Age range at time of imaging (years)	22-45	22-45	22-42	22-45	22-40
Archaeological	Number of individuals	18	7	9	2	
	Number of individuals with manubrium porosity	8	3	5	0	
	Number of individuals without manubrium porosity	10	4	4	2	
	Mean midpoint age-at-death estimate (years)	29	32	27	28	
	Range of midpoint age-at-	18-45	18-45	18-40	25-30	

2.2 Archaeological sample

Individuals from three 18th-19th century Quebec collections were included in the archaeological sample and originated from the following cemeteries: Saint-Antoine (1799–1855) (Ethnoscop, 2016a), Sainte-Marie (1709–1843) (Ethnoscop, 2006), and Pointe-aux-Trembles (1748–1878) (Ethnoscop, 2016b). Age-at-death was estimated by assessing the auricular surface, pubic symphysis, sternal rib ends, vertebral annular rings, and epiphyseal fusion (Lovejoy et al., 1985; Brooks & Suchey, 1990; Schmitt, 2005; Schaefer et al., 2009; Hartnett, 2010), while sex was estimated using standard morphological features of the skull and pelvis (Buikstra & Ubelaker, 1994). From these collections, 18 adults (over 18 years) with midpoint age estimates ≤ 45 years and with well-preserved manubria were chosen for the micro-CT sample (Table 2). The presence/absence of porosity on the posterior manubrium for these individuals was also recorded based on criteria described by Sanchez (2014).

Table 2-9: Demographic composition of archaeological and clinical samples.

		All	Male	Female	Anemic	Non-anemic
Clinical	Number of individuals	23	12	11	7	16
	Mean age at time of imaging (years)	33	33	33	36	33
	Age range at time of imaging (years)	22-45	22-45	22-42	22-45	22-40
		All	**Male**	**Female**	**Unknown**	
Archaeological	Number of individuals	18	7	9	2	
	Number of individuals with manubrium porosity	8	3	5	0	
	Number of individuals without manubrium porosity	10	4	4	2	
	Mean midpoint age-at-death estimate (years)	29	32	27	28	
	Range of midpoint age-at-death estimates (years)	18-45	18-45	18-40	25-30	

3.0 Methods

3.1 Clinical metric data

CT images were evaluated in the Centricity Enterprise Viewer (v 3.0), and measurements were taken with the ruler tool. Window levelling was set to the automatic "Bone Window" settings (C570, W3077) for all individuals. On the coronal view, the sagittal axis was placed at the centre of the sternum, such that it passed through the most inferior portion of the jugular notch on the manubrium. After placement of this axis, the total length of the manubrium (from the most superior to most inferior point) was measured on the sagittal view. This measurement was divided by three to establish where the upper-third of the manubrium began, as recording of porosity on the archaeological manubria found that it tended to originate in the upper-third of the bone. At this point, the anterior cortical thickness, posterior cortical thickness, and trabecular space thickness were measured. A ratio of trabecular space thickness to total cortical thickness was calculated for the final manubrium ratio.

The same ratio measurement of trabecular space to cortical thickness was calculated for the sternal body. The length of the sternal body was measured on the sagittal view after placement of the sagittal axis. This measurement was divided in half, and the same procedure for measuring and then calculating the ratio of trabecular space thickness to total cortical thickness was used at this midway point (Figure 2-1). Sternal and manubrium measurements were taken at two different times, and an average was used for final ratio calculations. Technical error of measurement (TEM) was calculated for all measurements (Perini et al., 2005).

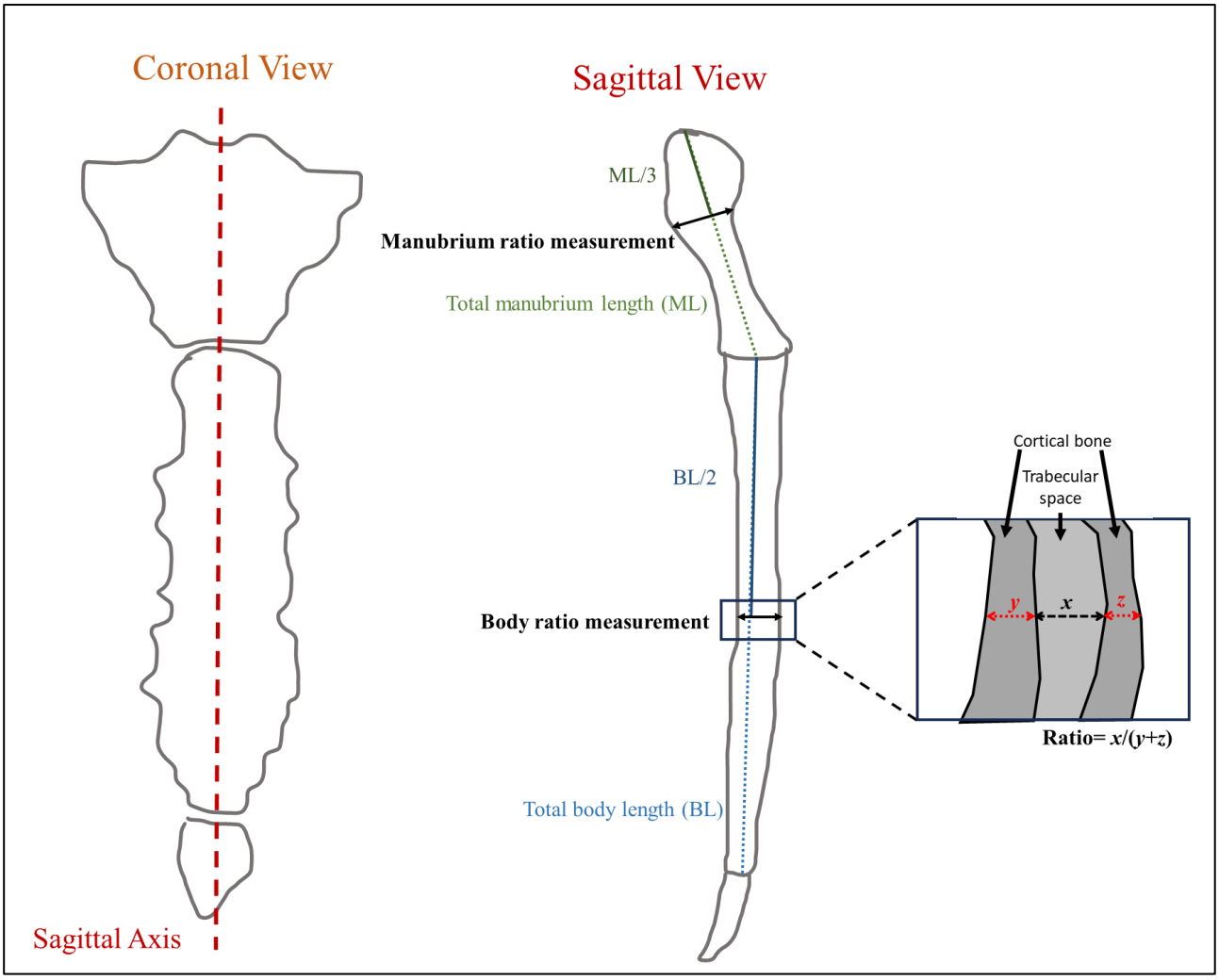

Figure 2-1: Diagram showing process of taking sternal body and manubrium measurements. Measurements for the final ratio calculation should be taken on the sagittal view at the bolded transverse lines corresponding to the bold text: **Manubrium ratio measurement** and **Body ratio measurement**.

3.2 Archaeological micro-CT analysis

Manubria underwent micro-CT imaging using a Nikon XTH-225ST micro-CT scanner at the Ancient Images Lab of the Museum of Ontario Archaeology. They were mounted within a Styrofoam cup and secured with green floral foam. Settings used were 115kV, 105µA, and 12.1 watts at a voxel size of 36.00 µm and panel gain of 18.0. A molybdenum target was used, and each scan used 3141 frames at a rate of 1 projection per second and took 53 minutes. The 3D volume was reconstructed in CT Pro 3D (v. 4.4.4) using an FDK-filtered back projection reconstruction algorithm. Dragonfly (v. 2021.3) was used to visualize and measure the manubria.

Micro-CT analysis allows for visualization of small-scale bone microarchitecture features, which was valuable for visually evaluating changes related to marrow hyperplasia in this study. However, due to the differences in resolution between the archaeological manubria's micro-CT imaging and the clinical sample's CT imaging, the initial ratios derived from the micro-CT analysis could not be directly compared to the CT-derived measurements. The micro-CT analysis allowed for more precise definition of the cortical bone borders, resulting in consistently larger ratios overall, as the total cortical thickness was smaller compared to the measured values from the CT images. To directly compare the ratios derived from the archaeological manubria to the clinical manubria, the resolution of the micro-CT reconstructions was downgraded to match the CT images (Figure 2-2). A set of adjusted measurements using the equivalent resolution to the clinical CT images were then taken, following the same protocol as above (Figure 2-1).

Figure 2-5: Original micro-CT resolution(a) versus adjusted resolution for comparison to CT images(b) for the same individual. Sagittal micro-CT (a) and CT (b) reconstructions.

3.3 Ratio analysis

The range of sternal and manubrium ratios was tested for normality using Shapiro-Wilk tests since they are appropriate for small sample sizes; both were normally distributed, so independent sample t-tests (two-tailed, $\alpha=0.05$) were used for further analysis. In the clinical sample, average ratios between the anemic and non-anemic groups and the overall manubrium and sternal body ratios were compared. Ratio values in males and females were also compared, and Pearson correlation tests were used to test the relationship between age and ratios. Minimum and maximum values were recorded to capture the range of variation.

In the archaeological sample, midpoint age estimates were used to assess if there was a difference in age between those with and without porosity. The adjusted ratios from the archaeological sample were compared to the anemic/non-anemic ratios from the clinical sample to determine if any individuals exceeded the clinical non-anemic values. A t-test (two-tailed,

α=0.05) was also used to assess whether there were significant differences in adjusted ratios between archaeological individuals with and without porosity. Statistical analysis was carried out using SPSS Statistics v29.0 and Microsoft Excel v16.0.

3.4 Visual microarchitecture analysis

To explore further skeletal manifestations of marrow hyperplasia, the original, high-resolution micro-CT reconstructions were used to assess if visually-observable microarchitecture changes correlated with the quantitative ratios. A scoring rubric for evaluating visual microstructure changes related to marrow hyperplasia (Table 2-3) was developed by reviewing literature that discussed the skeletal features associated with marrow hyperplasia.

The features associated with marrow hyperplasia were cortical thinning, trabecular thinning, and increased trabecular separation (Reynolds, 1962, 1965; Jaffe, 1972; Agarwal et al., 1970; Hoffbrand & Steensma, 2019). For the scoring rubric, these features were evaluated on a scale of 0-3, with scores of 3 representing the most significant expression of changes. Odds ratios were used to assess if individuals with ratios over the threshold identified from the clinical sample or individuals with posterior manubrium porosity were more likely to score higher. Odds ratios were calculated using logistic regression, with microarchitecture scores of over 2 as the dependant variable. Age and sex were also included as covariates. Odds ratios indicate the

Table 2-13: Full description of each score for the microstructure visual assessment of the manubrium. Scored across entire manubrium.

Cortical Thinning	
0-Absent	No cortical thinning is present.
1-Mild	Some patches of thinned cortex are present, but occur on less than 50% of the manubrium cortex.
2-Moderate	Mild cortical thinning is consistent across more than 50% of the manubrium, OR, marked cortical thinning (as seen in scores of 3) is present in less than 50% of the manubrium.
3- Significant	Marked cortical thinning is consistently present across more than 50% of the manubrium.
Increased Trabecular Separation	
0-Absent	No abnormally large trabecular spacing is present throughout the marrow space.
1-Mild	Abnormally large trabecular spacing is seen throughout less than 50% of the marrow space.
2-Moderate	Mildly abnormally large trabecular spacing is seen throughout more than 50% of the trabeculae in the marrow space OR marked abnormally large trabecular spaces (score of 3) are present throughout less than 50% of the marrow space.
3- Significant	Marked trabecular space enlargement is seen consistently throughout more than 50% of the marrow space.
Trabecular Thinning	
0-Absent	No trabecular thinning is present throughout the marrow space.
1-Mild	Trabecular thinning is seen throughout less than 50% of the trabeculae in the marrow space.
2-Moderate	Mild trabecular thinning is seen throughout more than 50% of the trabeculae in the marrow space OR marked trabecular thinning (score of 3) is present throughout less than 50% of the marrow space.
3- Significant	Marked trabecular thinning is seen consistently throughout more than 50% trabeculae in the marrow space.

likelihood of a particular outcome in the dependant variable given a set of independent variables; in this case, they represent the likelihood of scoring above a 2 in a microarchitecture category based on age, sex, and presence of a ratio over 3.6/presence of porosity. Significance was set at 0.05.

4.0 Results

4.1 Ratio comparisons

Table 2-4 reports the range of trabecular space to cortical thickness ratios for the clinical and archaeological cohorts, while Table 2-5 shows results of independent sample t-tests comparing average ratios between groups. TEM was found to be 0.596 mm. Average measurements are presented in Supplemental Table S2. When all clinical patients were grouped, a significant difference was also observed between the ratios measured in the manubrium compared to the sternal body; the sternal body tended to have a smaller ratio overall (range of 1.1-3.8) compared to the manubrium (range of 1.7-4.6). No significant differences were observed between males and females in the clinical sample, although the female ratios were smaller on average, particularly for the manubrium. In the sternal body, age was not found to be significantly associated with ratios (R=0.11, p-value=0.632). In the manubrium, there was a slightly stronger relationship between an elevated ratio and age, but it was also not significant (R=0.24. p-value= 0.387). In the clinical sample, there is a significant difference between the mean ratio for anemic versus non-anemic individuals in the manubrium and sternal body. In both cases, the ratio for anemic individuals is significantly higher, indicating wider trabecular space compared to cortical bone thickness.

Table 2-22: Range of measured cortical thickness to trabecular space thickness ratios for clinical and archaeological cohorts.

		Minimum Ratio	**Maximum Ratio**
Clinical Manubrium	*All (N=15)*	1.7	4.6
	Anemic (n=4)	3.6	4.6
	Non-Anemic (n=11)	1.7	3.6
Clinical Sternal Body	*All (N=22)*	1.1	3.8
	Anemic (n=6)	2.4	3.8
	Non-Anemic (n=16)	1.1	2.3
Archaeological Manubrium	*All (N=18)*	2.0	5.0
	Porotic (n=8)	2.4	5.0
	Non-Porotic (n=10)	2.0	4.5

Table 2-30: Average ratio of cortical thickness to trabecular space thickness for all cohorts, and results of t-tests comparing average ratios between various sample groups. Bold p-values are significant.

	Mean Ratio	Standard Deviation	p-value
All Clinical Manubrium (N=15)	3.2	0.86	**<0.001**
All Clinical Sternal Body (N=22)	2.1	0.69	
Clinical Female Manubrium (n=5)	2.3	1.5	0.165
Clinical Male Manubrium (n=10)	3.4	0.70	
Clinical Female Sternal Body (n=11)	1.9	0.78	0.308
Clinical Male Sternal Body (n=11)	2.2	0.59	
All Clinical Manubrium (N=15)	3.2	0.86	0.515
All Archaeological Manubrium (N=18)	3.4	0.83	
Anemic Clinical Manubrium (n=4)	4.1	0.43	**0.008**
Non-Anemic Clinical Manubrium (n=11)	2.8	0.74	
Anemic Clinical Sternal Body (n=6)	2.9	0.66	**<0.001**
Non-Anemic Clinical Sternal Body (n=16)	1.8	0.38	
Porotic Archaeological Manubrium (n=8)	3.7	0.88	0.260
Non- Porotic Archaeological Manubrium (n=10)	3.2	0.76	

No significant differences were found between the adjusted ratios measured from the archaeological and clinical manubria. These results suggest that the adjusted archaeological ratios and clinical ratios are viable comparisons. Within the archaeological sample, the average age-at-death of those with posterior manubrium porosity was 27 years and 30 years for those without, but this difference was not significant (p-value=0.361). No significant ratio difference was found between individuals with and without porosity on the posterior manubrium.

4.2 Assessment of marrow hyperplasia ratio measures

In the clinical sample, the minimum manubrium ratio for anemic patients was 3.6, which is equal to the maximum manubrium ratio for non-anemic patients (Figure 2-3). In the sternal body, the minimum ratio for anemic patients was 2.4, while the maximum for non-anemic individuals was 2.3. As non-anemic patients did not exceed 2.3 or 3.6 in their sternal body or manubrium ratios respectively, these values were then used as an approximate threshold value to differentiate between individuals with/without changes related to marrow hyperplasia in the archaeological manubria. The ratios are conservative estimates due to the challenges in accounting for all aspects of patient anemia history (see Section 5.1). In the archaeological sample, 38.9% (7/18) of individuals displayed ratios greater than 3.6. The mean ratio of those with ratios greater than 3.6 was 4.2 (standard deviation=0.46), and was 2.8 (standard deviation=0.48) for those with ratios less than 3.6.

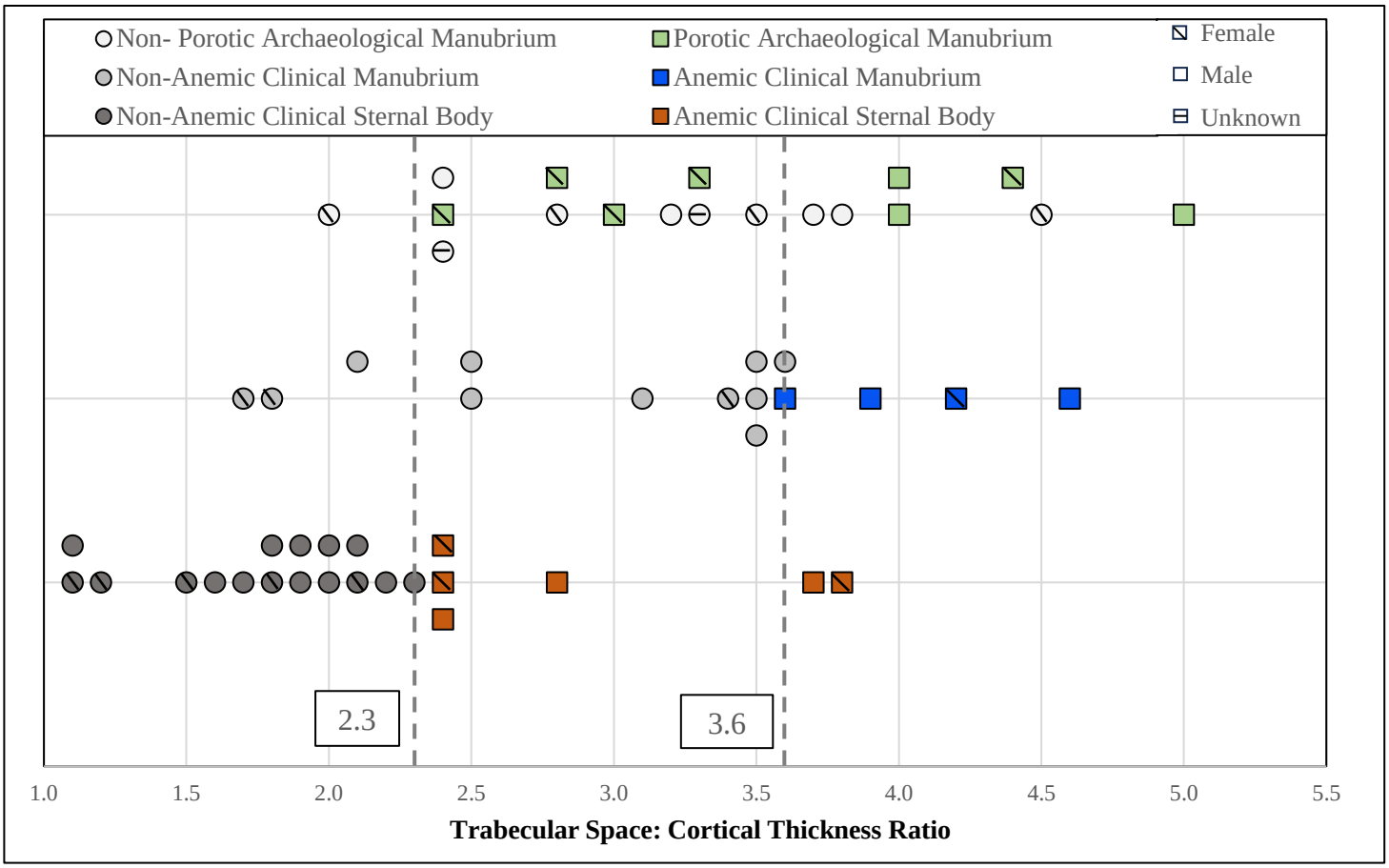

Figure 2-11: All measured ratios in this study. The proposed values used to differentiate between individuals with/without skeletal manifestations of marrow hyperplasia in the manubrium (3.6) and sternal body (2.3) are indicated by the vertical dashed lines.

4.3 Visual microarchitecture assessment

The archaeological individuals who were identified as having ratios >3.6 in the manubrium displayed higher scores when assessed visually using the rubric (Supplemental Table 2-S3). Individuals with a ratio of over 3.6 were nearly 20 times more likely to score over 2 in the trabecular separation category; this was the only significant relationship between microstructure scoring and elevated ratios (Table 2-6). Only 14.3% (1/7) of individuals with a ratio over 3.6 did not score 2 or a 3 for increased trabecular separation, while 72.7% (8/11) of individuals with a ratio under 3.6 did not score a 2 or 3. All (7/7) of the individuals with ratios >3.6 showed some evidence of cortical thinning (scores of 1-3), while only 27.3% (3/11) of individuals with ratios under the threshold scored above 0. All individuals (7/7) with ratios >3.6 showed some evidence of trabecular thinning (scores of 1-3), but 72.7% (8/11) of the individuals with ratios <3.6 also scored above 0.

During the visual scoring, sparse trabeculae and thinned cortical bone were identified in individuals with and without posterior porosity (Figure 2-4, Supplemental Data Table 2-S3). Odds ratios indicate that individuals with porosity were not significantly more likely to score over 2 for increased trabecular separation or cortical thinning categories. Those with porosity

were 33 times more likely to score above 2 for trabecular thinning; this is approaching significance. For increased trabecular separation scoring, 40% (4/10) of individuals without porosity and 63% (5/8) of individuals with porosity scored either 2 or 3. For cortical thinning, 20% (2/10) of those without porosity scored 2 or 3, which was a similar result for those with porosity (25%, 2/8). For trabecular thinning, 20% (2/10) of those without porosity scored a 2 or 3 compared to 63% (5/8) of those with porosity. Logistic regression models are presented in Supplemental Data Table 2-S4.

Table 2-38: Odds ratios showing the association between the presence of a pathological manubrium ratio (>3.6) or posterior porosity and microstructure changes scoring. Bold ratios are significant.

		Odds Ratio	***Confidence Interval***	***P-Value***
Ratio Indicative of Marrow Hyperplasia	*Increased Trabecular Separation (scores of 2-3)*	**19.62**	1.21-317.20	**0.036**
Ratio Indicative of Marrow Hyperplasia	*Trabecular Thinning (scores of 2-3)*	3.25	0.40-26.32	0.270
Ratio Indicative of Marrow Hyperplasia	*Cortical Thinning (scores of 2-3)*	1.9E+009	0- +Infinite	0.998
Posterior Porosity	*Increased Trabecular Separation (scores of 2-3)*	3.76	0.42-34.01	0.238
Posterior Porosity	*Trabecular Thinning (scores of 2-3)*	33.01	0.88-1235.2	0.058
Posterior Porosity	*Cortical Thinning (scores of 2-3)*	1.45	0.09-22.87	0.791

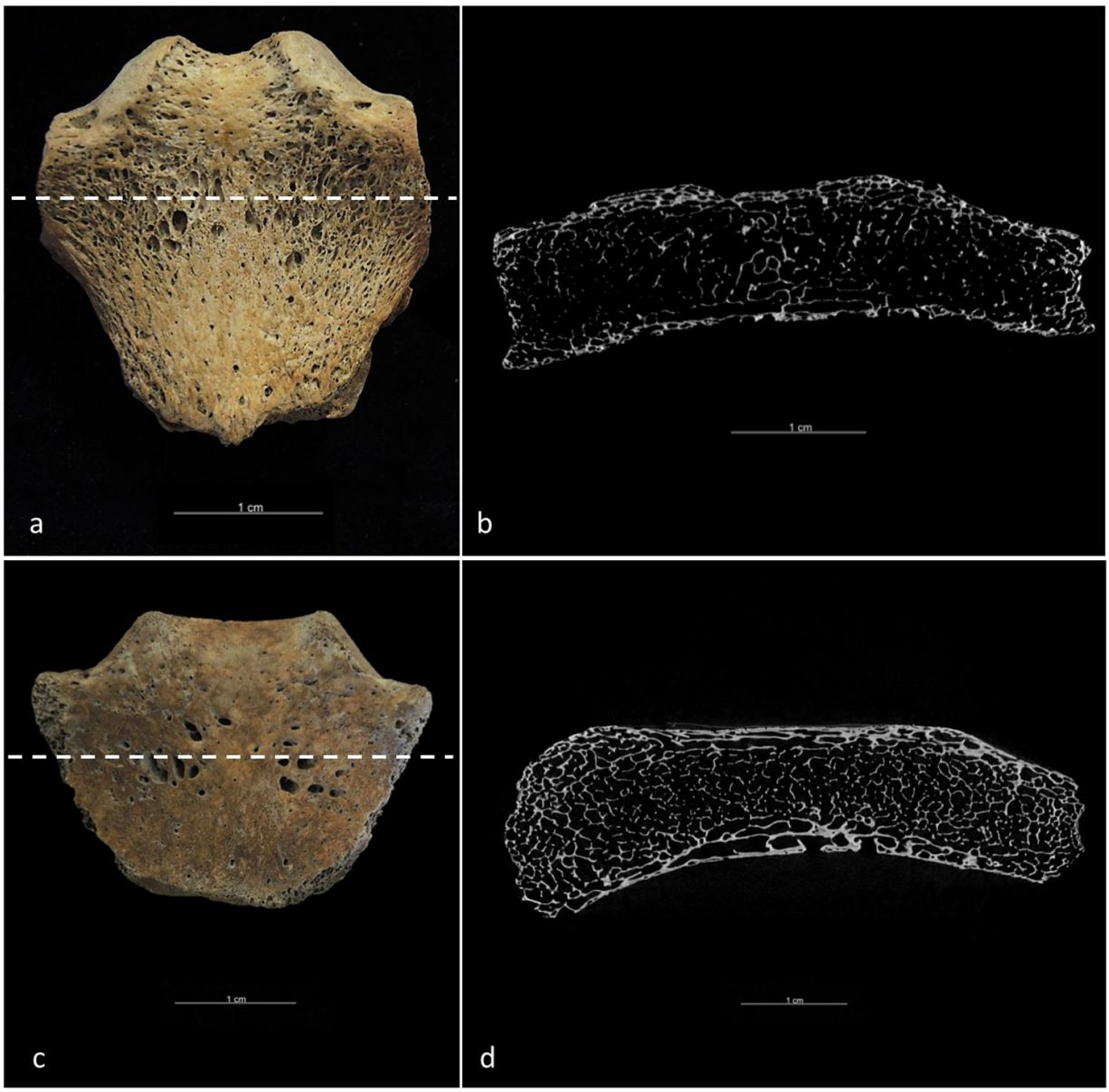

Figure 2-12: Comparison of two macroscopic archaeological manubria and micro-CT reconstruction of the same bone. The dashed lines in a) and c) indicate the approximate location of the micro-CT slice in b) and d). In the micro-CT images, anterior is towards the top of the image, while posterior is towards the bottom. a) Posterior view of manubrium with porosity present. b) Axial micro-CT reconstruction of the manubrium displaying sparse trabecular structure and cortical thinning. c) Posterior view of manubrium with porosity present. d) Axial micro-CT reconstruction of a manubrium with no visual evidence of changes related to marrow hyperplasia. The trabeculae and cortical bone are thicker, and there is little visible widening of intertrabecular spacing.

5.0 Discussion

5.1 Use of sternal metric data for evaluation of anemia

This study adds to the existing literature demonstrating that there are metric differences in cortical thickness and trabecular space that can develop in individuals with anemia. Previous methods of quantifying skeletal changes associated with anemia have focused on the cranium (e.g. Panzer et al., 2023; Stuart-Macadam, 1987), and this study shows the feasibility of further metric studies of marrow hyperplasia across the skeleton.

The quantitative study by Reynolds (1962) illustrates some of the difficulties of utilizing a clinical population to research anemia and bone; many included individuals were adults and were assessed for cranial changes, which would have been initiated during childhood. Although details on the control population are limited, they are described as being "comparable" (Reynolds, 1965: 72), and if they were also adults, it would be important to establish that they did not experience any form of anemia as children, not just at the time they underwent imaging. As anemia is a condition that can present non-specific symptoms that may not cause someone to seek immediate treatment (Maakaron, 2021), it is possible for individuals to experience anemia for longer than initially documented in their patient records or to be affected by it without ever undergoing a blood test that would confirm this in their clinical history. Reynolds (1962) also measured individuals with sickle-cell anemia to establish a cranial ratio threshold of 2.3, which may have resulted in more elevated ratios. These limitations mean that the proposed threshold ratio that differentiates anemic and non-anemic individuals in the research by Reynolds (1962, 1965) and later by Sebes & Digges (1979) are conservative values compared to those from a sample in which all aspects of patient history were known.

The estimates proposed in this study are similarly conservative. Although care was taken to select a non-anemic sample with no specific anemia diagnoses in the three years prior to their CT imaging, it is still possible that some of these individuals could have been anemic at some point and were never tested. As measurements were obtained from a modern sample, they may also be specific to modern populations, and should be interpreted conservatively in archaeological contexts. In their study of frontal ratio measurements in Egyptian mummies, Panzer and colleagues (2023) also highlight the issue of comparing ratios across contexts. They state that their identification of ratios over threshold values are also conservative estimates due to size differences between the archaeological mummies and the 20th-century samples from which the comparison ratios were derived. The above limitations mean that ratios for the manubrium and sternal body found in this research (>2.3 and 3.6, respectively) provide a starting point, not a definitive cutoff, for differentiating between individuals with and without skeletal manifestations of marrow hyperplasia in archaeological contexts. The sample size was small overall, and one non-anemic individual did have a manubrium ratio of 3.6. Although this value was exceeded only in anemic patients, this demonstrates that there is variation in ratio values, and that other factors beyond anemia may also affect measurements.

Despite limitations, quantitative measurements have the added benefit of being highly reproducible and are less prone to individual interpretation compared to visual analysis (Anderson et al., 2021), which is more typically used for anemia diagnosis in skeletal remains.

Although the results of the visual analysis scoring in this study were generally good, the wide odds ratio confidence intervals and the few individuals whose visual microstructure scores did not correlate as expected to their ratio result suggest that visual scoring alone should not be given as much diagnostic weight as the quantitative assessment. The ratio values proposed in this study are measurable diagnostic parameters that can be directly tied to known cases of anemia and should, therefore, be valued more strongly when assigning diagnostic certainty. However, it is also important to be considerate of imaging source and quality when comparing metric data; as evidenced in this study, the original micro-CT analysis and resolution resulted in measured ratios that could not be compared to the known clinical data without manipulation of the images. Micro-CT can offer greater precision in measurements and allows for visualization of microarchitecture (Saers et al., 2021), but clinical imaging is typically done using CT-analysis, which can complicate comparisons.

Considering contextual information and whole-skeleton pathology will be necessary for ruling out other possible causes of skeletal changes (Klaus, 2017; Mays, 2020), even when using metric methods of anemia diagnosis. Other variables that can affect ratios or bone microarchitecture should be evaluated as part of assigning individuals to categories of diagnostic certainty (Brickley & Morgan, 2023). In this study, no significant associations were found between age and sex and ratio measurements in the clinical sample, but average ratios were smaller for females, and it is possible that different ratio thresholds may need to be considered for males and females. As discussed by Brickley (2024), factors that affect bone quantity should also be considered when interpreting metric data, including taphonomy, environmentally-dependant activity levels, and diet/nutrition (Van Spelde et al., 2021; Cowgill et al., 2023; Swan et al., 2023).

Pathology is also an important variable to consider; for example, age-related bone loss and osteoporosis could skew cortical thickness measurements or evaluation of trabecular separation, meaning that multivariate statistical approaches will be required to allow the effects of age-related bone changes to be considered (Brickley, 2024). Neoplastic conditions can lead to marrow hyperplasia (Chan et al., 2016), and were not used as part of the exclusion criteria in this study, but should be considered as part of differential diagnosis in archaeological contexts. Infectious disease, trauma, and metabolic bone diseases can also cause changes in the marrow space (Chan et al., 2016), and would also need to be incorporated into differential diagnosis when evaluating changes related to marrow erythroid hyperplasia that could be potentially linked to anemia.

5.2 Posterior manubrium porosity

One hypothesis investigated in this study was whether posterior manubrium porosity was associated with anemia and could result from marrow hyperplasia. Porous lesions are commonly used for anemia diagnosis in skeletal remains, and investigating whether such lesions in the manubrium could be associated with anemia was an objective of this study. Although the average ratio in individuals with porosity was higher, no significant difference in ratios was found between those with and without porosity (Table 2-5). Only trabecular thinning approached significance when evaluating odds ratios, meaning that those with porosity were not more likely

to show other common signs of marrow hyperplasia, such as cortical thinning and increased trabecular spacing, and that the link between posterior porosity and marrow hyperplasia is not straightforward. Due to the resolution of the clinical CT images and the diameter/depth of manubrium porosity, visualization of porosity in the clinical sample could not be achieved confidently; porosity initially identifiable in the original micro-CT analysis often disappeared in the downgraded reconstructions. Similarly, CT quality has also been recognized as a limitation in identifying orbital porosity on CT images (Anderson et al., 2021; Panzer et al., 2023).

Other possible hypotheses for posterior manubrium porosity that have been proposed include lytic lesions related to tuberculosis (Sanchez, 2014; Khudaverdyan & Hobossyan, 2017), vascularization (Tayles & Buckley, 2004), neoplastic conditions (Mann & Tuamsuk, 2005), aortal aneurysm (Kelley, 1979) and growth/development (Sanchez, 2014). The relationship between posterior manubrium porosity and lytic lesions caused by tuberculosis was investigated using archaeological collections by Sanchez (2014), and no significant association between porosity and disease was found. Both Tayles & Buckley (2004) and Sanchez (2014) note that the general anatomy/development of the manubrium could also affect development of porosity; blood vessels enter the manubrium through the posterior surface, which could result in porosity, and its ossification centers during growth/development are typically located close to where porosity develops (see O'Neal et al., 1998: Figure 1), meaning that porosity could be an artifact of the ossification process. In the current study, no significant difference in age was found between those with and without porosity, but Sanchez (2014) noted that it was most common in adolescents, which could indicate a relationship between sternal porosity and growth and development.

Cortical thinning due to marrow hyperplasia may exacerbate pre-existing vascular foramina/growth-related porosity, but this would need to be evaluated on a case-by-case basis. For example, in Figure 2-4a-b, which displays cortical thinning and increased trabecular separation, thinning and trabecularization of the cortical bone may have resulted in new porosity and enhanced pre-existing pores. In contrast, Figure 2-4c-d displays macroscopically-different porosity that is not accompanied by microarchitecture changes, and is unlikely to be related to marrow hyperplasia. Carefully evaluating the appearance and skeletal manifestation of manubrium porosity will be necessary for suggesting possible etiologies. As with porous orbital lesions, which can be caused by processes other than marrow hyperplasia, the development and overall appearance of posterior manubrium porosity is likely affected by a wide variety of contributing factors, and evaluating internal features is an effective way of identifying changes related to marrow hyperplasia.

5.3 Future directions

The current study demonstrates the utility of using available clinical data to investigate skeletal features suggestive of anemia. In this way, it is similar to many of the original studies on skeletal manifestations of anemia, from which original criteria for diagnosing anemia in archaeological remains was developed (e.g. Angel, 1966). Future research that builds on this paper and seeks to identify other skeletal manifestations of anemia, or clarify which factors affect these skeletal changes will necessitate interdisciplinary research with clinical

collaborators. The challenges of working with anemia specifically will mean that future clinical sample cohorts should include detailed, longitudinal imaging and medical history data acquired over the course of an individual's lifetime as part of the study design.

Skeletal manifestations of marrow hyperplasia are highly dependant on age, and further investigation of the relationship between age and development of skeletal changes will help to establish when changes were initiated. In the current study, expanded ratios were seen in individuals aged 22-45 years; however, none of the individuals were under 18 years old, meaning it is impossible to establish a minimum age based on this data. There is also likely to be a maximum age at which sternal skeletal changes will develop. The capacity for marrow to reconvert from yellow to red to correct anemia-related deficiency is a further complication to establishing a maximum age for skeletal changes during anemia; there may be instances where marrow reconverts and/or expands, particularly at older ages when more mixed marrow is present (Blebea et al., 2007; Brickley, 2018).

The effects of bone remodelling and development on lesion appearance should also be investigated to establish a timeline for sternal skeletal changes during anemia. The sternum can have high bone resorption and remodelling rates, as it is constantly engaged in respiration (Klein et al., 1990). Therefore, skeletal manifestations of marrow hyperplasia in an adult sternum may represent episodes of anemia that have occurred closer to the current age of the individual, instead of those that have persisted from a childhood episode. Other areas of the skeleton that have the potential to be used for establishing episodes of anemia initiated in adulthood could include the vertebrae and iliac crest, as both areas maintain active marrow into adulthood (Burkhardt et al., 1987). Understanding how long changes persist in different bones will be important for estimating the age an archaeological individual experienced anemia.

6.0 Conclusion

Anemia diagnosis in archaeological skeletal remains is complex, and continued exploration of cranial and postcranial manifestations of the condition is still necessary. The current study demonstrated the difficulties of associating skeletal porosity with other skeletal evidence of marrow hyperplasia, which further emphasizes the need to consider evidence outside of porotic lesions when assessing anemia in the skeleton. Using metric data, this research demonstrates a novel approach of assessing anemia in the skeleton and the feasibility of using quantitative methods to evaluate anemia in archeological human remains. Although the sample size is small, it shows significant differences reflective of marrow hyperplasia in the measured ratios of trabecular space to cortical thickness in individuals diagnosed with anemia in modern clinical settings. Individuals without anemia did not display ratios of over 3.6 in the manubrium, or over 2.3 in the sternal body. This principle can be used to build future studies with larger sample sizes to establish more definitive parameters for ratio measurements and improve diagnostic methods for evaluating anemia in archaeological remains.

Acknowledgements
Thank you to Ville de Montréal (François Bélanger) for providing access and information for the Saint-Antoine and Pointe-aux-Trembles collections. Additional thanks to Conseil de la Fabrique de Sainte-Marie-de-Beauce for access to the Sainte-Marie collection. Thanks also to Kayla Lucier and Maryam Akbari-Moghaddam for assistance with TRUST data collection and access, to Dr. Andrew Nelson for facilitating micro-CT imaging, Dr. Heather Hatch at the Museum of Ontario Archaeology for access to micro-CT facilities, and to Dr. Jay Stock for suggestions on comparing micro-CT vs. CT imaging. This research was supported by a Social Science and Humanities Research Council (SSHRC) Joseph-Armand Bombardier Canada Graduate Scholarship (award number 767-2020-1835), the McMaster University Shelley Saunders/Koloshuk Family Scholarship, a SSHRC Insight Grant (File Number: 435-2021-0665), the Canadian Association for Biological Anthropology Shelley R. Saunders Thesis Research Grant, and undertaken, in part, thanks to funding from the Canada Research Chairs program. MZ is supported by an Internal Mid Career Award, Department of Medicine, McMaster University. Michael G. DeGroote Centre for Transfusion Research receives part infrastructure funding from Canadian Blood Services and Health Canada.

Supplemental Data

Table 2-S1: Exact clinical sample selection criteria, used for data search and extraction.

Criteria	Anemic Sample	Non-Anemic Control Sample
Age (years)	Over 18, under 45	Over 18, under 45
Date of CT - Imaging	January 1st, 2010-December 31st, 2017.	January 1st, 2010-December 31st, 2017.
Hemoglobin Level (g/L)	Either: <90, or 90-110	>130
CT Available (Specific Codes)	At least one of: CT CHE W/CONT ABD W/WOUT CONT CT CHE/PEL W/CONT ABD W/WO CT CHEST CT CHEST + ABD W/WOUT CONTRAST CT CHEST AND ABD CT CHEST AND ABD W/CONTRAST CT CHEST W/WO CONTRAST W/3D CT CHEST W/WOUT CONTRAST CT CHEST WITH CONTRAST CT CHEST/ABD/PEL W/CONTRAST CT CHEST/ABD/PEL W/WOUT CONT CT CHEST/ABD/PELVIS CT ABD + PELVIS W/WO CONT W/3D CT ABD AND PELVIS CT ABD AND PELVIS W/CONTRAST CT ABD AND PELVIS W/WOUT CONT CT ABD W/WITHOUT AND PEL WCONT CT ABDOMEN CT ABDOMEN W/WOUT CONTRAST CT ABDOMEN WITH CONTRAST CT EXTREMITY + ABD/PEL W/CONT	At least one of: CT CHE W/CONT ABD W/WOUT CONT CT CHE/PEL W/CONT ABD W/WO CT CHEST CT CHEST + ABD W/WOUT CONTRAST CT CHEST AND ABD CT CHEST AND ABD W/CONTRAST CT CHEST W/WO CONTRAST W/3D CT CHEST W/WOUT CONTRAST CT CHEST WITH CONTRAST CT CHEST/ABD/PEL W/CONTRAST CT CHEST/ABD/PEL W/WOUT CONT CT CHEST/ABD/PELVIS CT ABD + PELVIS W/WO CONT W/3D CT ABD AND PELVIS CT ABD AND PELVIS W/CONTRAST CT ABD AND PELVIS W/WOUT CONT CT ABD W/WITHOUT AND PEL WCONT CT ABDOMEN CT ABDOMEN W/WOUT CONTRAST CT ABDOMEN WITH CONTRAST CT EXTREMITY + ABD/PEL W/CONT
ICD-10 Code Criteria	Include: • D50.0-D53 (Nutritional anemias) • Or D64.9 (Anemia, unspecified) Must Exclude: • D55.0-D59.9 (Hemolytic anemias) • M80.0/M81.0 (Osteoporosis with/without current pathological fractures)	Must Exclude: • D50.0-D69.9 (Nutritional anemias; Hemolytic anemias; Anemia, unspecified) • M80.0/M81.0 (Osteoporosis with/without current pathological fractures)

CHE: Chest
ABD: Abdomen
PEL: Pelvis
W/3D: With 3D
W/CONT or W/: With contrast
WOUT CONT or WO CONT: Without contrast

Table 2-S2: Raw data of metric and demographic information from archaeological and clinical individuals included in this study.

Individual ID	Age (years)*	Sex	Known Anemia Diagnosis	*Manubrium*					*Sternal Body*			
				Porosity (P/A)	PCT (mm)	ACT (mm)	TbSpT (mm)	TbSpT:CT Ratio	PCT (mm)	ACT (mm)	TbSpT (mm)	TbSpT:CT Ratio
PaT-7A2S2	25	F	----	A	0.8	0.7	6.7	4.5	----	----	----	----
PaT-7A9S38	18	F	----	A	1.1	1.2	8.11	3.5	----	----	----	----
SA-21SS4	27.5	F	----	A	1	1.7	5.5	2.0	----	----	----	----
SA-23CS11	30	U	----	A	1.2	2.4	8.6	2.4	----	----	----	----
SA-24ES12	25	U	----	A	1.2	1.3	8.2	3.3	----	----	----	----
SA-25CS18	40	F	----	A	1.7	1.1	7.9	2.8	----	----	----	----
SM-2B7	25	M	----	A	2	1.3	8	2.4	----	----	----	----
SM-2B8	30	M	----	A	1.4	1.3	10	3.7	----	----	----	----
PaT-7A2S7	45	M	----	A	1.4	1.1	9.4	3.8	----	----	----	----
SA-11FS1	37.5	M	----	A	1.4	1.4	8.9	3.2	----	----	----	----
PaT-7A9S27	37.5	F	----	P	0.8	1	8	4.4	----	----	----	----
SA-17ZS1	18	M	----	P	1.2	1.1	11.6	5.0	----	----	----	----
SA-20FS35	25	F	----	P	1.4	1.1	8.3	3.3	----	----	----	----
SM-2B14	25	F	----	P	1.5	1.2	8.2	3.0	----	----	----	----
SM-2B15	36	M	----	P	1.3	1.3	10.3	4.0	----	----	----	----
PaT-7A2S5	30	M	----	P	1.4	1.2	10.5	4.0	----	----	----	----
SA-23BS2	25	F	----	P	1.1	1.7	7.9	2.8	----	----	----	----
SA-11AS2	18	F	----	P	1.2	1.8	7.1	2.4	----	----	----	----
Clinical-1	38	F	Non-anemic	----	2.1	2.5	8.2	1.8	2.0	2.3	4.6	1.1
Clinical-2	40	F	Non-anemic	----	1.5	1.5	9.9	3.4	1.9	1.9	5.7	1.5
Clinical-3	37	M	Non-anemic	----	2.0	1.6	11.0	3.1	2.1	2.1	8.8	2.1
Clinical-4	25	M	Anemic	----	----	----	----	----	1.4	1.5	7.8	2.8
Clinical-5	22	F	Anemic	----	----	----	----	----	1.6	1.4	7.1	2.4
Clinical-6	42	F	Anemic	----	----	----	----	----	1.3	1.3	6.0	2.4
Clinical-7	40	F	Non-anemic	----	2.3	1.8	10.1	2.5	2.3	2.0	7.9	1.8
Clinical-8	25	F	Non-anemic	----	----	----	----	----	2.1	2.2	9.2	2.1
Clinical-9	35	F	Non-anemic	----	----	----	----	----	2.3	2.2	5.0	1.1
Clinical-10	22	M	Non-anemic	----	1.6	1.7	11.8	3.6	1.4	1.9	7.5	2.3
Clinical-11	26	M	Non-anemic	----	2.2	3.5	14.3	2.5	2.5	2.1	7.4	1.6
Clinical-12	26	F	Non-anemic	----	2.4	1.8	7.0	1.7	2.2	1.8	4.6	1.2
Clinical-13	36	M	Non-anemic	----	2.1	3.2	10.9	2.1	1.9	1.5	6.4	1.9
Clinical-14	33	F	Anemic	----	1.4	1.5	11.8	4.2	1.3	1.2	9.2	3.8
Clinical-15	39	M	Non-anemic	----	1.6	1.8	11.6	3.5	1.5	1.8	7.5	2.3
Clinical-16	39	M	Anemic	----	1.4	1.6	10.9	3.6	1.4	1.4	6.7	2.4
Clinical-17	42	M	Anemic	----	1.6	1.4	11.6	3.9	----	----	----	----
Clinical-18	28	F	Non-anemic	----	----	----	----	----	1.5	1.8	5.9	1.8
Clinical-19	45	M	Anemic	----	1.3	1.8	14.4	4.6	1.2	1.1	8.5	3.7
Clinical-20	23	M	Non-anemic	----	1.7	1.5	11.1	3.5	1.9	2.2	8.3	2.0
Clinical-21	38	F	Non-anemic	----	----	----	----	----	1.1	1.4	5.0	2.0
Clinical-22	35	M	Non-anemic	----	----	----	----	----	2.2	1.7	7.3	1.9
Clinical-23	32	M	Non-anemic	----	2.0	2.2	14.5	3.5	1.8	1.9	8.0	2.2

PaT= Pointe-aux-Trembles
SA=Saint-Antoine
SM=Sainte-Marie-de-Beauce
P=Present A=Absent
*For archaeological individuals, age is reported as the midpoint age estimate. For clinical cohort, age is at time of imaging.
PCT=Posterior cortical thickness
ACT=Anterior cortical thickness
CT=Total cortical thickness (anterior + posterior cortical thickness)
TbSpT= Trabecular space thickness

Table 2-S3: Visual microstructure scoring for all archaeological individuals. Scores of 3 represent the most significant expression of each trait, and 0 represents no change.

	Individual ID	Increased Trabecular Separation Score	Trabecular Thinning Score	Cortical Thinning Score	Posterior Porosity
Individuals with a ratio indicative of marrow hyperplasia	PaT-7A2S2	2	1	2	A
	PaT-7A9S27	3	3	2	P
	SA-17ZS1	2	2	1	P
	SM-2B8	2	1	1	A
	SM-2B15	0	1	1	P
	PaT-7A2S5	2	2	1	P
	PaT-7A2S7	3	3	2	A
Individuals without a ratio indicative of marrow hyperplasia	PaT-7A9S38	0	0	0	A
	SA-11FS1	1	1	0	A
	SA-20FS35	1	1	1	P
	SA-21SS4	0	0	0	A
	SA-23CS11*	3	2	0	A
	SA-24ES12	1	1	0	A
	SA-25CS18	1	1	0	A
	SM-2B7	1	1	1	A
	SA-23BS2*	3	2	0	P
	SA-11AS2	1	0	0	P
	SM-2B14	2	2	2	P

PaT= Pointe-aux-Trembles
SA=Saint-Antoine
SM=Sainte-Marie-de-Beauce
P=Present A=Absent
* Although these individuals display increased trabecular separation, they also have some evidence of taphonomy affecting internal structures (i.e. dirt on the inside of the manubrium), and the destruction of trabeculae is thought to be related to this process. They have no evidence of cortical thinning, suggesting that their ratio measurements were unaffected by taphonomy.

Table 2-S4: Output of logistic regression models.

Dependant Variable	Predictors	Coefficient	SE	Odds Ratio	p-value	Lower 95% CI	Upper 95% CI
Increased Trabecular Separation (scores of 2-3)	Constant	-0.05	2.34	0.95	0.982		
	Ratio Indicative of Marrow Hyperplasia	2.98	1.42	19.62	0.036	1.21	317.20
	Age	-0.04	0.09	0.96	0.669	0.81	1.14
	Sex	0.11	0.82	1.12	0.890	0.22	5.59
Trabecular Thinning (scores of 2-3)	Constant	-1.48	2.04	0.23	0.469		
	Ratio Indicative of Marrow Hyperplasia	1.18	1.07	3.25	0.270	0.40	26.32
	Age	0.01	0.07	1.01	0.716	0.88	1.16
	Sex	0.28	0.75	1.32	0.716	.30	5.78
Cortical Thinning (scores of 2-3)	Constant	-5.39	3.48	0.00	0.121		
	Ratio Indicative of Marrow Hyperplasia	21.37	8145.65	1.9E+009	0.998	0.00	Infinity
	Age	0.13	0.11	1.14	0.240	0.92	1.42
	Sex	-21.86	8145.65	3.22E-010	0.998	0.00	Infinity
Increased Trabecular Separation (scores of 2-3)	Constant	-2.11	0.84	0.12	0.359		
	Prescence of Posterior Porosity	1.33	1.12	3.76	0.238	0.42	34.01
	Age	0.04	0.07	1.04	0.538	0.91	1.19
	Sex	0.50	0.78	`.64	0.522	0.36	7.54
Trabecular Thinning (scores of 2-3)	Constant	-6.12	3.70	0.00	0.098		
	Prescence of Posterior Porosity	3.50	1.85	33.01	0.058	0.88	1235.20
	Age	0.10	0.09	1.11	0.250	0.93	1.32
	Sex	1.39	1.10	4.02	0.207	0.46	34.94
Cortical Thinning (scores of 2-3)	Constant	-5.13	1.61	0.12	0.181	0.00	2.72
	Prescence of Posterior Porosity	0.37	1.41	1.45	0.791	0.09	22.87
	Age	0.15	0.10	1.17	0.126	0.96	1.42
	Sex	-2.16	1.61	0.12	0.181	0.00	2.72

References

Agarwal, K. N., Drar, N., Shah, M. M., & Bhardwaj, O. P. (1970). Roentgenologic changes in iron deficiency anemia. *American Journal of Roentgenology, 110*(3), 635-637.

Anderson, A. S., Sutherland, M. L., O'Donnell, L., Hill, E. C., Hunt, D. R., Blackwell, A. D., & Gurven, M. D. (2021). Do computed tomography findings agree with traditional osteological examination? The case of porous cranial lesions. *International Journal of Paleopathology*, *33*, 209-219.

Angel, J. L. (1966). Porotic hyperostosis, anemias, malarias, and marshes in the prehistoric eastern Mediterranean. *Science, 153*(3737), 760-763.

Berger, A. J., & Kahn, D. (2012). Growth and development of the orbit. *Oral and Maxillofacial Surgery Clinics*, *24*(4), 545-555.

Blebea, J. S., Houseni, M., Torigian, D. A., Fan, C., Mavi, A., Zhuge, Y., ... & Alavi, A. (2007). Structural and functional imaging of normal bone marrow and evaluation of its age-related changes. *Seminars in Nuclear Medicine, 37*(3), 185-194.

Brickley, M. B. (2018). Cribra orbitalia and porotic hyperostosis: A biological approach to diagnosis. *American Journal of Physical Anthropology*, 167(4), 896-902.

Brickley, M. B. (2024). Perspectives on anemia: Factors confounding understanding of past occurrence. *International Journal of Paleopathology*.

Brickley, M. B., & Morgan, B. (2022). Metabolic and endocrine diseases. In *The Routledge Handbook of Paleopathology* (pp. 338-359). Routledge.

Brickley, M. B., & Morgan, B. (2023). Assessing diagnostic certainty for scurvy and rickets in human skeletal remains. *American Journal of Biological Anthropology*, *181*(4), 637-645.

Brickley, M. B., Ives, R., & Mays, S. (2020). *The bioarchaeology of metabolic bone disease*. Academic Press.

Brooks, S., & Suchey, J. M. (1990). Skeletal age determination based on the os pubis: a comparison of the Acsádi-Nemeskéri and Suchey-Brooks methods. *Human Evolution*, *5*, 227-238.

Buikstra, J. E., & Ubelaker, D. H. (1994). Standards for data collection from human skeletal remains. Arkansas Archaeological Survey Research Series No. 44. *Fayetteville: Arkansas Archaeological Survey*.

Burkhardt, R., Kettner, G., Böhm, W., Schmidmeier, M., Schlag, R., Frisch, B., ... & Gilg, T. H. (1987). Changes in trabecular bone, hematopoiesis and bone marrow vessels in aplastic anemia, primary osteoporosis, and old age: a comparative histomorphometric study. *Bone*, *8*(3), 157-164.

Clynes, M. A., Harvey, N. C., Curtis, E. M., Fuggle, N. R., Dennison, E. M., & Cooper, C. (2020). The epidemiology of osteoporosis. *British Medical Bulletin, 133*(1), 105-117.

Cowgill, L., Harrington, L., MacKinnon, M., & Kurki, H. K. (2023). Gains in relative cortical area during growth and their relationship to nutrition, body size, and physical activity. *American Journal of Biological Anthropology, 182*(2), 177-193.

Cristy, M. (1981). Active bone marrow distribution as a function of age in humans. *Physics in Medicine & Biology, 26*(3), 389.

El-Najjar, M. Y., Ryan, D. J., Turner, C. G., & Lozoff, B. (1976). The etiology of porotic hyperostosis among the prehistoric and historic Anasazi Indians of southwestern United States. *American Journal of Physical Anthropology, 44*(3), 477-487.

Ethnoscop. (2006). Site du premier cimetière de Sainte-Marie, CcEs-1. Inventaire et fouilles archéologiques 2003-2004. Internal archaeological report. Ministère des transports du Québec, Direction de Chaudière-Appalaches.

Ethnoscop. (2016a). Projet de réaménagement de la place du Canada. Site archéologique du cimetière Saint-Antoine (1799–1854), BiFj-37, Montréal. Fouille et supervision archéologique (2014). Internal archaeological report. Ville de Montréal.

Ethnoscop. (2016b). Interventions archéologiques dans le cadre du projet de construction de la Maison du citoyen à Pointe-aux-Trembles, 2014, BjFi-17. Internal archaeological report. Rivière-des-Prairies, Pointe-aux-Trembles et Ville de Montréal.

Grauer, A. L. (2019). Circulatory, reticuloendothelial, and hematopoietic disorders. In J.E Buikstra's (Ed.) *Ortner's identification of pathological conditions in human skeletal remains (3rd edition)* (pp. 491-529). Academic Press.

Guillerman, R. P. (2013). Marrow: red, yellow, and bad. *Pediatric Radiology, 43*, 181-192.

Hartnett, K. M. (2010). Analysis of age-at-death estimation using data from a new, modern autopsy sample—Part II: Sternal end of the fourth rib. *Journal of Forensic Sciences, 55*(5), 1152-1156.

Hoffbrand, V., & Steensma, D. P. (2019). *Hoffbrand's essential haematology*. John Wiley & Sons.

Jaffe, H. L. (1972). *Metabolic, degenerative, and inflammatory diseases of bones and joints*. Lea and Febeiger.

Kelley, M. A. (1979). Skeletal changes produced by aortic aneurysms. *American Journal of Physical Anthropology, 51*(1), 35-38.

Khudaverdyan, A. Y., & Hobossyan, S. G. (2017). Bioarchaeological evidence for the health status of a Late Bronze Age and Early Iron Age Bakheri chala population (Armenia). *Anthropologie*, *55*(3), 319-336.

Kirbas, A., Celik, S., Gurer, O., Yildiz, Y., & Isik, O. (2011). Sternal wrapping for the prevention of sternal morbidity in elderly osteoporotic patients undergoing median sternotomy. *Texas Heart Institute Journal*, *38*(2), 132.

Klaus, H. D. (2017). Paleopathological rigor and differential diagnosis: Case studies involving terminology, description, and diagnostic frameworks for scurvy in skeletal remains. *International Journal of Paleopathology*, *19*, 96-110.

Klein, L., Li, Q. X., Donovan, C. A., & Powell, A. E. (1990). Variation of resorption rates in vivo of various bones in immature rats. *Bone and Mineral*, *8*(2), 169-175.

Lagia, A., Eliopoulos, C., & Manolis, S. (2007). Thalassemia: macroscopic and radiological study of a case. *International Journal of Osteoarchaeology*, *17*(3), 269-285.

Lopez, A., Cacoub, P., Macdougall, I. C., & Peyrin-Biroulet, L. (2016). Iron deficiency anaemia. *The Lancet*, *387*(10021), 907-916.

Lovejoy, C. O., Meindl, R. S., Pryzbeck, T. R., & Mensforth, R. P. (1985). Chronological metamorphosis of the auricular surface of the ilium: A new method for the determination of adult skeletal age at death. *American journal of Physical Anthropology*, *68*(1), 15-28.

Maakaron, J.E. (2021). *Anemia*. Medscape. https://emedicine.medscape.com/article/198475-overview. (accessed November 2023).

Mann, R. W., & Tuamsuk, P. (2005). Case report: Differential diagnosis of severe diffuse skeletal pathology in an adult Thai male. *Photographic regional atlas of bone disease: A guide to pathologic and normal variation in the human skeleton*, 213-221.

Mays, S. (2018). How should we diagnose disease in palaeopathology? Some epistemological considerations. *International Journal of Paleopathology*, *20*, 12-19.

Mays, S. A. (2020). A dual process model for paleopathological diagnosis. *International Journal of Paleopathology*, *31*, 89-96.

McFadden, C., & Oxenham, M. F. (2020). A paleoepidemiological approach to the osteological paradox: Investigating stress, frailty, and resilience through cribra orbitalia. *American Journal of Physical Anthropology*, *173*(2), 205-217.

Morgan, J. A. (2014). *The methodological and diagnostic applications of micro-CT to palaeopathology: a quantitative study of porotic hyperostosis* [Doctoral thesis]. The University of Western Ontario (Canada).

Moseley, J. E. (1965). The paleopathologic riddle of" symmetrical osteoporosis". *American Journal of Roentgenology*, *95*(1), 135-142.

O'Donnell, L., Buikstra, J. E., Hill, E. C., Anderson, A. S., & O'Donnell Jr, M. J. (2023). Skeletal manifestations of disease experience: Length of illness and porous cranial lesion formation in a contemporary juvenile mortality sample. *American Journal of Human Biology*, e23896.

O'Donnell, L., Hill, E. C., Anderson, A. S. A., & Edgar, H. J. (2020). Cribra orbitalia and porotic hyperostosis are associated with respiratory infections in a contemporary mortality sample from New Mexico. *American Journal of Physical Anthropology*, *173*(4), 721-733.

O'Neal, M. L., Dwornik, J. J., Ganey, T. M., & Ogden, J. A. (1998). Postnatal development of the human sternum. *Journal of Pediatric Orthopaedics*, *18*(3), 398-405.

Panzer, S., Schneider, K. O., Zesch, S., Rosendahl, W., Thompson, R. C., & Zink, A. R. (2023). Anemias in ancient Egyptian child mummies: Computed tomography investigations in European museums. *International Journal of Osteoarchaeology*, *33*(3), 532-545.

Reynolds, J. (1962). An evaluation of some roentgenographic signs in sickle cell anemia and its variants. *Southern Medical Journal*, *55*(11), 1123-8.

Reynolds, J. (1965). The roentgenological features of sickle cell disease and related hemoglobinopathies. Charles C Thomas Publisher.

Riley, R. S., Hogan, T. F., Pavot, D. R., Forysthe, R., Massey, D., Smith, E., ... & Ben-Ezra, J. M. (2004). A pathologist's perspective on bone marrow aspiration and biopsy: I. Performing a bone marrow examination. *Journal of Clinical Laboratory Analysis*, *18*(2), 70-90.

Rivera, F., & Mirazón Lahr, M. (2017). New evidence suggesting a dissociated etiology for cribra orbitalia and porotic hyperostosis. *American Journal of Physical Anthropology*, *164*(1), 76-96.

Saers, J. P., DeMars, L. J., Stephens, N. B., Jashashvili, T., Carlson, K. J., Gordon, A. D., ... & Stock, J. T. (2021). Automated resolution independent method for comparing in vivo and dry trabecular bone. *American Journal of Physical Anthropology*, *174*(4), 822-831.

Saint-Martin, P., Dedouit, F., Rérolle, C., Guilbeau-Frugier, C., Dabernat, H., Rougé, D., ... & Crubézy, E. (2015). Diagnostic value of high-resolution peripheral quantitative computed tomography (HR-pQCT) in the qualitative assessment of cribra orbitalia–A preliminary study. *Homo*, *66*(1), 38-43.

Sanchez, J. (2014). *In search of a cause: an etiological analysis of manubrial porosity* [Masters thesis]. The University of Western Ontario (Canada).

Schaefer, M., Black, S. M., Schaefer, M. C., & Scheuer, L. (2009). *Juvenile osteology*. London: Academic Press.

Schmitt, A. (2005). Une nouvelle méthode pour estimer l'âge au décès des adultes à partir de la surface sacro-pelvienne iliaque. *Bulletins et Mémoires de la Société d'Anthropologie de Paris*, *17*(17 (1-2)), 89-101.

Sebes, J. I., & Diggs, L. W. (1979). Radiographic changes of the skull in sickle cell anemia. *American Journal of Roentgenology*, *132*(3), 373-377.

Smith-Guzmán, N. E. (2015). The skeletal manifestation of malaria: An epidemiological approach using documented skeletal collections. *American Journal of Physical Anthropology*, *158*(4), 624-635.

Stuart-Macadam, P. (1987). A radiographic study of porotic hyperostosis. *American Journal of Physical Anthropology*, *74*(4), 511-520.

Sullivan, A. (2005). Prevalence and etiology of acquired anemia in Medieval York, England. *American Journal of Physical Anthropology*, *128*(2), 252-272.

Swan, K. R., Humphrey, L. T., & Ives, R. (2023). The impact of vitamin D deficiency on cortical bone area and porosity at the femoral midsection in children from post-medieval London. *American Journal of Biological Anthropology*, *180*(2), 272-285.

Tayles, N., & Buckley, H. R. (2004). Leprosy and tuberculosis in Iron Age southeast Asia? *American Journal of Physical Anthropology*, *125*(3), 239-256.

Van Spelde, A. M., Schroeder, H., Kjellström, A., & Lidén, K. (2021). Approaches to osteoporosis in paleopathology: How did methodology shape bone loss research? *International Journal of Paleopathology*, *33*, 245-257.

Vande Berg, B. C., Malghem, J., Lecouvet, F. E., & Maldague, B. (1998). Magnetic resonance imaging of the normal bone marrow. *Skeletal Radiology*, *27*, 471-483.

Wapler, U., Crubézy, E., & Schultz, M. (2004). Is cribra orbitalia synonymous with anemia? Analysis and interpretation of cranial pathology in Sudan. *American Journal of Physical Anthropology*, *123*(4), 333-339.

World Health Organization. (2011). *Haemoglobin concentrations for the diagnosis of anaemia and assessment of severity* (No. WHO/NMH/NHD/MNM/11.1). World Health Organization.

CHAPTER 3: A FRAMEWORK FOR ANEMIA DIAGNOSIS IN PALEOPATHOLOGY INCORPORATING METRIC METHODS

Title: A Framework for Anemia Diagnosis in Paleopathology Incorporating Metric Methods

Brianne Morgan [a], Meghan Langlois [a], Rachel Schats [b], Alie E. Van der Merwe [c], Isabelle Ribot [d], Andrea Waters-Rist [e], & Megan B. Brickley [a]

[a] McMaster University, Department of Anthropology, Hamilton, Ontario, Canada, L8S 4L9, morgab5@mcmaster.ca, langlm5@mcmaster.ca, brickley@mcmaster.ca

[b] Leiden University, Faculty of Archaeology, Leiden, Netherlands, 2333CC
r.schats@arch.leidenuniv.nl

[c] Amsterdam UMC, University of Amsterdam, Department of Medical Biology, Section Clinical Anatomy and Embryology, Amsterdam, Netherlands, 1105 AZ
a.e.vandermerwe@amsterdamumc.nl

[d] University of Montréal, Department of Anthropology, Montréal, Québec, Canada, QCH3T 1N8
i.ribot@umontreal.ca

[e] Western University, Department of Anthropology, London, Ontario, Canada, N6A 3K7
awaters8@uwo.ca

Under review at the American Journal of Biological Anthropology.

Abstract

Objectives: This paper explores metric manifestations of anemia in crania undergoing growth and development using micro-CT imaging. It presents a framework for assigning diagnostic certainty for anemia, based on evaluating the diagnostic parameters proposed in this study.

Materials and Methods: Sixty-eight orbits/frontal bones of individuals aged birth to 15 years from Quebecois and Dutch archaeological collections dating to the 18th and 19th century underwent micro-CT analysis. Individuals were visually assessed for skeletal manifestations of marrow hyperplasia within the internal marrow space using a scoring rubric. Bone microarchitecture measurements were used to calculate T-scores and identify individuals who displayed potential manifestations of marrow hyperplasia. Relative cortical thickness ratios of the frontal bone were calculated for 16 individuals. Error testing was performed for all evaluations.

Results: Anemia was inferred in 16 percent (10/61) of the assessable sample based on our diagnostic framework and the micro-CT analysis. Trabecular separation T-scores were considered the most significant metric for assigning a diagnosis. Frontal ratios were regarded as less strong due to the imaging technique used. Observer agreement for visual assessments was substantial between observers with more experience, and high repeatability was seen for metric methods.

Discussion: The recommendations for assigning diagnostic certainty in this study prioritize evaluating metric features strongly related to anemia through a biological approach that considers the etiology of marrow hyperplasia. Including a combination of metric and internal visual evaluation criteria in the diagnostic process provides clearer lines of evidence for assessment of bone structures associated with anemia beyond the macroscopic evaluation of porous lesions.

Keywords: cribra orbitalia, porotic hyperostosis, porotic lesions, marrow hyperplasia, micro-CT

1.0 Introduction

Although anemia in skeletal remains has been studied by anthropologists since the 1960s (e.g. Angel, 1966), its diagnosis is still contentious, emphasizing the need to standardize and improve the diagnostic criteria. Paleopathologists are increasingly highlighting the complexity of recognizing anemia (Brickley, 2024; Grauer, 2019; O'Donnell, Hill, Anderson, & Edgar, 2020; Panzer et al., 2023). Issues such as reliance on porotic lesions, which can have many potential and overlapping etiologies (Wapler et al., 2004), minimal clinical data on skeletal manifestations of anemia (Grauer, 2019), a lack of clear diagnostic guidelines (Brickley, 2024), and high rates of interobserver error when evaluating lesions (Anderson, 2023; Buckberry et al., 2023; Santos et al., 2023) have hindered diagnosis of anemia in paleopathological research.

As an alternative to observation of porous lesions, quantitative methods have occasionally been used to assess anemia in skeletal remains (Galea, 2013; Morgan, 2014; Morgan, Zeller, Ribot, & Brickley, 2024; Panzer et al., 2023; Stuart-Macadam, 1987a, 1987b; Zuckerman et al., 2014). However, there is currently a limited amount of comparative metric data available, and establishment of metric standards is still in the initial stages (Anderson et al., 2021; Brickley, 2024) and will require the use of imaging techniques to develop. No standardized frameworks have yet been presented for incorporating metric methods and visual evaluation for anemia diagnosis in skeletal remains. Establishing a systematic framework with consistent terminology based on an understanding of the underlying biological mechanisms that affect the expression of skeletal changes (Klaus & Lynnerup, 2019) enables comparisons across diverse contexts, and ensures that anemia diagnosis based on identifying marrow hyperplasia has a formal basis moving forward. Therefore, this study aims to explore metric and visual methods of assessing marrow hyperplasia in the cranium using micro-CT images. Initial quantitative data that can be used to establish measurement baselines are proposed, and recommendations on assigning diagnostic certainty for anemia in skeletal remains are presented. This study focuses on a single skeletal area, the cranium, in individuals aged birth-15 years, as skeletal manifestations of marrow hyperplasia are known to develop in the cranium and are better understood in human skeletons undergoing growth and development.

2.0 Background

Anemia is a condition where the body cannot supply adequate oxygen to its tissues. Anemia can be caused by increased red blood cell (RBC) destruction, decreased RBC production, or excessive RBC loss (Walker, Bathurst, Richman, Gjerdrum, & Andrushko, 2009) resulting from a variety of etiologies, including micronutrient deficiencies (e.g., iron, folic acid, vitamin B12, vitamin B9), parasitic infections, infectious disease, chronic illness, and genetic traits (e.g., sickle cell anemia or thalassemia) (WHO, 2011; WHO, 2023). In response to a deficiency in RBCs, increased production may occur, triggering the expansion of bone marrow, where RBCs are produced (Hoffbrand & Steensma, 2019). This process, referred to as marrow hyperplasia, can potentially lead to skeletal changes as the bone adapts to accommodate the new volume of bone marrow (Brickley, 2018). Increased trabecular separation to account for the new marrow is expected and thinned cortical bone and sparser/thinned trabeculae can develop as a result, leading to increased diploic/trabecular space width (Agarwal, Drar, Shah, & Bhardwaj, 1970; Hoffbrand & Steensma, 2019; Jaffe, 1972; Reynolds, 1962, 1965; Stuart-Macadam,

1987a). In areas of the skeleton where cortical bone is already thin, such as the orbital lamina, the cortex may fully resorb in places, resulting in macroscopically visible porous lesions (Brickley, 2018; Hengen, 1971; Hoffbrand & Steensma, 2019; Jaffe, 1972).

Not all forms of anemia lead to marrow hyperplasia, and the forms that cause it are debated. Walker et al. (2009) argue that iron deficiency anemia cannot result in the excessive marrow proliferation that causes skeletal manifestations of marrow hyperplasia, a position contrasted by Oxenham and Cavill (2010). Additionally, McIlvaine (2015) and Schats (2023) point out the possibility for different forms of anemia to co-occur, meaning that associating one form of anemia with skeletal changes is further complicated. In the current study, the term 'anemia' will be used as a general descriptor encompassing any type of anemia that can result in skeletal manifestations of marrow hyperplasia.

To recognize marrow hyperplasia when it does occur, identifying bone microarchitecture or trabecular width changes within the marrow space is necessary (Angel, 1966; Brickley, 2024; Wapler et al., 2004). The application of different visualization techniques, such as radiography (e.g., Stuart Macadam 1987a, 1987b), CT imaging (e.g., Anderson et al., 2021; Durdin, 2020; Naveed, Abed, Davagnanam, Uddin, & Adds, 2012; O'Donnell et al., 2020; Panzer et al., 2023; Rivera & Lahr, 2017; Saint-Martin et al., 2015; Zuckerman, Garofalo, Frohlich, & Ortner, 2014) or micro-CT imaging (e.g., Galea, 2013; Morgan, 2014; Morgan et al., 2024) allows for the marrow space to be evaluated non-destructively, and for researchers to investigate the potential causes of cranial porosity.

As part of using imaging technology and visualization methods, quantitative methods of identifying skeletal changes associated with marrow hyperplasia have also been proposed and sometimes used (e.g., Durdin, 2020; Galea, 2013; Morgan, 2014; Morgan et al., 2024; Panzer et al., 2023; Stuart-Macadam, 1987a; Zuckerman et al., 2014). Stuart-Macadam (1987a) sets out protocols for measuring the cranial vault and identifying pathological measurements, and various studies have used cranial vault thickness to investigate porous cranial lesions and anemia (e.g., Durdin, 2020; Hengen, 1971; Zuckerman et al., 2014). Specific microstructure measurements, such as trabecular separation or trabecular number, are also likely to be affected by marrow hyperplasia, and have been linked to presence of porous orbital lesions in skeletal remains (e.g., Galea, 2013; Morgan, 2014).

Quantitative approaches often involve defining a range of non-pathological 'baseline' measurements against which abnormal patterns can be identified, potentially signalling the presence of pathology. For example, in the clinical assessment of osteoporosis, a patient's bone densitometry results from certain skeletal sites are compared to those from a standard group of individuals without osteoporosis who have been measured on the same instrument using T-scores to evaluate the significance of observed patterns (Binkley, Adler, & Bilezikian, 2014; Karaguzel & Holick, 2010). When using quantitative methods for assessing marrow hyperplasia related to anemia in skeletal remains, identifying a baseline group of individuals without anemia is challenging due to the lack of accompanying hematological data. However, absence of any skeletal manifestations of marrow hyperplasia could be used as a conservative method to identify a baseline group.

Following the approaches to paleopathological diagnosis proposed by Mays (2018), quantitative analysis of archaeological bone can yield a "direct measurement of a diagnostic parameter" (Mays, 2018; p. 13), which is fundamentally different from traditional lesion-based methods used for anemia diagnosis (Brickley, 2024). Although metric approaches require the application of skeletal imaging techniques which may be challenging or prohibited in certain contexts due to cost and the accessibility of equipment, employing quantitative methods can help reduce discrepancies among observers and diminish overreliance on the assessment of porous lesions as the sole basis for anemia diagnosis (Brickley, 2024).

3.0 Materials

Individuals from seven archaeological skeletal collections were evaluated: three were from 18th-19th century Quebec, Canada, and four were from 18th-19th century Netherlands (Table 3-1). Although there are socioeconomic differences between sites, which could cause differences in bone quality, individuals were grouped into age categories (see Table 3-1) regardless of burial type so that metric analysis could be done with the largest sample size possible. For the purpose of differential diagnosis, all individuals underwent a full paleopathological macroscopic assessment with special focus on the identification of porotic orbital lesions. Age estimation was done by assessing dental development (Gustafson & Koch, 1974), and all individuals under 15 years of age at the time of death with an orbit were included in the initial micro-CT sample (N=68, Table 3-1).

Table 3-1: Summary of orbits that underwent micro-CT imaging, by site and by age category.

ORBIT MICRO-CT SAMPLE-SITE COMPOSITION		
SITE	*CONTEXT*	*NUMBER OF INDIVIDUALS*
Saint-Antoine	Quebec, CA, 1799–1855	19
Pointe-aux-Trembles	Quebec, CA, 1748–1878	17
Sainte-Marie	Quebec, CA, 1709–1843	8
Alkmaar (GRK)	Netherlands, 1716–1830	8
Arnhem (ARJB)	Netherlands, 1650–1829	12
Eindhoven (EHV-CK)	Netherlands, 1650-1850	3
Zwolle (ZW87)	Netherlands, 1675-1828	1

ORBIT MICRO-CT SAMPLE-AGE COMPOSITION	
AGE CATERGORY	*NUMBER OF INDIVIDUALS*
0-1.9 years	38
2-5.9 years	19
6-15 years	11

Table complied from Arts & Altena, 2013; Baetsen, 2001; Baetsen & Zielman, 2020; Bitter, 2002; Clevis & Constandse-Westermann, 1992; Ethnoscop, 2006; Ethnoscop, 2016a; Ethnoscop, 2016b.

4.0 Methods

4.1 Micro-CT imaging and sample preparation

Orbits were analyzed using the Nikon XTH-225ST micro-CT scanner at the Ancient Images Lab of the Museum of Ontario Archaeology. Smaller single orbits were mounted inside Styrofoam cups and secured with low-density green florist foam to minimize movement. For complete frontal bones that could not fit inside the Styrofoam cup, a block of green florist foam was carved to secure each bone. Samples were scanned using 95 kV, 165 µA, a molybdenum

target, at 24.00 µm voxels. Each scan used 3141 frames, at a rate of 1 projection per second, and took 53 minutes. The 3D volume reconstruction was done in CT Pro 3D (v. 4.4.4), using a FDK filtered back projection reconstruction algorithm. Visualization, orbit microarchitecture measurements, and frontal ratio measurements were performed using Dragonfly (v. 2021.3) (https://www.theobjects.com/dragonfly/index.html).

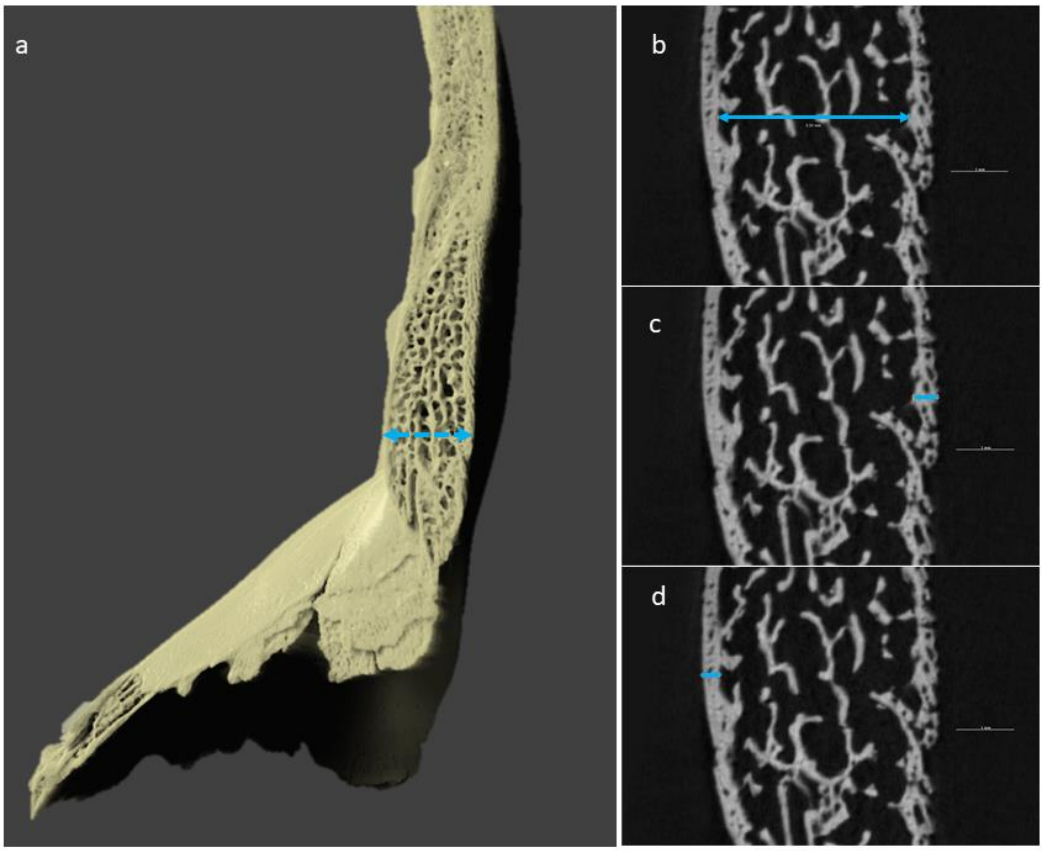

Figure 3-1: Method of taking measurements for the frontal ratio calculation. a) Arrow indicates location of frontal ratio measurement on 3D model. b) Trabecular space measurement, which is a 2D linear measurement. Arrows indicate the length of the measurement. c) Ectocranial cortical measurement, indicated by arrows. d) Endocranial cortical measurement, indicated by arrows. Final ratio is calculated by dividing the measurement from b) by the sum of the measurements from c) and d).

4.2 Frontal ratio measurements

Frontal ratios of trabecular space thickness to cortical thickness were calculated following Panzer et al. (2023). Measurements were taken on a mid-sagittal view of the frontal bone, just above the nasal bones and the orbital roof (Figure 3-1). This area was only accessible in 16 of the scanned samples. Although the frontal sinus may interfere with these measurements in older juveniles, this was not encountered in the current study. To assess the repeatability of the ratio measurements, six frontal bones (~40% of the sample) were assessed by two observers (BM and ML), and the final ratio outcomes for each observer were compared. To evaluate if there was a relationship between ratio and age, a two-tailed Pearson correlation test (α=0.05) was performed using all 16 individuals who could be measured. The original research by Reynolds

(1962, 1965) and Sebes and Diggs (1979) considered a ratio over 2.5 to be indicative of diploic expansion based on measurements from radiographs.

4.3 Visual microstructure assessment

Visual microstructure assessment of each orbit reconstruction was done with the criteria used in Table 3-2. Examples are provided in Figures 3-2 to 3-4. Cortical thinning of the orbital roof, increased trabecular separation, and trabecular thinning were all evaluated on a scale of 0 to 3, with 3 representing the most significant expression of each trait. Based on initial observation, changes were most evident in the lower third of the orbit, just above the orbital lamina. Accordingly, features were scored in this location throughout the 3D orbit (see Figures 3-3,3-4).

In addition to the three microarchitecture features, the possible sources of observable porous lesions were evaluated. Lesions could be assigned to any number of etiologies listed in Table 3-3 (examples provided in Figure S3-1). All features were evaluated for a final visual assessment of whether there was evidence of skeletal manifestations of marrow hyperplasia (Table 3-4). Individuals (n=7) with internal evidence of post-mortem damage (e.g., sediment within intertrabecular spaces) were excluded from visual analysis and further measurements, as taphonomic damage would have affected measurements and scoring.

Table 3-2: Description of microarchitecture features for visual scoring.

CORTICAL THINNING OF ORBITAL LAMINA	
Score across entire orbital lamina.	
0-Absent	No cortical thinning is present throughout the orbital lamina.
1-Mild	Some patches of thinned cortex are present, but occur on less than 50% of the orbital lamina.
2-Moderate	Mild cortical thinning is consistent across more than 50% of the orbital lamina, OR marked cortical thinning (as seen in scores of 3) is present in less than 50% of the orbital lamina.
3-Marked	Marked cortical thinning is consistently present across more than 50% of the orbital lamina.
INCREASED TRABECULAR SEPARATION	
Score in lower third of marrow space above orbital lamina.	
0-Absent	No abnormally large trabecular spacing is present throughout the marrow space.
1-Mild	Abnormally large trabecular spacing is seen throughout less than 50% of the marrow space.
2-Moderate	Mildly abnormally large trabecular spacing is seen throughout more than 50% of the trabeculae in the marrow space OR marked abnormally large trabecular spaces (score of 3) are present throughout less than 50% of the marrow space.
3-Marked	Marked trabecular space enlargement is seen consistently throughout more than 50% of the marrow space.
TRABECULAR THINNING	
Score in lower third of marrow space above orbital lamina.	
0-Absent	No trabecular thinning is present throughout the marrow space.
1-Mild	Trabecular thinning is seen throughout less than 50% of the trabeculae in the marrow space.
2-Moderate	Mild trabecular thinning is seen throughout more than 50% of the trabeculae in the marrow space OR marked trabecular thinning (score of 3) is present throughout less than 50% of the marrow space.
3-Marked	Marked trabecular thinning is seen consistently throughout more than 50% trabeculae in the marrow space.

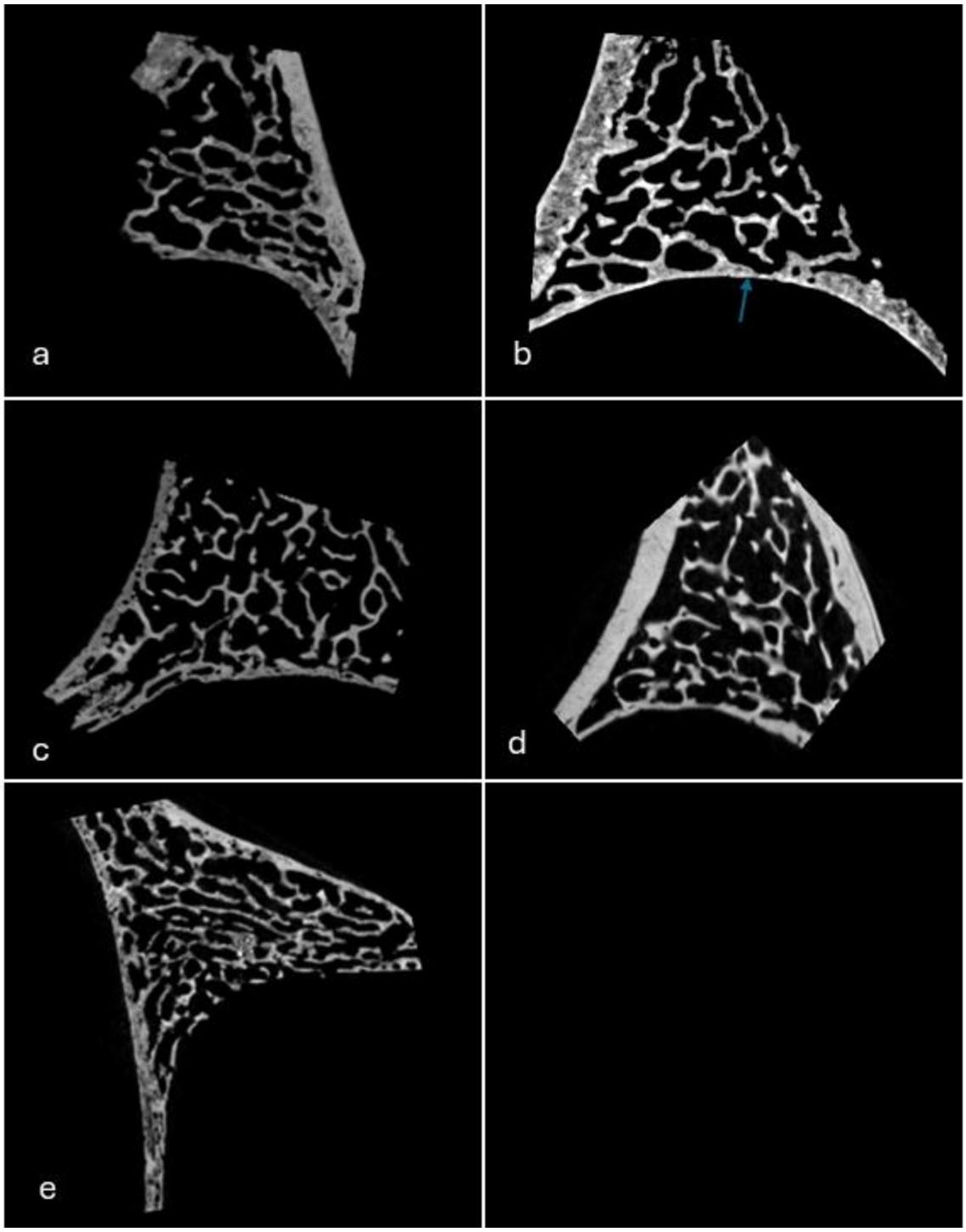

Figure 3-2: Examples and description of cortical thinning for each scoring category. a) Cortical thinning score of 0. b) Cortical thinning score of 1. Arrow indicates a patch of mild thinning, which was present throughout this orbit. c) Cortical thinning score of 2, where mild thinning is present over more than 50% of the visible cortex. d) Cortical thinning score of 2, where marked thinning on is present on less than 50% of the visible cortex. e) Cortical thinning score of 3, where marked thinning on is present on more than 50% of the visible cortex. In this case, the cortex is so thin that it has worn away in patches.

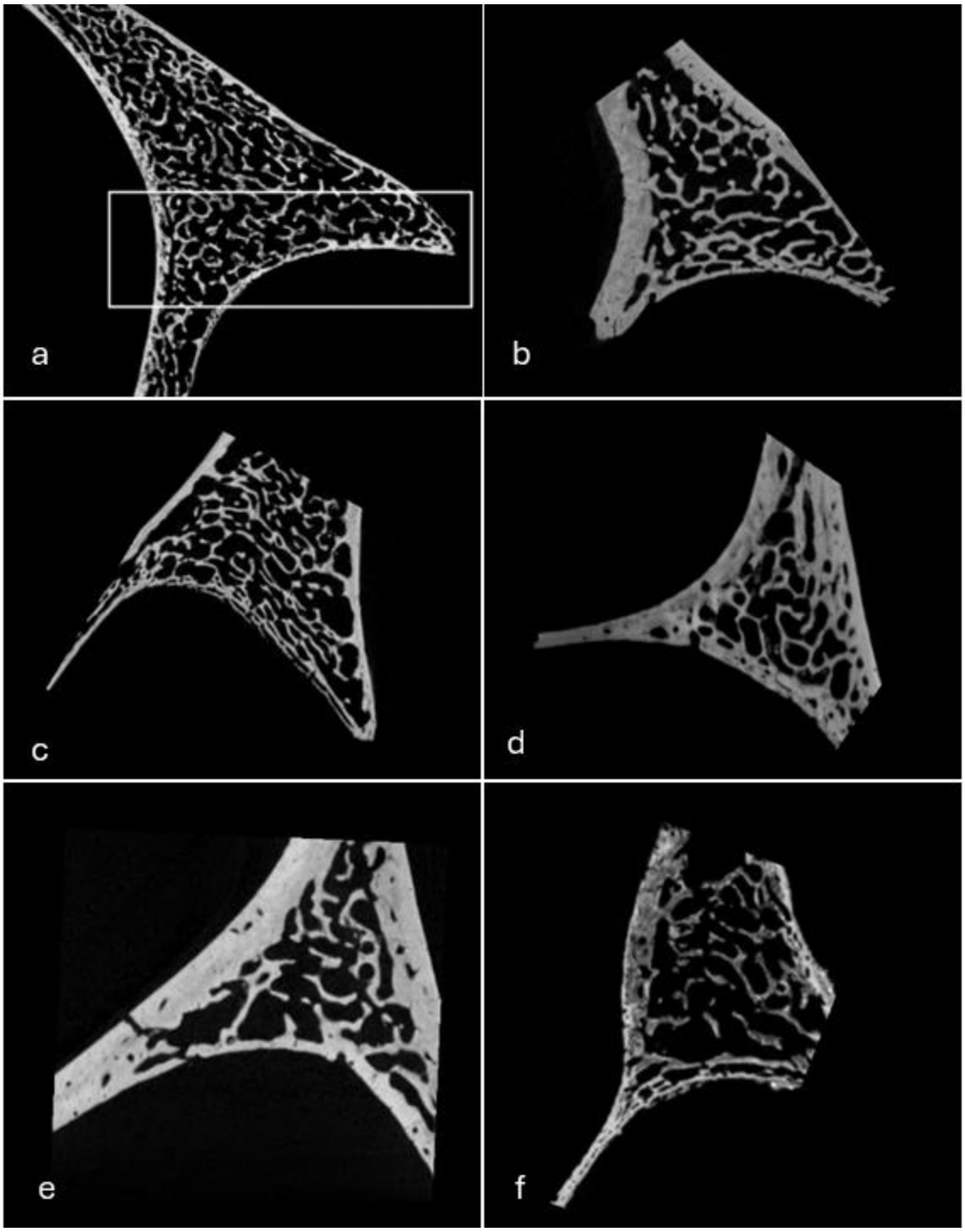

Figure 3-3: Examples of increased trabecular separation for each scoring category, and location of scoring. a) Location where orbit should be scored (lower third) is highlighted by the box. b) Increased trabecular separation score of 0. c) Increased trabecular separation score of 1. d) Increased trabecular separation score of 2, where mildly abnormally large trabecular separation is seen throughout more than 50% of the marrow space. e) Increased trabecular separation score of 2, where marked abnormally large trabecular separation (score of 3) is present throughout less than 50% of the marrow space. f) Increased trabecular separation score of 3.

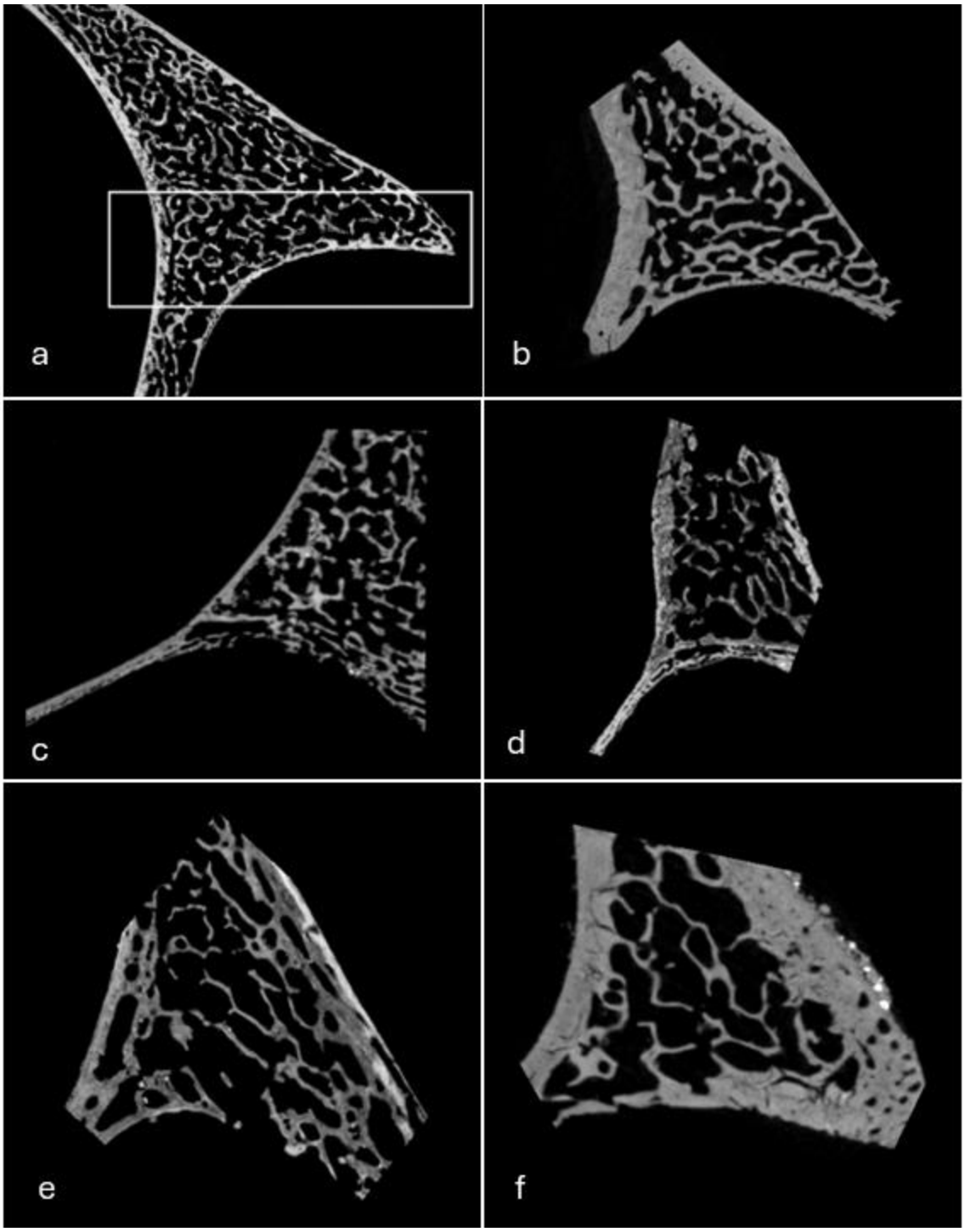

Figure 3-4: Examples of trabecular thinning for each scoring category. a) Location where orbit should be scored (lower third) is highlighted by the box. b) Thinned trabeculae score of 0. c) Trabecular thinning score of 1. The cortical bone is thin in general, and the trabeculae do not look markedly thin in comparison. d) Trabecular thinning score of 2 where mild trabecular thinning is seen throughout more than 50% of the trabeculae in the marrow space. e) Trabecular thinning score of 2 where marked trabecular thinning (score of 3) is present throughout less than 50% of the marrow space. f) Trabecular thinning score of 3.

The visual assessment serves as a conservative method of identifying baseline individuals, as those with no evidence of skeletal manifestations of marrow hyperplasia were assigned to the 'no evidence' category. Visual assessment using this rubric is meant to be a simple, binary assessment that can contribute to a final diagnosis, but should be combined with other methods when assigning diagnostic certainty.

To test for interobserver reliability, and to evaluate the scoring rubric's ease of use, seven (~10%) of the orbit reconstructions were evaluated by three additional observers with experience in evaluating porous lesions and/or micro-CT images, and four who had some experience in evaluating skeletal remains, but not necessarily in metabolic bone disease or porous lesions. Cohen's Kappa coefficient was used to evaluate average interobserver agreement for the final visual assessments.

Table 3-11: Description of porous lesion etiologies, and what they look like on micro-CT images. Note that orbits can be scored with more than one lesion source.

POROUS LESION POSSIBLE SOURCE	
1-Marrow hyperplasia	Porosity will originate from inside the orbital roof. The cortex may appear thin, and porosity may look as though the trabecular structure has penetrated through the cortex. Trabeculae may also extend through the cortex. Porosity may be irregular in shape and size.
2-Vascular response	Signs of an inflammatory response are present. Individual pores, or channels, will be circular and less than 1 mm in diameter. Channels will generally originate on the outer surface of the cortex, and may or may not penetrate through to the trabecular space.
3-Impaired mineralization	Impaired mineralization causes bone to look spiculated and porous. Pores may be relatively fine, but irregular in shape.
4- Porous subperiosteal new bone formation	Layers of new bone may appear as highly porous. Observing new bone formation is key for this score.
5- Post-mortem damage	Porosity due to post-mortem damage may be the result of corrosion, root damage, cracks, or weathering. Pores may have sharp, discoloured edges with obvious soil inside.
6- Normal growth and development	Porosity will be uniform and fine. Will be more common in those undergoing growth and development. In the orbit, this may be accompanied by lamination of bone, as the bone develops through mesenchymal ossification (Tawfik & Dutton, 2018).

Table 3-15: Orbit visual assessment categories and features.

	EXPECTED FEATURES
EVIDENCE OF Skeletal Manifestations of Marrow Hyperplasia	• Porotic lesions linked to marrow hyperplasia (i.e. source score of 1) are present. • Increased trabecular separation is present to at least some extent, and is accompanied by some level of cortical/trabecular thinning (scores ≥1).
NO EVIDENCE OF Skeletal Manifestations of Marrow Hyperplasia	• Multiple key features expected in marrow hyperplasia (cortical/trabecular thinning, increased trabecular separation, porous lesions caused by cortical thinning) are all absent or mild. • Increased trabecular separation is mild or absent (scores of 0-1). • Cortical thinning or trabecular thinning may be present, but are milder (scores of 1-2) and not accompanied by increased trabecular separation.

4.4 Orbit microarchitecture measurements

During macroscopic observation of orbits, the location of porous lesions was recorded on orbit diagrams. A 10x10x15 mm sample placed on the lateral 2/3s of the orbital roof was used for microarchitecture measurements, as this was the most common lesion location from the diagrams, and because active marrow is present in only this section of the orbit for individuals over 8 years (O'Donnell et al., 2023). Instructions on placing this sample box are provided in Figure 3-5. Orbit measurements were taken using Dragonfly's Bone Analysis Wizard tool using Buie segmentation (Buie, Campbell, Klinck, MacNeil, & Boyd, 2007). These measurements are done using 3D volume reconstruction, so measurements are an average from across the entire bone, which differs from the 2D point measurement used for ratio assessments (e.g., Figure 3-1). Measurements taken included average cortical thickness of the orbital lamina (CtThOL, mm), average trabecular separation (TbSp, mm), and average trabecular thickness (TbTh, mm). To test intraobserver reliability in this method, the entire process of obtaining measurements was repeated on a random selection of seven (~10% of the sample) orbit reconstructions one week later, and differences between the two sets of measurements were calculated. Two-tailed Pearson correlation tests at 0.05 significance level were used to assess the relationship between an individual's midpoint age estimate and orbit microarchitecture measurements for the entire sample.

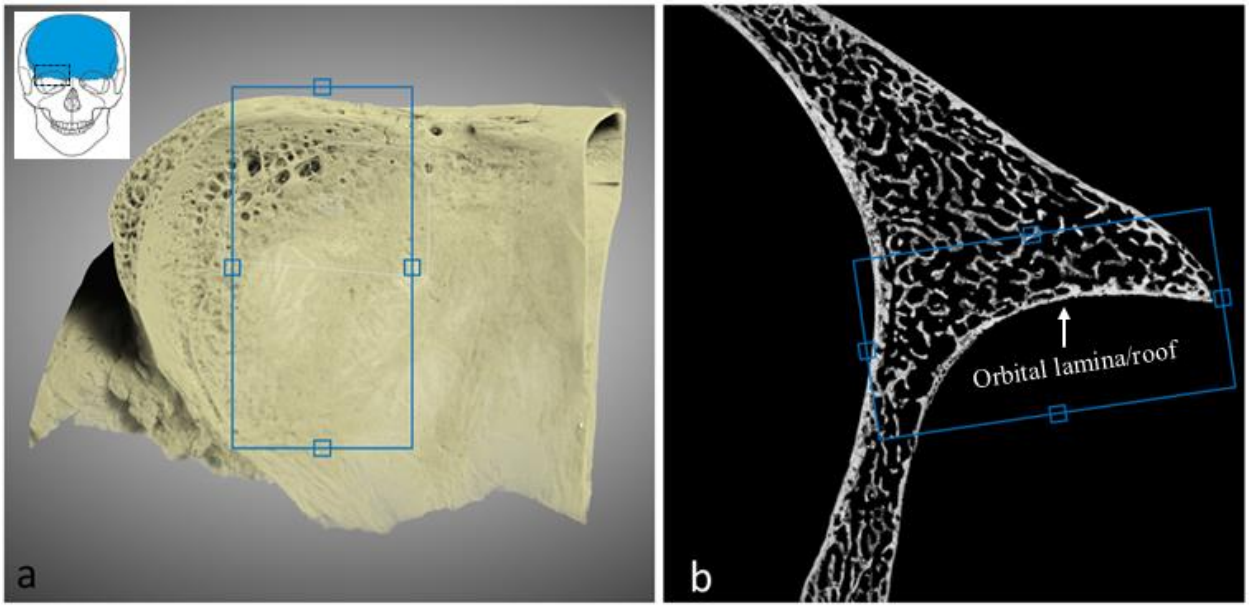

Figure 3-11: Placement for the measurement sample box, where microarchitecture measurements were taken. The sample box measures 10x10x15mm. The longest edge of the rectangular box was aligned parallel to the orbital lamina, and the lateral edge of the rectangle was aligned with the zygomatic process of the frontal bone, just before where the supraorbital margin begins to curve inferiorly (Figure 3-5a, inferior view of right orbital lamina). On the medial-lateral 2D view, the centre of the box was aligned with the orbital lamina, and oriented such that the most inferior edge was parallel to the centre of the orbital roof (Figure 3-5b).

The method used to evaluate the relationship between microstructure measurements and marrow hyperplasia related to anemia used in this study was derived from the T-score method used in osteoporosis diagnosis. T-scores are calculated as follows: T-score = (patient bone

mineral density –normal mean bone mineral density)/standard deviation of the normal population, and scores of -1 to -2.5 standard deviations (SD) at particular sites are considered osteopenic, while scores of <-2.5 SD are considered osteoporotic (Binkley et al., 2014; Kanis et al., 1994). To carry out the same procedure in this study, the average and standard deviation of all measurements for each age category were calculated using only the visually-identified baseline group. T-scores for all individuals not included in that group were calculated, and scores of ≤-1 for average cortical thickness of the orbital lamina (CtThOL) and average trabecular thickness (TbTh) were considered evidence of cortical/trabecular thinning and scores of ≥1 for average trabecular separation (TbSP) were considered evidence of increased trabecular spacing. In osteoporosis assessment, different T-score thresholds are used for different skeletal sites (Binkley et al., 2014), and more metric data will help to refine these thresholds for the orbit in the future.

4.5 Assessment of possible anemia status

Different levels of diagnostic certainty exist when evaluating pathological lesions present on skeletal remains, and the framework by Appleby, Thomas, & Buikstra (2015) sets out terminology that can capture these differences in certainty. To apply this framework to anemia assessment, we outlined important considerations in Figure 3-6, and defined terminology for assigning diagnostic certainty for anemia in Table 3-5. The basic steps in Figure 3-6 and the standardized terminology set out by Appleby, Thomas, & Buikstra (2015) were used to construct a decision tree (Figure 3-7) to facilitate consistent evaluation and assignment of diagnostic certainty for the current study, where frontal ratios, visual assessments, and microstructure T-scores were evaluated. Genetic anemias were not thought to be a factor for any of the individuals in this study, but in contexts where genetic anemias are considered, skeletal manifestations of marrow hyperplasia may be more marked, and there may be additional bone features (Hershkovitz et al., 1997; Lewis, 2012). Assessments on the assigned diagnostic certainty were made following the decision tree in Figure 3-7, and three observers repeated assessments on 20% of the sample to evaluate agreement. Although Figure 3-7 is specific to the data used in this study, it could be used as a model and adapted for future use depending on the data available.

Table 3-23: Categories of diagnostic certainty for anemia.

CERTAINTY CATEGORY	DESCRIPTION
Diagnostic of	Features and metric changes could only have been caused by anemia. Visual features of the bone (e.g. hair-on-end appearance of the crania) should be highly indicative of marrow hyperplasia. Metric data should strongly reflect skeletal manifestations of marrow hyperplasia, and be supported by robust clinical data.
Highly consistent with	Features and metric changes could have been caused by anemia, but a few other possible causes exist. Internal visual changes expected for skeletal manifestations of marrow hyperplasia (e.g. for the orbit, this includes cortical thickness, trabecular thickness, and trabecular separation) must be observable, and metric data supports skeletal manifestations of marrow hyperplasia.
Consistent with	Features and metric changes may be caused by anemia, but there are many other possible causes. Internal visual changes (e.g. for the orbit, this includes cortical thickness, trabecular thickness, and trabecular separation) are present but may be mild. Metric data does indicate the potential for skeletal manifestations of marrow hyperplasia, but many other possible causes cannot be excluded as contributing to the observed features and measurements.
Not consistent with	Features and metric changes expected for skeletal manifestations of marrow hyperplasia caused by anemia are absent, or could not have been caused by anemia.

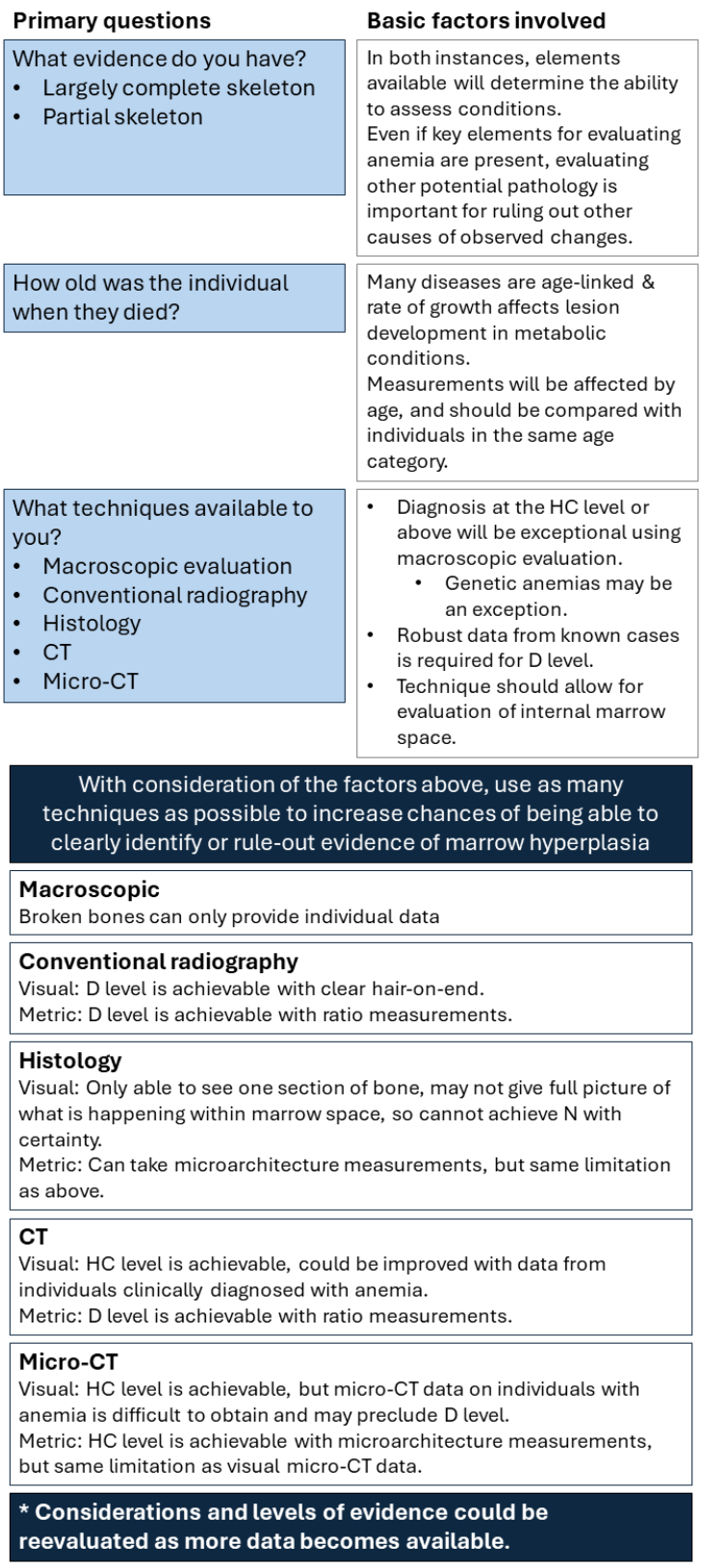

Figure 3-17: Flow diagram showing the various considerations for assigning diagnostic certainty during anemia assessment. N=not consistent with, HC= Highly consistent with, D=Diagnostic of.

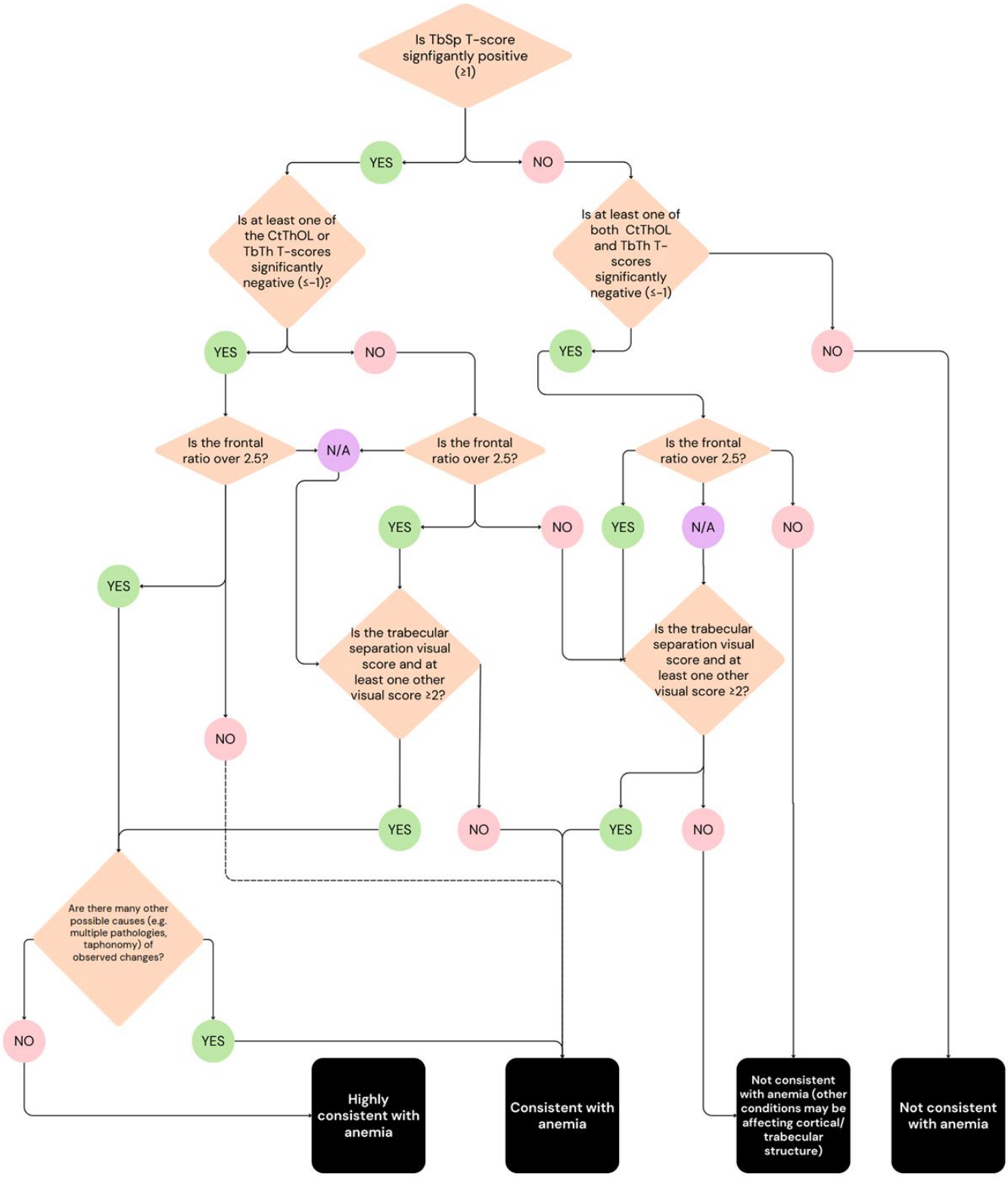

Figure 3-18: Decision tree demonstrating how anemia assessments were done using the available data from this study.

Other diseases, conditions, or sources of variation (e.g. scurvy, rickets) that could have resulted in microarchitecture changes were excluded through the process of differential diagnosis, based on a paleopathological analysis of the full skeleton (Klaus, 2017; Mays, 2020). When other conditions could not be excluded as contributing to the observed changes, this was reflected in the assigned diagnostic certainty. Although the protocol used in this study priorities micro-CT analysis of the orbit, it is important that the entire skeleton is assessed macroscopically, so that other possible causes of microarchitecture changes could be evaluated.

4.5.1 'Diagnostic of'

At the 'diagnostic of' level of certainty, only anemia could have caused the features and metric skeletal changes observed in an individual. The term 'diagnostic of' should be used in cases where observed features and measurements can be directly linked to those found in known cases of anemia. Visual changes that meet this criterion includes hair-on-end trabeculae, and metric data must be supported by robust clinical data (e.g. ratio measurements derived from clinically-diagnosed individuals). To use the 'diagnostic of' certainty category, other pathological conditions (e.g. osteoporosis, neoplastic conditions) or growth-related features must be excluded as contributing to observed metric and visual changes.

4.5.2 'Highly consistent with'

In cases where observed bone metrics and features could have been caused by anemia, and few other possible causes for changes exist, the term 'highly consistent with' can be used. The term 'highly consistent with' may be appropriate when observed visual features and metric changes are indicative of marrow hyperplasia, but a few other possible causes cannot be excluded with available evidence. Strong visual indicators and high-level metric data that reflects skeletal manifestations of marrow hyperplasia should be present.

4.5.3 'Consistent with'

The 'consistent with' category can be used when metric and visual changes could have been caused by anemia, but several other possible causes cannot be excluded. Changes are may be non-specific, and there are many other possible causes of the observed features. When metric parameters are contradictory (e.g., the TbSp T-score is over 1, but so is the CtThOL T-score), higher categories of diagnostic certainty should not be used. The nature of possible confounding factors, such as age, origin of reference data (i.e., imaging source), and other pathology, which could be causing the contradictions, should be considered in order to determine if 'consistent with' is still appropriate.

4.5.4 'Not consistent with'

When observed features or metric data could not have been caused by anemia, the term 'not consistent with' should be used. This term may be appropriate in cases where skeletal manifestations of marrow hyperplasia can be evaluated, but there is no observable visual evidence, or no metric deviation from baseline data, such as the microarchitecture measurements in the current study. It may also be appropriate in cases where anemia can be excluded as a contributing factor to observed skeletal changes based on all available evidence.

4.5.5 Co-morbidity and co-occurrence

Co-occurrence of anemia and other conditions can contribute to variation in the expression of skeletal changes and may affect diagnostic certainty. If skeletal indicators of other conditions are present in addition to metric changes indicative of marrow hyperplasia related to anemia, then co-occurrence should be considered. Conditions should be individually evaluated following established guidelines for assigning diagnostic certainty (e.g., Appleby et al., 2015; Brickey & Morgan, 2023). Expression of metric and visual changes when conditions co-occur will depend on a variety of factors, such as order of development, severity, and age. Whether co-occurrence may have affected metric data, or whether skeletal manifestations of marrow hyperplasia could have affected the expression of skeletal changes for other conditions should be considered. The final level of diagnostic certainty for anemia and any co-occurring conditions should be reported.

Skeletal manifestations of marrow hyperplasia can exacerbate the lesions caused by other diseases. For example, cortical thinning of the orbital roof could enhance porosity caused by other conditions. Similarly, conditions that also affect bone microarchitecture may exacerbate any metric microarchitecture or ratio differences. Assessment of diagnostic certainty must therefore consider the idea that other diseases can no longer be excluded as causing the observed metric changes.

5.0 Results

5.1 Interobserver error

For the orbit microstructure measurements, the average difference between the original and the repeated measurements was ≤ 0.005mm for all three measurements, indicating a high level of repeatability in the sampling procedure and Dragonfly software. For the frontal ratio measurements, there was agreement on the ratio assessment (i.e., whether they were over or under 2.5) in five of six cases. A third set of measurements was taken for the individual who did not show agreement, and the average was used for the final frontal ratio.

Figure 3-19: Micro-CT reconstruction of orbit (sagittal view, anterior towards the right) from individual 7A11-S57, who displays significant trabecular and cortical thinning, and increased trabecular separation. All observers agreed that skeletal manifestations of marrow hyperplasia were present in this individual.

The Cohen's Kappa coefficient across all observers in the visual rubric assessment was 0.34 (fair agreement). Between the experienced observers only, the average Cohen's Kappa was calculated to be 0.76 (substantial agreement) (McHugh, 2012), demonstrating that experience in evaluating porous lesions and familiarity with micro-CT analysis did help in ensuring consistency

when using the visual scoring rubric. Orbits with more extreme changes (e.g., Figure 3-8) showed the highest level of agreement, while those with more ambiguous changes showed less agreement. When using the decision tree in Figure 3-7 to assign diagnostic certainty, observers unanimously agreed on all assessments during the blind testing, indicating high repeatability.

5.2 Age and microarchitecture measurements

The three microarchitecture measurements are significantly associated with age (CtThOL: Pearson R=-0.73, P-value= < .001; TbSp: Pearson R=-0.56, P-value= < .001; TbTh: Pearson R=-0.49, P-value= < .001). For all three measurements, a positive relationship exists (Figure 3-9), meaning that as age increases, so does average cortical thickness, trabecular thickness, and trabecular separation. For TbTh, the overall range of measurements was narrow (0.14-0.26 mm); the range of variation is much wider for both CtThOL (0.11-0.52 mm) and TbSp (0.22-0.71 mm). In contrast, the frontal ratios are not significantly associated with age (Pearson R=-0.10, P-value=0.711).

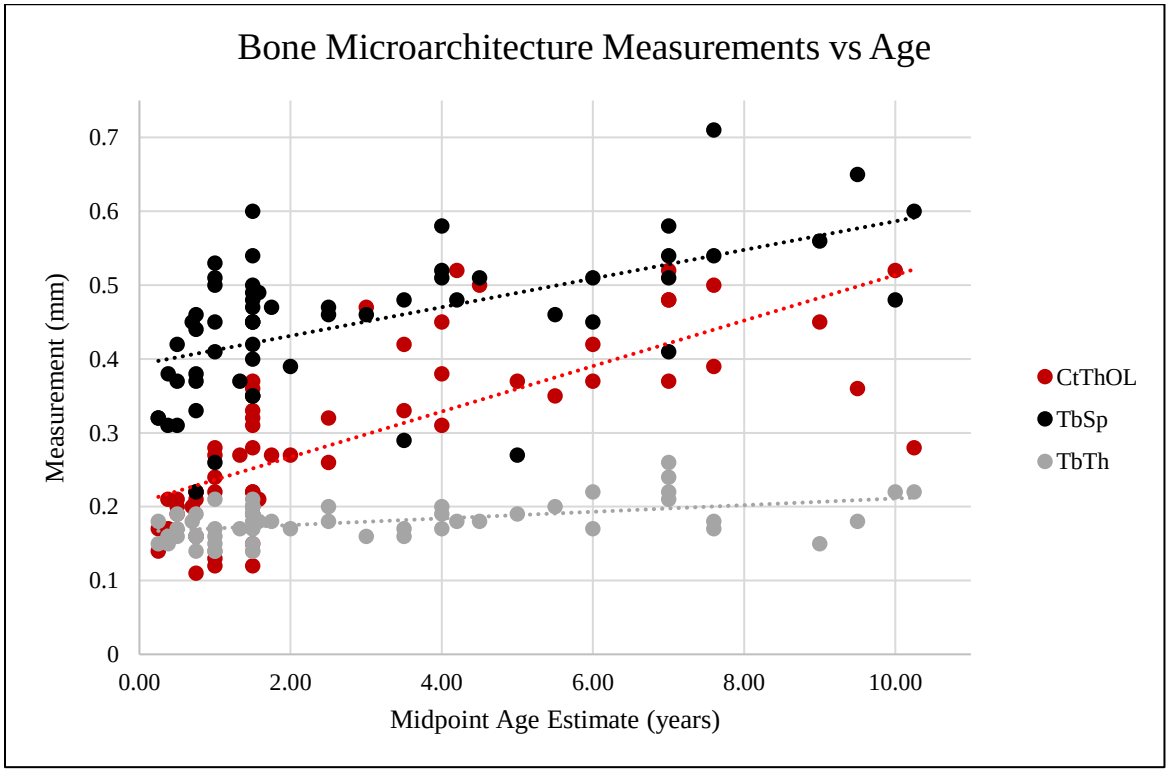

Figure 3-20: Bone microarchitecture measurements plotted against age estimate midpoints. Trendlines demonstrate the positive relationship between age and increased measurements.

5.3 Anemia assessment results

In total, 27 individuals were assessed as showing no visual evidence of skeletal manifestations of marrow hyperplasia and had frontal ratio measurements under 2.5. These individuals were therefore included in the baseline sample to calculate T-scores.

Table 3-27: Compiled results of all evaluations, plus assessments for individuals with visual evidence of skeletal manifestations of marrow hyperplasia, which manifests as cortical/trabecular thinning and widened intertrabecular separation.

SKELETON ID	SITE	AGE (YEARS)*	CORTICAL THINNING SCORE	TRABECULAR SEPARATION SCORE	TRABECULAR THINNING SCORE	OVERALL VISUAL	FRONTAL RATIO[1]	CTTHOL T-SCORE[2]	TBTH T-SCORE[2]	TBSP T-SCORE[3]	ANEMIA DIAGNOSIS
7A2-S6	Pointe-aux-Trembles, CA	0.38	2	1	1	EMH	4.6	-0.7	0.1	**-1.1**	N
20F-S39	St-Antoine, CA	0.50	2	1	1	EMH	2.0	-0.4	0.6	-0.7	N
7A11-S59	Pointe-aux-Trembles, CA	0.70	2	2	1	EMH	----	-0.3	**1.0**	0.3	C
ARJB-V1625	Arnhem, NL	0.75	1	1	1	EMH	**4.0**[4]	-0.1	0.9	-0.7	N
GRK-V807	Alkmaar, NL	1.00	3	1	2	EMH	----	**-1.5**	**1.0**	**-1.6**	H
7A11-S57	Pointe-aux-Trembles, CA	1.00	3	3	3	EMH	----	0.1	**1.8**	-0.7	H
21E-S8	St-Antoine, CA	1.40	1	3	1	EMH	0.9	1.0	**1.7**	**-1.1**	C
GRK-V326	Alkmaar, NL	1.50	2	2	2	EMH	----	-0.4	0.6	**-1.6**	N
GRK-V532	Alkmaar, NL	1.50	3	2	1	EMH	----	**-1.5**	-0.3	**-1.6**	N
GRK-V63	Alkmaar, NL	1.50	1	1	1	EMH	----	1.7	0.3	0.8	N
ARJB-V1777	Arnhem, NL	1.50	3	1	2	EMH	**4.5**	**-1.0**	-0.3	**-1.1**	N
7A2-S22	Pointe-aux-Trembles, CA	1.50	2	2	1	EMH	**2.8**	0.1	**1.7**	1.2	C
7A2-S24	Pointe-aux-Trembles, CA	1.50	2	2	2	EMH	----	-0.3	**1.3**	-0.2	H
17L-S4[5]	St-Antoine, CA	1.50	2	2	3	EMH	----	0.4	**2.0**	-0.2	C
2E3	Ste-Marie, CA	1.50	1	2	1	EMH	----	2.2	**2.2**	1.7	N
1G2	Ste-Marie, CA	1.50	2	1	2	EMH	1.4	2.3	**1.5**	0.8	N
20A-S3	St-Antoine, CA	1.50	2	2	2	EMH	----	1.6	**3.0**	0.3	C
7A2-S32	Pointe-aux-Trembles, CA	1.58	2	1	1	EMH	**4.9**	-0.1	**1.5**	0.3	H
ARJB-V478	Arnhem, NL	2.00	2	1	0	EMH	----	**-1.53**	0.06	-0.73	N
ARJB-V1812	Arnhem, NL	2.50	1	1	0	EMH	**3.4**	**-1.66**	0.64	1.02	N
2G3	Ste-Marie, CA	2.50	3	2	2	EMH	**6.9**	-0.88	0.73	-0.15	C
ARJB-V667	Arnhem, NL	3.00	0	2	3	EMH	----	1.07	0.64	**-1.32**	N
21E-S4	St-Antoine, CA	3.00	0	2	1	EMH	----	1.73	0.81	-0.15	N
21F-S5	St-Antoine, CA	3.00	1	2	2	EMH	----	**-1.01**	**1.14**	1.02	H
ARJB-V1762	Arnhem, NL	3.50	1	0	1	EMH	0.5	0.42	0.81	-0.73	N
ARJB-V1319	Arnhem, NL	4.00	1	2	2	EMH	----	0.81	**1.64**	-0.73	C
1G6	Ste-Marie, CA	4.00	3	2	3	EMH	----	-0.10	**1.06**	0.44	H
20F-S2	St-Antoine, CA	7.00	2	2	2	EMH	**4.0**	**-1.42**	0.37	-0.06	C
21E-S14	St-Antoine, CA	7.00	0	2	1	EMH	----	1.12	0.84	-0.36	N
21R-S5	St-Antoine, CA	7.60	2	3	3	EMH	0.6	**-1.08**	0.84	**-1.55**	C
30R-S7	St-Antoine, CA	7.6	2	3	3	EMH	**3.5**	0.78	**3.49**	**-1.25**	H
ARJB-V1258	Arnhem, NL	9.00	1	2	0	EMH	----	-0.07	**1.15**	**-2.15**	H
ARJB-V1735	Arnhem, NL	9.50	2	2	1	EMH	----	**-1.59**	**2.55**	**-1.25**	H
21U-S6	St-Antoine, CA	10.25	2	3	2	EMH	----	**-2.95**	**1.77**	-0.06	H

* Midpoint age estimate

EMH=Evidence of skeletal manifestations of marrow hyperplasia

[1]Bolded values are over 2.5, which was considered pathological by Panzer et al.,(2023) and Sebes & Diggs (1979), based on radiographic ratios from Reynolds (1962, 1965). See Section 5 for further discussion on how frontal ratios were used in this study.

[2]Bolded values ≤ -1, and are considered evidence of cortical or trabecular thinning.

[3] Bolded values are ≥ 1, and are considered evidence of increased trabecular separation.

CtThOL= Average cortical thickness of the orbital lamina

TbSp= Average trabecular separation

TbTh=Average trabecular thickness

D= Diagnostic of H= Highly consistent with C= Consistent with N= Not consistent with

[4] The frontal ratio was not considered for diagnosis, due to poor preservation of the cortical bone.

[5] This individual was fragmentary, and few skeletal elements beyond the orbit were available for analysis, meaning that although they did show strong metric and visual changes indicative of marrow hyperplasia, other conditions could not be excluded as contributing to these features.

Ten individuals were assessed as having evidence of skeletal manifestations of marrow hyperplasia using the metric and visual data in conjunction with the decision tree in Figure 3-7. Table 3-6 compiles all metric and visual analyses and presents the level of diagnostic certainty for each case. Measurements for the baseline group are presented in Supplemental Data Table 3-S1. All raw measurements and visual scores are presented in Supplemental Data Table 3-S2.

6.0 Discussion

Anemia assessment in the current study used a variety of metric data, and followed a consistent diagnostic framework that considered the biological mechanisms of microarchitecture changes, relative bone ratios, and lesion development. The quantitative approach taken here is rooted in the biological approach (Mays, 2018), and emphasizes consideration of the underlying process (i.e., marrow hyperplasia) that contributes to metric changes during anemia. In contrast, evaluation and scoring of porous lesions is not always tied to assessing lesion etiology (Anderson, 2023; Brickley, 2024), and recent studies have demonstrated the high amount of interobserver error that exists when recording porotic lesions (Anderson, 2023; Santos et al., 2023). Additionally, not all porous lesions are caused by skeletal manifestations of marrow hyperplasia (Wapler et al., 2004); many individuals in the current study, such as individual 7A9-S21, showed no internal visual evidence of microarchitecture changes related to anemia, but did have porous orbital lesions consisting of new bone formation and cortical porosity. These issues demonstrate the importance of understanding skeletal manifestations of marrow hyperplasia and analyzing internal changes as part of anemia diagnosis in paleopathology (Grauer, 2019; Brickley, 2024).

Using a standardized framework and terminology for paleopathological diagnosis helps ensure consistency and rigor in the process (Buikstra, Cook, & Bolhofner, 2017; Klaus & Lynnerup, 2019). For anemia, the proposed framework can help ensure that the pathogenesis of lesions and skeletal changes (i.e. skeletal manifestations of marrow hyperplasia) is considered more consistently, and allows for improved comparisons of anemia across contexts. Metric methods help to improve reproducibility and reduce subjectivity, further improving consistency. However, pathological metric measurements should not confer a ‘diagnostic of’ diagnosis without considering the other factors that may have contributed to calculated metric differences.

In the current study, for example, frontal ratios over 2.5 did not necessarily confer a high level of diagnostic certainty, even though this threshold value is derived from individuals clinically diagnosed with anemia (Reynolds, 1962, 1965; Sebes & Diggs, 1979), and is therefore a parameter that could be used to assign the ‘diagnostic of’ level of certainty (Table 3-5). However, this value is derived from measurements taken on radiographs, which have been found to differ from those performed during micro-CT analysis (Belgın, Serindere, & Orhan, 2019). The greater resolution of micro-CT allows for more accurate placement of the cortical bone borders, which can result in smaller cortical thickness measurements, and therefore larger ratios. For this reason, frontal ratios had to be interpreted conservatively and were not as highly prioritized in the decision tree (Figure 3-7) created for this study, but could be for future analyses where imaging modalities are more comparable. Improved consistency and diagnostic certainty

are achievable using metric data and standardized frameworks, but researchers must still consider confounding technical and biological factors as part of diagnosis.

As more metric data become available for comparison, it is expected that some of the assessments presented in the current study may change, and some cases could be assigned as 'diagnostic of.' Further adjustments could result from improved frontal ratio comparisons, and adding more data to baseline measurements may change T-score calculations. Metric evaluation of anemia in skeletal remains is still in the early stages, and may be difficult to compare across studies due to variation in instruments, or measurement protocols. In the future, new visual or metric criteria from a variety of skeletal areas may also be sufficient to propose various levels of diagnostic certainty. Accumulating measurement data is a key step towards differentiating between normal variation and possible pathology, and will be a necessary part of adopting these techniques in the future. Furthermore, while the decision tree in Figure 3-7 is specific to the data that was available in the current study, it could be adapted for future research depending on the metric data that is available and the relationship of that data to the recommended terminology in Table 3-5 and Section 4.5, and the considerations in Figure 3-6. For example, in our decision tree, trabecular separation T-scores were prioritized, as cortical thinning was thought to be most sensitive to taphonomic factors, and trabecular thickness was less variable than the other two scores, but studies in other contexts may produce data that support adoption of different configurations.

6.1 Interobserver error

The results from interobserver error testing of the visual assessment rubric show high agreement amongst individuals with experience in evaluating metabolic conditions/porotic lesions, and less agreement for those with limited experience. Microarchitecture measurements had strong agreement and were highly repeatable when using the Dragonfly program. Frontal ratios showed good agreement, but did introduce additional subjectivity, as the users had to determine where to take the measurements and assess the borders of the cortical bone. For the one individual in which there was no agreement on the outcome of the ratio, there was considerable weathering of the cortical bone, resulting in a high degree of variation in cortical thickness. Diploe measurements were consistent between observers, but differences in cortical thickness measurements affected the final ratios. The frontal ratio for this individual was not considered for the final diagnosis, as it may have been skewed by preservation. It is recommended that researchers repeat frontal ratio measurements and use an average to reduce error.

6.2 Age and microarchitecture changes

Age was found to be a major factor when considering bone microarchitecture measurements, which is expected as part of normal bone growth and development. The orbit undergoes 50% of its expected growth by the age of two years (Berger & Kahn, 2012), meaning that individuals under this age may show significantly different microarchitecture and increased variation compared to those who are past this developmental threshold. The significant positive relationship between age and microstructure measurements means that age must be considered

when selecting a metric baseline for determining pathological ratios and/or T-scores. It is expected that possible cases of anemia in individuals under 2 years of age may be less likely to be classified as 'diagnostic', since they are less likely to have straightforward metric results.

Frontal ratios were not significantly associated with age, possibly because ratio calculations help to standardize values. Non-ratio measurements of cranial vault thickness have been found to increase with age in those undergoing growth and development (De Boer, Van der Merwe, & Soerdjbalie-Maikoe, 2016), but Panzer et al., (2023) found that frontal ratio values did not appear to be associated with age.

6.3 Future directions

Establishing baseline measurements and ratios is crucial for evaluating marrow hyperplasia and anemia-related changes in the cranium with a greater degree of confidence. Additional measurements across various age categories are especially needed to further explore how skeletal manifestations of marrow hyperplasia are affected by growth and development. In this study, individuals older than two years were underrepresented, so more data on older age groups will be essential, particularly for calculating more robust T-scores. Evaluating microstructure measurements in individuals clinically diagnosed with anemia would be ideal and contribute greatly to establishing baseline measurements.

Specific investigation of measurement differences between micro-CT, CT, and conventional radiography will be essential for improving the use of frontal ratios. Micro-CT and CT-derived measurements tend to be more equivalent (Lillie, Urban, Weaver, Powers, & Stitzel, 2015), but data on the amount of error that exists when comparing ratios derived via conventional radiographs versus micro-CT analysis will help to clarify when certain metric data can be used, and what limitations researchers should be aware of when making such comparisons. Previous studies have measured frontal bone thickness at different locations (e.g., Stuart-Macadam, 1987a; De Boer et al., 2016; Rivera and Lahr, 2017), and it will also be important to establish if differences exist between locations.

7.0 Conclusion

This study demonstrates that metric data can provide another line of evidence for anemia diagnosis in skeletal remains, particularly when assessing crania of growing individuals. The results presented here reiterate the importance of specifically evaluating changes related to marrow hyperplasia for anemia assessment and highlight the utility of methods that allow for analysis of the internal marrow space. Developing a standardized framework for diagnosing and reporting anemia allows for continued progress by ensuring consistency and repeatability across studies. Evaluation of porous cranial lesions can play a role in this framework, but is not the primary feature for assessing anemia. By incorporating metric data into the diagnostic process, researchers can better understand the relationship between marrow hyperplasia and anemia, leading to improved diagnostic accuracy and rigor in skeletal remains.

Acknowledgements

Ethics approval granted by the Hamilton Integrated Research Ethics Board. Thank you to Ville de Montréal (François Bélanger) and Conseil de la Fabrique de Sainte-Marie-de-Beauce for

access to collections. Additional thanks to Dr. Andrew Nelson for facilitating micro-CT imaging, and to Dr. Heather Hatch at the Museum of Ontario Archaeology for access to imaging facilities. Observers who participated in error testing and rubric development include: Rebecca Christenson, Amanda Cooke, Lily Godwin, Celine Jacqueroud, Julie Nguyen, Isabel Sealey, Dr. Thomas Siek, and the winter 2023 McMaster ANTHROP 4R03 class. Thank you to all observers for their feedback and participation. Thanks to Emilie Dion (Université de Montréal) who did the dental age estimations of the Quebec collections. This research was supported by a Social Science and Humanities Research Council (SSHRC) Joseph-Armand Bombardier Canada Graduate Scholarship, the McMaster University Shelley Saunders/Koloshuk Family Scholarship, a SSHRC Insight Grant (File Number: 435-2021-0665), the Canadian Association for Biological Anthropology Shelley R. Saunders Thesis Research Grant, and undertaken, in part, thanks to funding from the Canada Research Chairs program.

Data Availability Statement

Data are available in the supplementary material of this article.

Supplemental Data

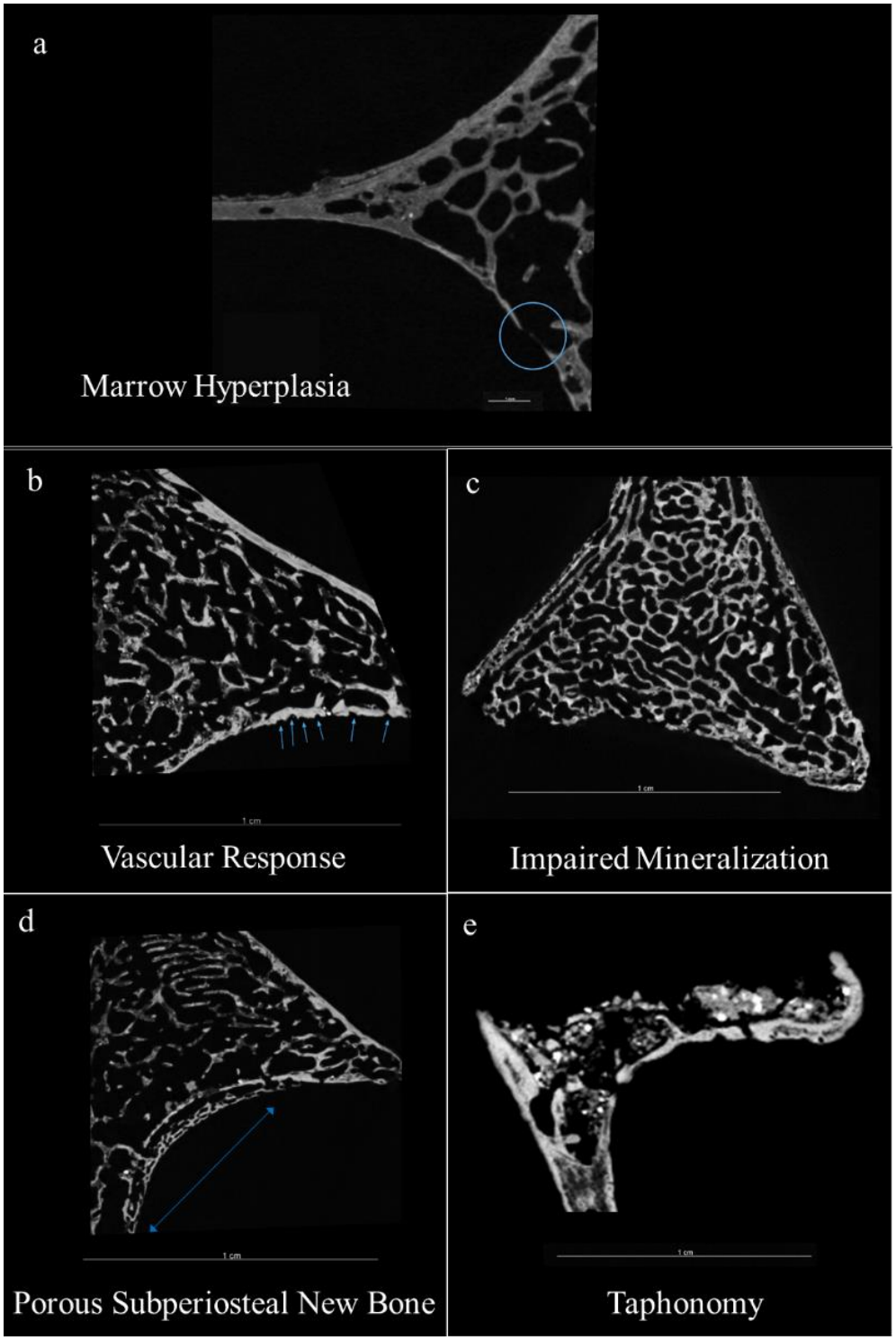

Figure 3-S1: a) Cortical thinning and subsequent porosity due to marrow expansion. b) Perforations due to vascular response. c) Gaps in the bone due to impaired mineralization. d) Periosteal new bone formation on the surface of the orbit, indicated by the arrow. e) Dirt and minerals inside the trabecular space mean that taphonomy cannot be excluded as a possible source of lesions.

Table 3-S1: Visual assessment scores for individuals used as part of the baseline group for measurement comparisons.

SKELETON ID	SITE	AGE (YEARS)*	CORTICAL THINNING SCORE	TRABECULAR SEPARATION SCORE	TRABECULAR THINNING SCORE	OVERALL VISUAL	FRONTAL RATIO[1]	ANEMIA ASSESSMENT
7A9-S44	Pointe-aux-Trembles, CA	0.25	3	0	1	NE	----	N
2E5	Ste-Marie, CA	0.25	1	1	1	NE	----	N
7A9-S48	Pointe-aux-Trembles, CA	0.50	3	0	0	NE	----	N
GRK-V102	Alkmaar, NL	0.75	3	0	1	NE	2.0	N
7A11-S63	Pointe-aux-Trembles, CA	0.75	1	1	1	NE	----	N
7A9-S21	Pointe-aux-Trembles, CA	0.75	1	1	1	NE	----	N
21N-S12	St-Antoine, CA	0.75	2	0	1	NE	----	N
20F-S6	St-Antoine, CA	0.75	1	0	0	NE	----	N
ARJB-V1084	Arnhem, NL	1.00	3	0	1	NE	----	N
20F-S9	St-Antoine, CA	1.00	1	1	1	NE	----	N
21N-S11	St-Antoine, CA	1.33	1	1	1	NE	----	N
GRK-V181	Alkmaar, NL	1.50	2	0	1	NE	----	N
7A2-S1	Pointe-aux-Trembles, CA	1.50	0	0	0	NE	----	N
20Z-S5	St-Antoine, CA	1.50	0	1	0	NE	----	N
8J-S4.2	St-Antoine, CA	1.50	1	0	0	NE	----	N
GRK-V63	Alkmaar, NL	1.50	1	1	1	NE	----	N
7A9-S55	Pointe-aux-Trembles, CA	1.75	1	1	1	NE	----	N
GRK-V169	Alkmaar, NL	3.50	1	0	0	NE	----	N
ARJB-V1762	Arnhem, NL	3.50	1	0	1	NE	0.5	N
ARJB-V452	Arnhem, NL	4.50	0	0	0	NE	----	N
7A9-C6	Pointe-aux-Trembles, CA	5.00	0	0	1	NE	----	N
EHVCK-3115	Eindhoven, NL	5.50	1	1	0	NE	2.1	N
GRK-V1	Alkmaar, NL	6.00	1	1	0	NE	----	N
EHVCK-3537	Eindhoven, NL	6.00	0	1	0	NE	----	N
EHVCK-979	Eindhoven, NL	7.00	0	0	0	NE	----	N
ZW87-303	Zwolle, NL	7.00	0	1	0	NE	----	N
ARJB-V1630	Arnhem, NL	10.00	0	1	0	NE	----	N

* Midpoint age estimate

NE= No visual evidence of skeletal manifestations of marrow hyperplasia

[1]Values over 2.5 were considered pathological by Panzer et al.,(2023) and Sebes & Diggs (1979), based on radiographic ratios from Reynolds (1962, 1965). See Section 5for further discussion on how frontal ratios were used in this study.

D= Diagnostic of H= Highly consistent with C= Consistent with N= Not consistent with

Table 3-S2: Raw microstructure measurement data.

Skeleton ID	Site	Age (years)*	CtThOL (mm)	TbSp (mm)	TbTh (mm)
7A11-S59	Pointe-aux-Trembles, CA	0.70	0.2	0.45	0.18
ARJB-V1625	Arnhem, NL	0.75	0.21	0.44	0.16
21E-S8	St-Antoine, CA	1.40	0.28	0.5	0.15
GRK-V807	Alkmaar, NL	1.00	0.12	0.45	0.14
2E3	Ste-Marie, CA	1.50	0.36	0.54	0.21
1G2	Ste-Marie, CA	1.50	0.37	0.49	0.19
ARJB-V1777	Arnhem, NL	1.50	0.15	0.35	0.15
GRK-V63	Alkmaar, NL	1.50	0.33	0.4	0.19
7A2-S32	Pointe-aux-Trembles, CA	1.58	0.21	0.49	0.18
ARJB-V478	Arnhem, NL	2.00	0.27	0.39	0.17
21E-S4	St-Antoine, CA	4.20	0.52	0.48	0.18
ARJB-V667	Arnhem, NL	3.00	0.47	0.46	0.16
ARJB-V1762	Arnhem, NL	3.50	0.42	0.48	0.17
ARJB-V1319	Arnhem, NL	4.00	0.45	0.58	0.17
21E-S14	St-Antoine, CA	7.00	0.52	0.54	0.21
ARJB-V1258	Arnhem, NL	9.00	0.45	0.56	0.15
7A11-S57	Pointe-aux-Trembles, CA	1.00	0.22	0.51	0.16
ARJB-V1812	Arnhem, NL	2.50	0.32	0.47	0.18
1G6	Ste-Marie, CA	4.00	0.38	0.51	0.19
21R-S5	St-Antoine, CA	5.00	0.39	0.54	0.17
21U-S6	St-Antoine, CA	8.00	0.28	0.6	0.22
30R-S7	St-Antoine, CA	10.00	0.5	0.71	0.18
20F-S39	St-Antoine, CA	0.50	0.19	0.42	0.16
17L-S4	St-Antoine, CA	1.00	0.24	0.53	0.17
7A2-S22	Pointe-aux-Trembles, CA	1.50	0.22	0.5	0.2
7A2-S24	Pointe-aux-Trembles, CA	1.50	0.2	0.47	0.17
GRK-V326	Alkmaar, NL	1.50	0.19	0.42	0.14
GRK-V532	Alkmaar, NL	1.50	0.12	0.35	0.14
2G3	Ste-Marie, CA	2.50	0.26	0.46	0.2
20A-S3	St-Antoine, CA	4.00	0.32	0.6	0.18
21F-S5	St-Antoine, CA	4.00	0.31	0.52	0.2
20F-S2	St-Antoine, CA	7.00	0.37	0.51	0.22
ARJB-V1735	Arnhem, NL	9.50	0.36	0.65	0.18
7A2-S6	Pointe-aux-Trembles, CA	0.86	0.17	0.38	0.15
2E5	Ste-Marie, CA	0.25	0.17	0.32	0.18
7A2-S10	Pointe-aux-Trembles, CA	0.50	0.2	0.37	0.17
7A9-S44	Pointe-aux-Trembles, CA	0.25	0.14	0.32	0.15
7A9-S12	Pointe-aux-Trembles, CA	0.38	0.21	0.31	0.16
7A9-S48	Pointe-aux-Trembles, CA	0.50	0.21	0.31	0.19
21N-S11	St-Antoine, CA	1.33	0.27	0.37	0.17
21N-S12	St-Antoine, CA	0.75	0.16	0.33	0.16
7A11-S63	Pointe-aux-Trembles, CA	0.75	0.16	0.38	0.16
7A9-S21	Pointe-aux-Trembles, CA	0.75	0.22	0.46	0.16
GRK-V102	Alkmaar, NL	0.75	0.11	0.22	0.14
ARJB-V1084	Arnhem, NL	1.00	0.13	0.26	0.14
20F-S6	St-Antoine, CA	0.75	0.22	0.37	0.19

* Midpoint age estimate
CtThOL= Average cortical thickness of the orbital lamina
TbSp= Average trabecular separation
TbTh=Average trabecular thickness

Table 3-S2 Cont'd**:** Raw microstructure measurement data.

Skeleton ID	Site	Age (years)*	CtThOL (mm)	TbSp (mm)	TbTh (mm)
20Z-S5	St-Antoine, CA	1.50	0.35	0.48	0.2
7A2-S1	Pointe-aux-Trembles, CA	1.50	0.31	0.45	0.2
8J-S4.2	St-Antoine, CA	1.50	0.28	0.45	0.2
GRK-V181	Alkmaar, NL	1.50	0.22	0.45	0.17
7A9-S55	Pointe-aux-Trembles, CA	1.75	0.27	0.47	0.18
GRK-V169	Alkmaar, NL	3.50	0.33	0.29	0.16
20F-S9	St-Antoine, CA	1.00	0.27	0.41	0.21
ARJB-V452	Arnhem, NL	4.50	0.5	0.51	0.18
7A9-C6	Pointe-aux-Trembles, CA	5.00	0.37	0.27	0.19
EHVCK-3115	Eindhoven, NL	5.50	0.35	0.46	0.2
EHVCK-3537	Eindhoven, NL	6.00	0.42	0.51	0.22
GRK-V1	Alkmaar, NL	6.00	0.37	0.45	0.17
EHVCK-979	Eindhoven, NL	7.00	0.48	0.41	0.24
ZW87-303	Zwolle, NL	7.00	0.48	0.58	0.26
ARJB-V1630	Arnhem, NL	10.00	0.52	0.48	0.22

* Midpoint age estimate
CtThOL= Average cortical thickness of the orbital lamina
TbSp= Average trabecular separation
TbTh=Average trabecular thickness

References

Agarwal, K. N., Drar, N., Shah, M. M., & Bhardwaj, O. P. (1970). Roentgenologic changes in iron deficiency anemia. *American Journal of Roentgenology*, *110*(3), 635-637.

Anderson, A. S. (2023). Observer agreement on the morphology of porous cranial lesions: Results from a workshop at the 2019 meeting of the Paleopathology Association. *International Journal of Paleopathology*, *43*, 68-71.

Anderson, A. S., Sutherland, M. L., O'Donnell, L., Hill, E. C., Hunt, D. R., Blackwell, A. D., & Gurven, M. D. (2021). Do computed tomography findings agree with traditional osteological examination? The case of porous cranial lesions. *International Journal of Paleopathology*, *33*, 209-219.

Angel, J. L. (1966). Porotic hyperostosis, anemias, malarias, and marshes in the prehistoric eastern Mediterranean. *Science*, *153*(3737), 760-763.

Appleby, J., Thomas, R., & Buikstra, J. (2015). Increasing confidence in paleopathological diagnosis–Application of the Istanbul terminological framework. *International Journal of Paleopathology*, *8*, 19-21.

Arts, N., & Altena, E. (2013). *Een knekelveld maakt geschiedenis: het archeologisch onderzoek van het koor en het grafveld van de middeleeuwse Catharinakerk in Eindhoven, circa 1200-1850*. Uitgeverij Matrijs.

Baetsen, S. (2001). Graven in de Grote Kerk. Het fysisch antropologisch onderzoek van de graven in de St. Laurenskerk van Alkmaar. *Rapporten over de Alkmaarse Monumentenzorg en Archeologie (RAMA)*, *8*.

Baetsen, W. A., & Zielman, G (Eds.). (2020). *Wat de nieuwe Sint Jansbeek boven water bracht: dood en leven in het Arnhemse verleden; Archeologisch onderzoek Sint Jansbeek te Arnhem, volume 2. RAAP report 4476-2*. Weesp: RAAP Archeologisch Adviesbureau.

Belgın, C. A., Serindere, G., & Orhan, K. (2019). Accuracy and reliability of enamel and dentin thickness measurements on micro-computed tomography and digital periapical radiographs. *Journal of Forensic Radiology and Imaging*, *18*, 32-36.

Berger, A. J., & Kahn, D. (2012). Growth and development of the orbit. *Oral and Maxillofacial Surgery Clinics*, *24*(4): 545-555.

Binkley, N., Adler, R., & Bilezikian, J. P. (2014). Osteoporosis diagnosis in men: The T-score controversy revisited. *Current Osteoporosis Reports*, *12*, 403-409.

Bitter, P. (2002). *Graven en begraven: Archeologie en geschiedenis van de Grote Kerk van Alkmaar*. Verloren.

Brickley, M. B. (2018). Cribra orbitalia and porotic hyperostosis: A biological approach to diagnosis. *American Journal of Physical Anthropology*, 167(4), 896-902.

Brickley, M. B. (2024). Perspectives on anemia: Factors confounding understanding of past occurrence. *International Journal of Paleopathology*, *44*, 90-104.

Brickley, M. B., & Morgan, B. (2022). Metabolic and endocrine diseases. In A.L. Grauer (Ed.) *The Routledge Handbook of Paleopathology* (pp. 338-359). Routledge.

Brickley, M. B., & Morgan, B. (2023). Assessing diagnostic certainty for scurvy and rickets in human skeletal remains. *American Journal of Biological Anthropology*, *181*(4), 637-645.

Brickley, M. B., Ives, R., & Mays, S. (2020). *The bioarchaeology of metabolic bone disease*. Academic Press.

Buckberry, J., Ali, A., Hebda, M., Evans, A., Sparrow, T., Koon, H., & Wilson, A. (2023). Visualizing cribra orbitalia using modern imaging techniques [conference presentation]. In Monge Calleja, A. M., Santos, A. L., & Gomes, R.A.M.P. (Coord.). *International Meeting on Porous Skeletal Lesions: Achievements and future directions. Program and Abstract Book*. University of Coimbra, Research Centre in Anthropology and Health (CIAS). http://hdl.handle.net/10316/108791.

Buie, H. R., Campbell, G. M., Klinck, R. J., MacNeil, J. A., & Boyd, S. K. (2007). Automatic segmentation of cortical and trabecular compartments based on a dual threshold technique for in vivo micro-CT bone analysis. *Bone*, *41*(4), 505-515.

Buikstra, J. E., Cook, D. C., & Bolhofner, K. L. (2017). Introduction: Scientific rigor in paleopathology. *International journal of paleopathology*, *19*, 80-87.

Clevis, H. H. C. C., & Constandse-Westermann, T. (1992). *De doden vertellen. Opgraving in de Broerenkerk te Zwolle 1987-88.* Stichting Archaeologie Ijssel/Vechtstreetk.

De Boer, H. H., Van der Merwe, A. E., & Soerdjbalie-Maikoe, V. (2016). Human cranial vault thickness in a contemporary sample of 1097 autopsy cases: relation to body weight, stature, age, sex and ancestry. *International Journal of Legal Medicine*, *130*, 1371-1377.

Durdin, R. R. (2020). *A Diagnosis of Cribra Orbitalia and Porotic Hyperostosis Using Cranial Vault Thickness* [Doctoral dissertation]. The University of Mississippi (USA).

Ethnoscop. (2006). Site du premier cimetière de Sainte-Marie, CcEs-1. Inventaire et fouilles archéologiques 2003-2004. Internal archaeological report. Ministère des transports du Québec, Direction de Chaudière-Appalaches.

Ethnoscop. (2016a). Projet de réaménagement de la place du Canada. Site archéologique du cimetière Saint-Antoine (1799–1854), BiFj-37, Montréal. Fouille et supervision archéologique (2014). Internal archaeological report. Ville de Montréal.

Ethnoscop. (2016b). Interventions archéologiques dans le cadre du projet de construction de la Maison du citoyen à Pointe-aux-Trembles, 2014, BjFi-17. Internal archaeological report. Rivière-des-Prairies, Pointe-aux-Trembles et Ville de Montréal.

Galea, J. (2013). *Analysing the microarchitecture of cribra orbitalia via micro-computed tomography in post-medieval remains from the Bristol Royal Infirmary* [Doctoral dissertation]. University of Bristol (UK).

Grauer, A. L. (2019). Circulatory, reticuloendothelial, and hematopoietic disorders. In J.E Buikstra (Ed.) *Ortner's identification of pathological conditions in human skeletal remains* (pp. 491-529). Academic Press.

Gustafson, G., & Koch, G. (1974). Age estimation up to 16 years of age based on dental development. *Odontologisk revy*, *25*, 297-306.

Hengen, O. P. (1971). Cribra orbitalia: pathogenesis and probable etiology. *Homo*, *22*, 57-75.

Hershkovitz, I., Rothschild, B. M., Latimer, B., Dutour, O., Léonetti, G., Greenwald, C. M., ... & Jellema, L. M. (1997). Recognition of sickle cell anemia in skeletal remains of children. *American Journal of Physical Anthropology*, *104*(2), 213-226.

Jaffe, H. L. (1972). *Metabolic, degenerative, and inflammatory diseases of bones and joints*. Lea and Febeiger.

Kanis, J. A., Melton, L. J., Christiansen, C., Johnston, C. C., & Khaltaev, N. (1994). The diagnosis of osteoporosis. *Journal of Bone and Mineral Research*, *9*(8), 1137-1141.

Karaguzel, G., & Holick, M. F. (2010). Diagnosis and treatment of osteopenia. *Reviews in Endocrine and Metabolic Disorders*, *11*(4), 237-251

Klaus, H. D., & Lynnerup, N. (2019). Abnormal bone: considerations for documentation, disease process identification, and differential diagnosis. In *Ortner's identification of pathological conditions in human skeletal remains* (pp. 59-89). Academic Press.

Lewis, M. E. (2012). Thalassaemia: its diagnosis and interpretation in past skeletal populations. *International Journal of Osteoarchaeology*, *22*(6), 685-693.

Lillie, E. M., Urban, J. E., Weaver, A. A., Powers, A. K., & Stitzel, J. D. (2015). Estimation of skull table thickness with clinical CT and validation with microCT. *Journal of anatomy*, *226*(1), 73-80.

Mays, S. (2018). How should we diagnose disease in palaeopathology? Some epistemological considerations. *International Journal of Paleopathology*, *20*, 12-19.

McHugh, M. L. (2012). Interrater reliability: The Kappa statistic. *Biochemia Medica*, *22*(3), 276-282.

Morgan, B., Zeller, M., Ribot, I., & Brickley, M. B. (2024). Skeletal manifestations of anemia in the sternum in a modern clinical sample: An initial investigation. *Journal of Archaeological Science, 164*, 105942.

Morgan, J. A. (2014). *The methodological and diagnostic applications of micro-CT to palaeopathology: a quantitative study of porotic hyperostosis* [Doctoral thesis]. The University of Western Ontario (Canada).

Naveed, H., Abed, S. F., Davagnanam, I., Uddin, J. M., & Adds, P. J. (2012). Lessons from the past: Cribra orbitalia, an orbital roof pathology. *Orbit*, *31*(6), 394-399.

O'Donnell, L., Buikstra, J. E., Hill, E. C., Anderson, A. S., & O'Donnell Jr, M. J. (2023). Skeletal manifestations of disease experience: Length of illness and porous cranial lesion formation in a contemporary juvenile mortality sample. *American Journal of Human Biology*, e23896.

O'Donnell, L., Hill, E. C., Anderson, A. S. A., & Edgar, H. J. (2020). Cribra orbitalia and porotic hyperostosis are associated with respiratory infections in a contemporary mortality sample from New Mexico. *American Journal of Physical Anthropology*, *173*(4), 721-733.

Oxenham, M. F., & Cavill, I. (2010). Porotic hyperostosis and cribra orbitalia: the erythropoietic response to iron-deficiency anaemia. *Anthropological Science*, 118(3), 199-200.

Panzer, S., Schneider, K. O., Zesch, S., Rosendahl, W., Thompson, R. C., & Zink, A. R. (2023). Anemias in ancient Egyptian child mummies: Computed tomography investigations in European museums. *International Journal of Osteoarchaeology, 33(*3), 532-545.

Reynolds, J. (1962). An evaluation of some roentgenographic signs in sickle cell anemia and its variants. *Southern Medical Journal*, *55*(11), 1123-8.

Reynolds, J. (1965). The roentgenological features of sickle cell disease and related hemoglobinopathies. Charles C Thomas Publisher.

Rivera, F., & Mirazón Lahr, M. (2017). New evidence suggesting a dissociated etiology for cribra orbitalia and porotic hyperostosis. *American Journal of Physical Anthropology*, *164*(1), 76-96.

Saint-Martin, P., Dedouit, F., Rérolle, C., Guilbeau-Frugier, C., Dabernat, H., Rougé, D., ... & Crubézy, E. (2015). Diagnostic value of high-resolution peripheral quantitative computed tomography (HR-pQCT) in the qualitative assessment of cribra orbitalia–A preliminary study. *Homo*, *66*(1), 38-43.

Santos, A.L., Gomes, R., & Monge, A. (2023, August 9-11). *Lesiones esqueléticas porosas: Tiempos de parar, sopesar y reiniciar* [conference presentation]. 9th Annual PAMinSA Meeting, Bolivia.

Schats, R. (2023). Developing an archaeology of malaria. A critical review of current approaches and a discussion on ways forward. *International Journal of Paleopathology*, *41*, 32-42.

Sebes, J. I., & Diggs, L. W. (1979). Radiographic changes of the skull in sickle cell anemia. *American Journal of Roentgenology*, *132*(3), 373-377.

Stuart-Macadam, P. (1987a). A radiographic study of porotic hyperostosis. *American Journal of Physical Anthropology*, *74*(4), 511-520.

Stuart-Macadam, P. (1987b). Porotic hyperostosis: new evidence to support the anemia theory. *American Journal of Physical Anthropology*, *74*(4), 521-526.

Tawfik, H. A., & Dutton, J. J. (2018). Embryologic and fetal development of the human orbit. *Ophthalmic Plastic & Reconstructive Surgery*, *34*(5), 405-421.

Walker, P. L., Bathurst, R. R., Richman, R., Gjerdrum, T., & Andrushko, V. A. (2009). The causes of porotic hyperostosis and cribra orbitalia: A reappraisal of the iron-deficiency-anemia hypothesis. *American Journal of Physical Anthropology, 139*(2), 109-125.

Wapler, U., Crubézy, E., & Schultz, M. (2004). Is cribra orbitalia synonymous with anemia? Analysis and interpretation of cranial pathology in Sudan. *American Journal of Physical Anthropology*, *123*(4), 333-339.

World Health Organization. (2011). *Haemoglobin concentrations for the diagnosis of anaemia and assessment of severity* (No. WHO/NMH/NHD/MNM/11.1). World Health Organization.

Zuckerman, M. K., Garofalo, E. M., Frohlich, B., & Ortner, D. J. (2014). Anemia or scurvy: A pilot study on differential diagnosis of porous and hyperostotic lesions using differential cranial vault thickness in subadult humans. *International Journal of Paleopathology*, *5*, 27-33.

CHAPTER 4: CO-OCCURRENCE OF ANEMIA AND SCURVY IN 18TH-19TH CENTURY QUEBEC

Title: Co-Occurrence of Anemia and Scurvy in 18th-19th Century Quebec

Brianne Morgan[a], Julie Nguyen[a], Isabelle Ribot [b], & Megan B. Brickley [a]

[a] McMaster University, Department of Anthropology, Hamilton, Ontario, Canada, L8S 4L9, morgab5@mcmaster.ca, nguyj9@mcmaster.ca, brickley@mcmaster.ca

[b] University of Montréal, Department of Anthropology, Montréal, Québec, Canada, QCH3T 1N8 i.ribot@umontreal.ca

Prepared for submission to PLOS One.

Abstract

During the 18th-19th century, Quebec underwent political, environmental, and social transitions. Many urban and rural communities experienced food insecurity, and are likely to have been affected by multiple metabolic bone diseases. For vulnerable groups, such as children, clustering of multiple metabolic conditions may have significantly affected health and mortality. This research is the first broader-scale study of the specific co-occurrence of scurvy/anemia, and seeks to assess these conditions across urban and rural sites from 18th-19th century Quebec to understand how metabolic bone disease affected mortality in these contexts. Individuals under 15 years old from three skeletal collections were assessed for scurvy (n=55), anemia (n=37), and co-occurrence (n=31). Scurvy was evaluated macroscopically, anemia was assessed using micro-CT analysis, and co-occurrence was considered in those that could be assessed for both conditions. Prevalence and age-at-death data were compared between contexts and across diagnoses. Scurvy was associated with younger ages-at-death; this trend was most noticeable in the village site of Pointe-aux-Trembles, where scurvy prevalence was significantly higher and mean age-at-death was significantly lower. Co-occurrence was diagnosed in 6.5% of assessed individuals, and individuals with both conditions had a lower average age-at-death estimate than those with neither condition. The sample size of those who could be assessed for co-occurrence was small, making interpretations of trends difficult. Local variation in factors such as weaning practices contributed to some differences in trends between sites, but disease prevalence overall was high in comparison to other contexts, demonstrating the challenges that affected individuals in both urban and rural environments across Quebec at this time.

Keywords: metabolic bone disease, paleopathology, mortality trends, age-at-death, weaning

1.0 Introduction

Metabolic bone conditions are often related to nutrition and food insecurity, which tend to cluster in vulnerable groups, and increase the risk of individuals developing more than one metabolic bone condition (1). Contexts with known nutritional deficiencies or food insecurities allow for multiple metabolic bone diseases to be studied, and for consideration of the variables that might have affected disease dynamics. Broadly, Quebec during the 18th-19th century is one such context; metabolic bone conditions have been documented amongst colonial groups from this period and earlier as they adapted to new nutritional landscapes and underwent significant political changes (2,3,4,5,6). On a local level, urban and rural settlements in colonial Quebec contended with different risk factors that affected mortality, such as differences in subsistence pathways and variable levels of epidemic disease risk (7,8). Assessing metabolic bone disease co-occurrence and clustering is crucial for understanding how social, environmental, political, and biological variables can affect health and contribute to mortality risk (9,10,11).

Scurvy and acquired anemia from nutritional deficiencies are conditions that are particularly likely to co-occur. Scurvy is a deficiency in vitamin C, while anemia is a reduction in the body's capacity to transport oxygen (12,13). Despite the known associations between anemia and scurvy, there has been little investigation of how co-occurrence of these conditions might affect past communities. In paleopathology, the term co-occurrence means that multiple conditions are thought to have "exist[ed] at the same time, and [are] thought likely to be causally related" (10, p227); the relationship between vitamin C deficiency and anemia means that co-occurrence, under this definition, is highly likely in archaeological samples. Therefore, the purpose of this paper is to explore differences in mortality patterns and the prevalence of anemia, scurvy, and co-occurrence amongst individuals under the age of 15 years from urban (Saint-Antoine), rural (Sainte-Marie) and suburban (Pointe-aux-Trembles) communities in 18th-19th century Quebec. Furthermore, this research aims to better understand how these conditions may have differentially affected health and mortality risk amongst vulnerable individuals.

2.0 Background

2.1 Historical context

Throughout the 1700s and 1800s, Quebec underwent a series of political, cultural, and environmental shifts. The Conquest of 1760 marked the beginning of British governance of Quebec, and this event plus the subsequent passing of the Quebec Act in 1774 led to a general decline in socioeconomic status of Quebec's French Canadian (Catholic) population (3,15). The onset of industrialization in urban centres like Montréal and Quebec City led to rapid urbanization and a drastic increase in population size due to high fertility rates and immigration starting in the early-mid 19th century (7,16). These changes contributed to higher urban mortality (16, 17a,18a). Factors such as high population density, poor sanitary infrastructure, and difficulties in affording adequate housing contributed to large-scale epidemics of cholera, smallpox, and typhus that significantly increased urban mortality (3,16,19). Previous archaeological work has identified evidence for metabolic bone diseases in urban French Canadian (20) and English Protestant (21,22,23) samples.

In general, both urban and rural Quebecois communities consumed standard agricultural diets, which included beef, chicken, and pork, along with vegetables like potatoes, peas, and pumpkins (24, 25). Grain was a major food source, and wheat made up over 65% of the harvest for many rural agricultural villages (26). While this diet would provide adequate nutrition, access to these foods varied among different communities. Historical accounts depicting this idealized diet are primarily from middle- and upper-class individuals, and those from lower social classes did not likely have access to these same resources (27). Environmental challenges, such as long-lasting winters and crop failures, often meant that staple foods were not readily available, and prices subsequently increased (24). Children would also have consumed different foods from adults; for example, weaning foods typically included porridge or bread soaked in water, which do not contain any vitamin C or iron, and minimal folate (8,16,21), increasing the risk of developing scurvy and nutritionally-acquired anemia in the early years of life.

During this period, infant and childhood mortality rates in Quebec were notably higher compared to similar contexts in Britain and France (8,28). For urban children in particular, mortality was even higher, and was reported to be about 1.5 times higher than in rural villages (16,18). Rural villages were thought to be safer and healthier than cities like Montreal or Quebec City (8,29), and rural people may have had foodways (i.e. subsistence farming versus buying food) that ultimately decreased the risk of metabolic bone conditions.

2.2 Anemia and scurvy co-occurrence

In clinical settings, anemia is commonly reported in late-stage cases of scurvy (13). The association between scurvy and anemia is partially due to the various roles that vitamin C plays within the body. Vitamin C is essential for iron absorption, folate level maintenance, and wound healing (13,30,31), all of which mean that anemia can result if vitamin C is deficient. When anemia occurs as a direct result of scurvy, the type of anemia that can develop is highly variable, and is dependant on the presence of nutritional deficiencies and the length/severity of the vitamin C deficiency (13,31). For example, megaloblastic anemia in scurvy develops if folate/vitamin B12 levels are affected, while iron-deficiency anemia (IDA) can manifest due to a lack in dietary iron, blood loss, or impaired iron absorption, and it is possible for multiple forms of anemia to develop at the same time (31,32).

In addition to the physiological link between vitamin C deficiency and anemia, scurvy and anemia also co-occur due to the risk factors they have in common, such as low socioeconomic status, limited access to nutritious food, or an individual's higher nutritional requirements (33,34,35). When scurvy and anemia co-occur, overall immune function is worsened, and cardiac complications may result, which can lead to long term difficulties and heart failure, further heightening mortality risk (13).

2.3 Skeletal manifestations of anemia and scurvy

Skeletal lesions in scurvy are the result of an inflammatory response to haemorrhage and bleeding (36). Vitamin C is an essential catalyst for collagen formation and deficiency results in increased risk of blood vessel rupture and hemorrhage (37). When hemorrhage occurs near bone, abnormal porosity that is less than 1 mm in diameter can form because of new blood vessel

formation in that area, and a buildup of blood can cause irritation or elevation of the periosteum, leading to deposition of subperiosteal new bone (SPNB) (38,39,40). Its role in collagen formation means that vitamin C is essential for new bone formation, and generalized osteopenia can occur as a result of deficiency (39,41). However, as only small amounts of vitamin C are necessary for SPNB formation (39), deposition of new bone as an inflammatory response can occur even during active cases of vitamin C deficiency. Lesions in scurvy are concentrated near muscle origins/insertions, especially around muscles that are regularly used, and where a blood vessel is positioned between the muscle and the bone (36,39,40). Individuals in earlier stages of growth and development are more likely to develop lesions, as the periosteum is more loosely attached, making it easier to disrupt, and the body's capacity for capillary growth and new bone formation are elevated (10,36). Scurvy diagnosis in skeletal remains should consider the distribution of lesions and the age of the individual, as well as contextual information (42).

Anemia is characterized by a reduction in the body's ability to supply oxygen to its organs and tissues, often due to of blood loss, decreased red blood cell (RBC) production, or increased RBC destruction (42). Active bone marrow, where RBCs are produced, can expand to correct the RBC deficiency ('marrow hyperplasia'), and may lead to subsequent skeletal changes. Cortical thinning, trabecular thinning, loss of trabecular number and increased intertrabecular spacing are common microstructure manifestations of marrow hyperplasia (42,43), and these properties of bone can be measured to suggest anemia (44). Skeletal manifestations of marrow hyperplasia will only occur at sites of active bone marrow, which changes with age (45). In those under 6 years old, changes tend to develop in the cranium (45).

In the case of rickets and scurvy, co-occurrence can inhibit the formation of characteristic skeletal lesions for each individual disease (46). For scurvy and anemia, co-occurrence does not seem to prohibit the typical skeletal manifestations of each condition; medical and animal studies support the idea that marrow is increasingly hypercellular and therefore capable of undergoing marrow hyperplasia during periods of scurvy, and many clinical cases of co-occurrence display radiographic signs of scurvy (e.g. white lines of Fraenkel, Pelkin fractures) and subperiosteal new bone formation (47,48). In some cases, co-occurrence of anemia and scurvy may exacerbate the development of skeletal changes. Scurvy can lead to generalized osteopenia and in those with less bone than might normally be anticipated, reduced bone levels may mimic skeletal manifestations of marrow hyperplasia. Cortical thinning that occurs due to marrow hyperplasia can also exacerbate porosity caused by scurvy. Diagnosis of these conditions, therefore, should consider if the presence of the other condition has changed lesion appearance. Skeletal changes that could have multiple possible causes should never be attributed to just one condition.

3.0 Materials and Methods

3.1 Age-at-death estimation and sample composition

To investigate the local factors that could have been affecting childhood mortality, collections from both urban and rural environments were used in this study (Figure 4-1). The Sainte-Marie-de-Beuce cemetery collection (1748-1864) is from a rural village in southeastern

Quebec consists of 62 individuals excavated from a cemetery that contains over 600 burials (49). The site is located on the east bank of the Chaudière river, and preservation was notably poorer for some nonadult individuals at this site (49). The Pointe-aux-Trembles collection (1709-1843) consists of 63 individuals and also represents just part of the cemetery (50). Pointe-aux-Trembles was a suburban fortified village located just outside of Montréal and the proportion of children in this collection may be higher than the other collection due to the practice of sending children to the village to be wet-nursed (50). The Saint-Antoine collection (1799-1854) is from the Saint-Antoine French-Canadian cemetery within Montréal itself; over 600 burials have been identified during various archaeological projects from 1993 to 2015 (51). Preservation at Saint-Antoine was poorer than at the other two sites, which could have affected the proportion of nonadults in the collection.

Age-at-death estimation was done using dental development (52), and individuals from birth to the age of 15 years were evaluated. The initial sample size of nonadults included all individuals within this age range and was composed of 119 individuals (31 from Pointe-aux-Trembles, 30 from Sainte-Marie, and 58 from Saint-Antoine). However, not all individuals could be included in the total sample, leaving a final sample size of 61. Figure 4-2 shows the breakdown of this sample into smaller samples of those who could be evaluated for scurvy (n=55), anemia (n=37), and co-occurrence (n=31) from each site. To be included in the scurvy sample, individuals needed to have a combination of assessable skeletal features that included at least one of the greater wing of the sphenoid, foramen rotundum, and/or posterior scapula, plus at least one additional key location listed in Table 4-1. Exclusion from the sample was not based on a certain threshold preservation percentage, as diagnostic certainty can be assigned with relatively few lesions depending on their range and expression (41). To be included in the

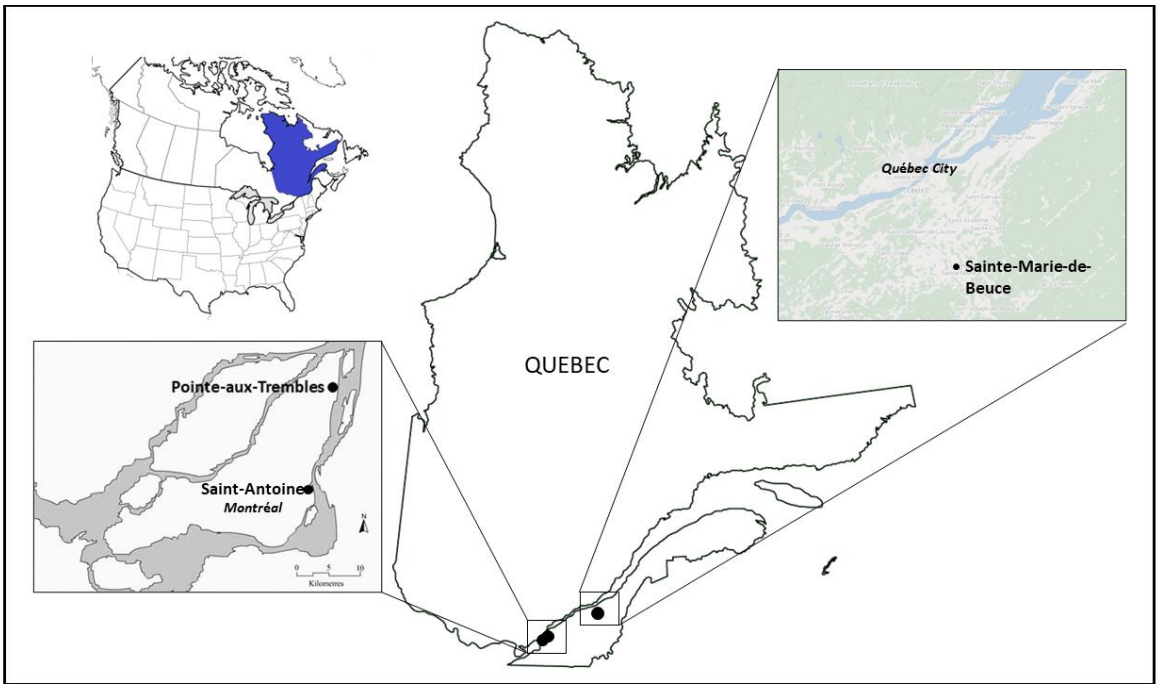

Figure 4-1: Map of the province of Quebec showing the sites of all samples. The insert in the top left shows Quebec (shaded) relative to the rest of North America.

anemia sample, individuals needed to have at least one orbit with no obvious outside taphonomic damage. The co-occurrence sample comprised individuals who could be evaluated for scurvy and an orbit that could undergo micro-CT analysis.

An important consideration when interpreting paleodemographic and paleopathological trends is the representativeness of the excavated samples. For all three collections, samples were derived from archaeological rescue excavations, and only a portion of the cemeteries were excavated (18a,49,50,51), meaning there may be missing individuals that affect interpretations. Duchemin (18a) found that individuals under one year may be underrepresented in the Saint-Antoine osteological sample based on comparisons to demographic census data, and that individuals under one year in the Pointe-aux-Trembles collection may be slightly overrepresented. Therefore, the interpretations of mortality trends and prevalence data derived from these samples are conservative, and further data may affect conclusions in the future.

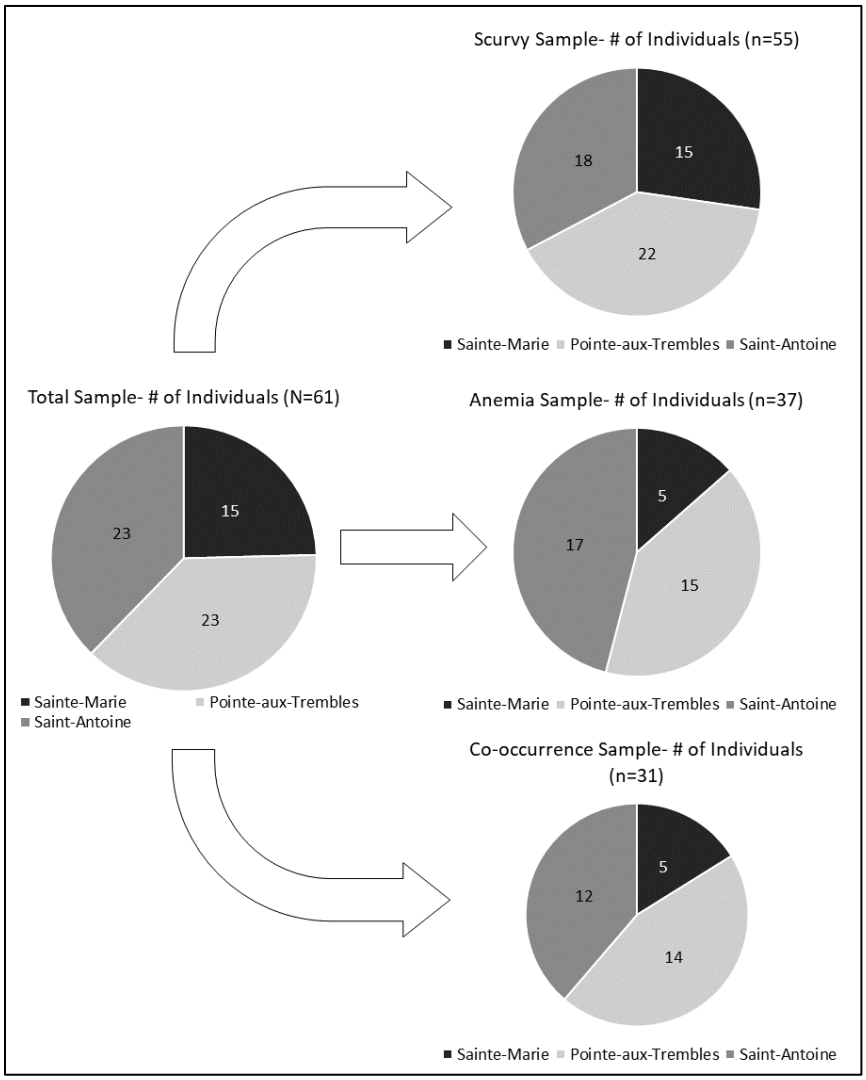

Figure 4-9: Breakdown of total sample into scurvy sample (those assessable for scurvy), anemia sample (those assessable for anemia), and co-occurrence sample (those assessable for co-occurrence), showing distribution of individuals in each sample by site. Number of individuals in each sample is presented.

3.1 Scurvy diagnosis

Scurvy diagnosis followed the process set out by Brickley and Morgan (41). To do this, the entire skeleton was evaluated macroscopically, and lesions associated with scurvy, including SPNB, porosity, and blood vessel impressions, were assessed at locations that are typically affected in scurvy (Table 4-1). Expression and development of lesions was evaluated, and lesion location, presence of mixed lesions and bilaterality of lesions was recorded. Microscopic examination of lesions was done using a Keyence Portable Digital microscope to clarify scoring of lesions. Porosity is expected as part of growth and development, and the use of microscopic imaging, in addition to thorough recording, helped to differentiate between etiologies of observed porosity.

The lesion locations and descriptions presented in Table 4-1 are not all equally associated with scurvy, for example, porosity on the alveolar process is also seen in dental disease and as a part of normal tooth development, while bilateral 'Ortner' porosity on the greater wing of the sphenoid is much more specific to scurvy (41). These differences were considered as part of diagnosis. Final scurvy diagnoses were done following Brickley & Morgan (41), and cases were classified as "diagnostic of scurvy", highly consistent with scurvy", "consistent with scurvy", and "not consistent with scurvy" based on the framework for assigning diagnostic certainty (Supplemental Tables 4-S1-S3). Using this framework, most cases diagnosed as scurvy are expected to be classified as 'highly consistent with', as cases need to meet more specific criteria (i.e. bilaterality of lesions must be assessable) to fall under the 'diagnostic of' category.

Table 4-2: List of key locations examined for lesions associated with scurvy.

Bone	**Location**	**Core Lesions Expected in Scurvy**
Sphenoid	*Greater wing*	SPNB, porosity, mixed lesions
	Foramen rotundum	SPNB, porosity, mixed lesions
Orbit		SPNB, porosity, mixed lesions
Maxilla	*Infraorbital Foramen*	SPNB, porosity, mixed lesions
	Posterior	SPNB, porosity, mixed lesions
	Palate	Porosity
	Alveolar Bone	SPNB, porosity, mixed lesions
Mandible	*Mylohyoid line*	SPNB, porosity, mixed lesions, blood vessel impressions
	Medial coronoid process	Porosity
	Alveolar bone	SPNB, porosity, mixed lesions
Scapula	*Supraspinous fossa*	SPNB, porosity, mixed lesions
	Infraspinous fossa	SPNB, porosity, mixed lesions
Medial zygomatic		SPNB, porosity, mixed lesions
Cranial vault	*Endocranial surface*	SPNB, porosity, blood vessel impressions
	Ectocranial surface	SPNB, porosity, mixed lesions
Medial ilium		SPNB, porosity, mixed lesions
Long bone metaphyses		SPNB, porosity (past cut-back zone)

Sources for table: 36,38-41,46,53

3.2 Anemia diagnosis

Individuals in this sample had been previously analyzed and assessed for anemia in a study by Morgan et al. (44) (Supplemental Data Table 4-S4). Those diagnoses were used in the

current study. In summary, the orbits were analyzed using the Nikon XTH-225ST micro-CT scanner at the Ancient Images Lab of the Museum of Ontario Archaeology and rreconstruction of the 3D volume was done in CT Pro 3D (v. 4.4.4). Analysis was done in Dragonfly (v. 2021.3) (https://www.theobjects.com/dragonfly/index.html). Visual evaluation of bone microstructure, microstructure measurement T-scores, and relative cortical bone ratios of the frontal bone were all used for the final anemia diagnoses.

Only the frontal bone (including orbits) was used for anemia diagnoses, as metric approaches are still in an early stage of development. Future development of approaches may allow for incorporation of post-cranial elements, and other data that allows for further refinement of anemia diagnoses. Therefore, the anemia diagnoses used in this study are conservative, and the highest diagnostic certainty that could be achieved with currently available methods is 'highly consistent with'.

3.3 Co-occurrence diagnosis and mortality trends

Co-occurrence was diagnosed in individuals who had been assigned to the 'diagnostic of' or 'highly consistent with' categories of certainty for scurvy, and the 'highly consistent with' category for anemia. As part of the diagnostic frameworks for both scurvy and anemia, other diseases or conditions that could have caused skeletal lesions or changes are considered, and for this study, interpretations of observed skeletal features and assignment of diagnostic certainty specifically considered if co-occurrence could have exacerbated skeletal manifestations of either scurvy or anemia. Comparisons of crude prevalence were made across sites in the scurvy sample (n=55), anemia sample (n=37), and co-occurrence sample (n=31). Fisher's Exact tests were used when total sample sizes were under 30 (two-tailed, α=0.05), and chi-square tests were used for other cases (two-tailed, α=0.05). Using midpoint age-at-death estimates, age-at-death distributions were created for each of the three contexts using the total sample, and for those with different diagnoses. Welch's independent two-sample t-tests (α=0.05) were used to assess if mean-age-at-death differed between sites, and two-sample Kolmogorov–Smirnov tests (α=0.05) were used to assess if age-at-death distributions differed between those diagnoses with and without different conditions. Statistical analysis was done in SPSS Statistics 29.0 and Microsoft Excel 2016.

4.0 Results

4.1 Scurvy, anemia, and co-occurrence crude prevalence

Table 4-2 shows the crude prevalence of scurvy, anemia, and co-occurrence across the individuals assessable for each. Supplemental Data Table 4-S1-S3 shows recording of lesions specific to scurvy, Table 4-S4 shows the data used for the anemia assessments, and Table 4-S5 shows categories of diagnostic certainty assigned for all cases. Anemia prevalence was not significantly different between any of the three sites. In the scurvy sample, scurvy prevalence was highest at Pointe-aux Trembles compared to the other two sites; these differences in prevalence were significant (Table 4-2). See Figure 4-3 for examples of lesions associated with scurvy that were observed in these samples.

Across the individuals who could be assessed for co-occurrence, 6.5% (2/31) were diagnosed with both scurvy and anemia (Figure 4-4). Both individuals were from Pointe-aux-Trembles. For 35.5% (11/31) of individuals, cases were considered 'consistent with' one or both conditions based on the available evidence, meaning that these cases cannot be completely excluded from representing co-occurrence or considered as cases where neither condition was present. For 19.3% (6/31) of cases, both conditions were classified as 'not consistent with', representing true cases of individuals diagnosed with neither condition.

Table 4-3: Comparison of crude prevalence (%) data between sites. Prevalence data above the horizontal line are calculated using the scurvy (N=55) and anemia (N=37) samples respectively, while data below the line was calculated with the co-occurrence sample (N=31). Bold p-values are significant.

	Pointe-aux-Trembles	**Sainte-Marie**	**p-value**	**Pointe-aux-Trembles**	**Saint-Antoine**	**p-value**	**Sainte-Marie**	**Saint-Antoine**	**p-value**
All Scurvy (n=17)	59.1% (13/22)	13.3% (2/15)	**0.005**	59.1% (13/22)	11.1% (2/18)	**0.002**	13.3% (2/15)	11.1% (2/18)	0.846
All Anemia (n=7)	20.0% (3/15)	20.0% (1/5)	1.000	20.0% (3/15)	17.6% (3/17)	1.000	20.0% (1/5)	17.6% (3/17)	1.000
Neither Condition (n=6)	7.1% (1/14)	20% (1/5)	0.468	7.1% (1/14)	33.3% (4/12)	0.148	20% (1/5)	33.3% (4/12)	1.000
Co-Occurrence (n=2)	14.3% (2/14)	0.0% (0/5)	1.000	14.3% (2/14)	0.0% (0/12)	0.483	0.0% (0/5)	0.0% (0/12)	1.000
Scurvy Only (n=8)	42.9% (6/14)	40% (2/5)	1.000	42.9% (6/14)	0% (0/12)	**0.017**	40% (2/5)	0% (0/12)	0.074
Anemia Only (n=4)	7.1% (1/14)	20% (1/5)	0.468	7.1% (1/14)	16.7% (2/12)	0.580	20% (1/5)	16.7% (2/12)	1.000

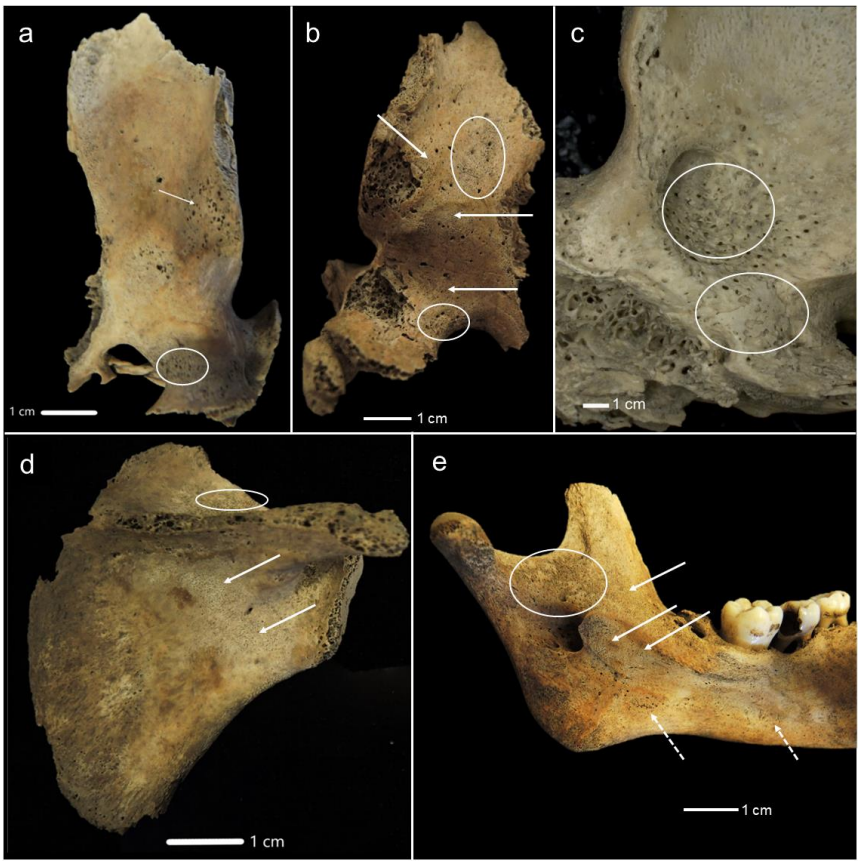

Figure 4-10: Lesions seen in individuals diagnosed with scurvy in this sample. Examples include porosity and SPNB on the greater wing of the sphenoid of 7A11-S57 (a) and 20A-S3 (b); new bone formation and fine porosity surrounding the foramen rotundum of 7A11-S57 (c), microscopic image); fine porosity on the infraspinous fossa of a right scapula and SPNB on the supraspinous fossa of 7A11-S57 (d); fine porosity, SPNB, and blood vessel impressions on the internal surface of the mandible pf 20F-S2 (e). Arrows indicate areas of abnormal porosity, circles indicate SPNB, and dashed arrows indicate blood vessel impressions.

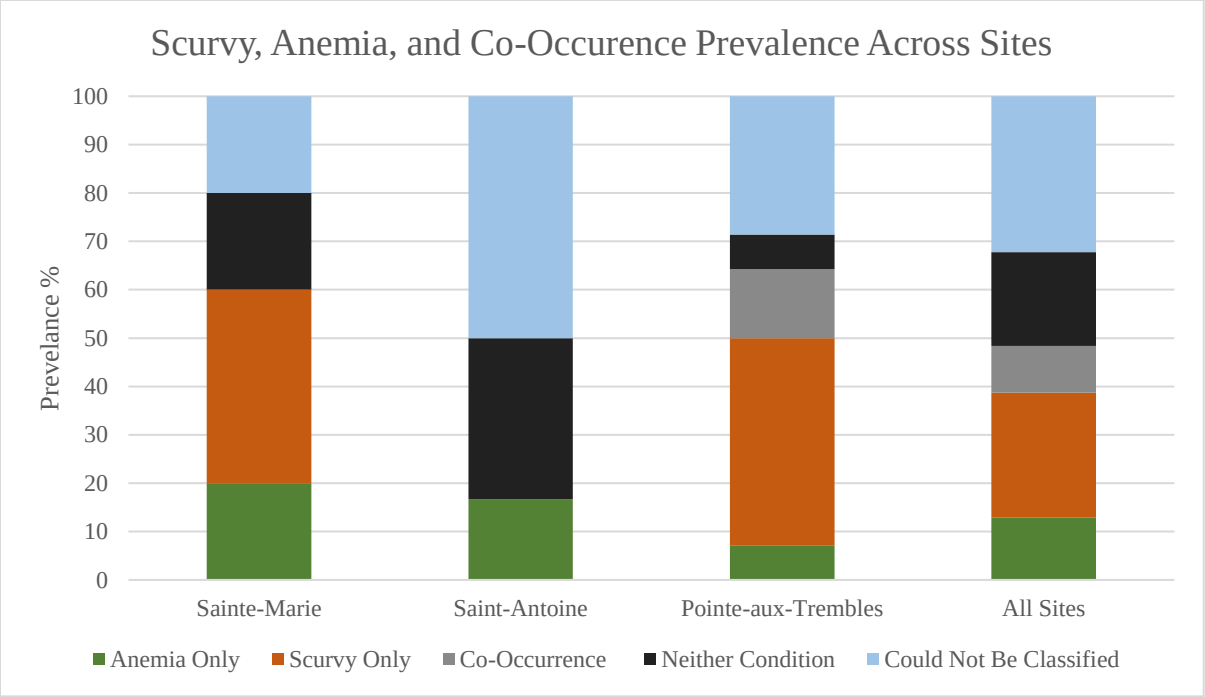

Figure 4-11: Prevalence across the three sites and overall sample calculated using the co-occurrence sample (n=31). Cases in the 'could not be classified' category could not be definitively assigned to any category, as they were considered 'consistent with' for scurvy and/or anemia.

4.2 Age-at-death data

Mean age-at-death for the entire sample is 2.9 years (SD=2.9), and mean age-at-death per site is reported and compared across sites in Table 4-3. Pointe-aux-Trembles had a significantly lower mean age-at-death compared to both other sites, and there was no significant difference between Saint-Antoine and Sainte-Marie.

Mean age-at-death for individuals diagnosed with scurvy was 1.3 years (SD=1.5) compared to 4.1 years (SD=3) for those who showed no indicators of scurvy. The age distribution of these two groups was found to be significantly different (D-crit=0.5566, p=0.003). The mean age-at-death for those diagnosed with anemia was 4.1 years (SD=3.5) compared to 1.4 years (SD=1.6) those with no evidence of anemia. No significant difference in the distributions of these groups was found (D-crit=0.5325, p=0.099). The number of individuals with both scurvy and anemia was too small (n=2) for meaningful calculations of statistical difference, but the mean age-at-death for these individuals (1.3 years, SD=0.4) was less than the mean age-at-death for those with neither condition (n=6, 2.1 years, SD=2.3).

The age-at-death distribution by site (Figure 4-5a) shows a very different pattern for Pointe-aux-Trembles in particular. Over 50% of the Pointe-aux-Trembles individuals were estimated to be aged under one year at death, representing the peak mortality for Pointe-aux-Trembles. Mortality at Sainte-Marie peaks between ages 3-5.9 years, and only 7% of the sample (1/15) were estimated to be under one year at death. At Saint-Antoine, mortality peaks at ages 1-2.9, and 17% (4/23) were estimated to be under one year old at death.

When breaking down the age-at-death data by diagnosis (Figure 4-5b), 94% (16/17) of individuals diagnosed with scurvy were estimated to be under three years old at death. For anemia, 43% (3/7) died before age three years. Of the two individuals diagnosed with scurvy and anemia, both were estimated to be under two years at time of death.

Table 4-8: Comparisons between mean age-at-death across sites. Bold p-values are significant. P-values were not calculated for co-occurrence comparisons due to the small sample size.

Site	Mean age-at-death	SD	Site	Mean age-at-death	SD	p-value
Pointe-aux-Trembles (n=23)	1.3 years	1.5	*Saint-Antoine (n=23)*	3.3 years	3.2	**0.012**
Pointe-aux-Trembles (n=23)	1.3 years	1.5	*Sainte-Marie (n=15)*	4.6 years	3.0	**0.001**
Saint-Antoine (n=23)	3.3 years	3.2	*Sainte-Marie (n=15)*	4.6 years	3.0	0.231

SD=Standard deviation

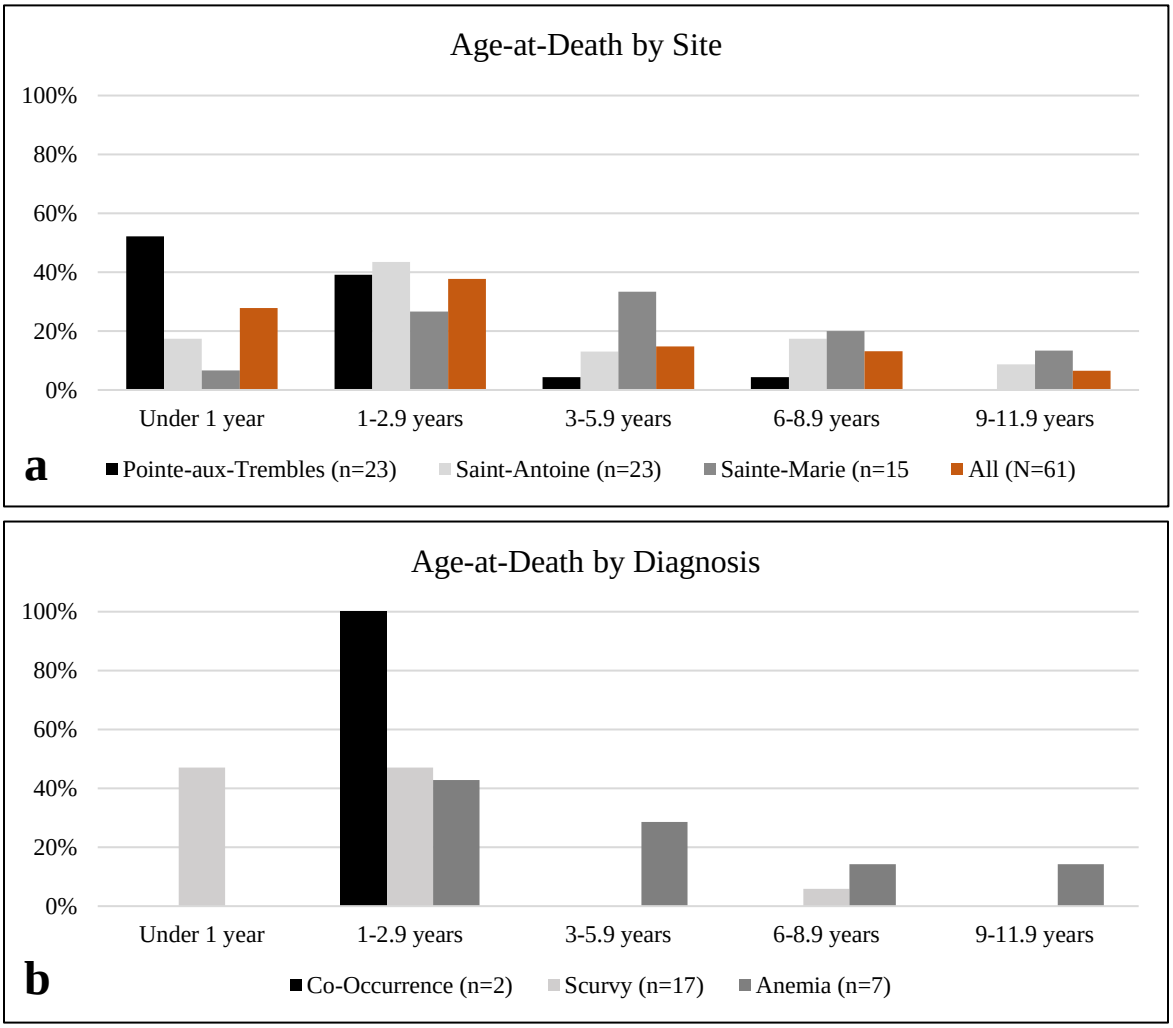

Figure 4-12: a) Age-at-death prevalence by site, using the total sample (N=61). b) Age-at-death prevalence by diagnosis (co-occurrence, scurvy, anemia).

5.0 Discussion

5.1 Mortality trends and metabolic bone disease

Infant and childhood mortality in 18th-19th century Quebec was high. By the middle of the 1700s, mortality rates were approximately 309 deaths per 1000 births in children under one year, and 85 deaths per 1000 births in those under five years (54). As population density increased, so did the probability of dying before one year of age, which meant that individuals living in urban environments undergoing rapid expansion were particularly affected (16,18,55). Cities faced frequent epidemics and higher mortality rates, while rural communities faced less exposure to infectious diseases, had a more stable food supply due to a reliance on subsistence farming, and tended to have higher fertility rates overall (16,29,56). In this study, the rural site of Sainte-Marie had a higher mean age-at-death than both Pointe-aux-Trembles and Saint-Antoine, but it is not significantly different from Saint-Antoine, which is a site directly in Montreal.

Out of the three sites, the Pointe-aux-Trembles sample exhibited the lowest mean age-at-death and the highest proportion of individuals who did not survive past one year of age. Pointe-aux-Trembles was a village just outside of Montreal, and in Quebec at this time, the practice of sending children away from urban centers was not uncommon, particularly amongst wealthier families (57). Children in rural environments were thought to be better protected from epidemics and other health risks than those living in urban environments (29). In the contemporary population of 18th century Paris, it is estimated that only around 30% of infants were nursed by those that had given birth to them (58). Similarly, in Montreal, 62 children were sent to be wet-nursed at Pointe-aux-Trembles over the 50-year period from 1754-1806 (8). However, as the cemetery sample at Pointe-aux-Trembles was composed of nearly two-thirds of children (50), and the mean age-at-death for this sample was significantly lower compared to samples at both other sites, this suggests that the practice of sending infants to rural settings did not necessarily confer protection from early childhood mortality; indeed it may have resulted in increased mortality risk for local children, who may have received less care as a result. We can look to patterns of disease and other contextual information to help explain some of these trends, although interpretations are conservative, due to the limitations of the sample.

One notable trend is the high proportion of individuals under the age of three years who were diagnosed with scurvy. These findings are consistent with other paleopathological studies; scurvy prevalence tends to be highest in those under five years old (40,53,59). In part, this is due to the mechanisms of lesions development in scurvy, which is strongly linked to rates of growth (10). Additionally, although scurvy can resolve rapidly if adequate vitamin C is introduced to the diet, it will lead to fatality if untreated (2), which can happen quickly in children (60). Prevalence of scurvy in those under 15 years was significantly higher at Pointe-aux-Trembles (see Section 5.2), which likely contributes to the significantly lower mean age-at-death at Pointe-aux-Trembles compared to the other two sites.

It was expected that co-occurrence would be associated with an increased likelihood of dying at a younger age. Although the mean age-at-death for those diagnosed with both scurvy and anemia was less than for those diagnosed with neither condition, the sample size is very small (n=2), and it is difficult to say if this difference is meaningful. The high prevalence of

metabolic bone disease in these samples may also be a contributing factor to the limited number of individuals diagnosed with co-occurrence, as individuals with scurvy may have died before skeletal manifestations of marrow hyperplasia could develop.

Infants are normally protected from scurvy until five months after birth, provided their mother is also not deficient (46,61). Anemia that results from vitamin C deficiency usually develops after the soft-tissue manifestations of scurvy manifest (2,62). Therefore, individuals under one year old may not have lived long enough with scurvy to develop scurvy-induced anemia. While individuals under one year with scurvy could have developed anemia due to other nutritional deficiencies, anemia in children is most often diagnosed in children 6-24 months, and tends to develop between 6-12 months due to increased nutritional needs, a depletion in fetal iron stores, and a lack of adequate complementary foods (63,64). Agarwal et al. (65) noted a period of several months between clinical development of anemia and potential skeletal manifestations of marrow hyperplasia, so even those who developed the condition at or around 6 months would not necessarily have shown anemia-related changes detectable in bone until several months later, and may not have lived long enough with anemia for skeletal manifestations to develop.

Another factor when interpreting mortality trends in the context of scurvy and anemia is the effect of other diseases, particularly infectious disease epidemics. Saint-Antoine had a significantly higher proportion of individuals diagnosed with neither scurvy nor anemia compared to both other sites, which might initially indicate that they were less affected by disease. However, the osteological paradox (66) is one important consideration here; Saint-Antoine was used as a cholera cemetery during the 1832 Quebec cholera epidemic, and again during subsequent cholera outbreaks (18,67). Individuals without a diagnosis could represent people who were not exposed to metabolic/nutritional stress, or those who died quickly due to fast-acting infectious disease without manifesting skeletal evidence of any disease or condition (66). Nutritional stress at Saint-Antoine may have been less than at Sainte-Marie or Pointe-aux-Trembles, as implied by prevalence data, but other diseases are likely to have played a role in shaping mortality patterns for this community.

5.2 Diet and nutrition in 18th-19th century Quebec

Nutritional deficiencies and related conditions have been seen in colonial contexts (68), and evidence for scurvy has been previously identified in skeletal remains from Colonial Quebec/New France (4,6,20,21,22,23). However, a consideration of local differences in subsistence practices between each of the three sites can help to contextualize prevalence trends for anemia and scurvy. As a rural village, the French-Canadian inhabitants of Sainte-Marie would have lived a mostly agricultural lifestyle, cultivating mainly wheat in addition to potatoes, peas, and barley, and relying on bread as a main dietary staple (69,70). However, by 1815, wheat crop failures had become increasingly common, and by 1830, it was nearly impossible to farm due to poor soil conditions (69). This meant that many rural farmers could no longer grow wheat for their own consumption, or to export, making it even more difficult to purchase alternative food options. Harsh winters only exacerbated these problems (3). Rates of malnutrition and starvation in many rural villages increased after this time, and many farmers reverted to supporting themselves through subsistence agriculture (69). However, in the current study, the

prevalence of scurvy (13.3%) at the rural site of Sainte-Marie was higher than the prevalence for many contemporary European and North American groups (ranging from 0-4%) (40,71) except for famine samples (e.g. Geber & Murphy (46)). This suggests that subsistence agriculture in this context did not completely prevent development of nutritional conditions.

The prevalence of scurvy at Saint-Antoine (11.1%) was also higher than many other contemporary paleopathological assemblages (40,71). Prevalence of anemia at Saint-Antoine is 17.6%, but comparing this value to other paleopathological studies is difficult due to the differences in diagnostic methods used in this study versus typical methods of anemia analysis. Notably, scurvy prevalence at Saint-Antoine was not significantly different from rural Sainte-Marie. This pattern is consistent with what is seen in industrial England, where both urban and rural children were at risk for metabolic bone disease and early-life stress, although sometimes for different reasons (72,73). At the time, there was a perception that rural environments were healthier than urban ones, both in Quebec (29), and in other contexts undergoing industrialization (73), but this assumption is not supported by these findings from Sainte-Marie and Saint-Antoine. Montreal was dependent on rural villages to provide food (74), so long winters and crop failures would have affected food availability universally, which likely contributed to the high prevalence of scurvy and anemia across all sites.

Although the city had greater availability of markets to buy food, the French-Catholic community that mainly used the Saint-Antoine cemetery generally worked in low-to-middle status occupations, tended to live in lower rent properties (19,75), and may not have been able to utilize these resources. Social stratification along cultural and language lines divided Montreal, and the French-Canadian population was generally considered middle-low socioeconomic status; they were more prosperous than the Irish Catholic population, but not as well-off as the English Protestants (19). In their study of infant mortality across Montreal's three cultural communities, Thorton & Olson (76) found that 20% of French-Canadian infants in 1880 had "weakness" (which includes general malnutrition and anemia specifically) listed as their cause-of-death. In Irish and English communities, this drops to 13% and 5% respectively. In the late 19th century, microscopic blood analysis for anemia diagnosis was possible, but signs such as pallor and weakness were also commonly associated with the condition (77), and were likely part of diagnosis.

Overall infant mortality rates were highest amongst the French-Canadian population, and Thorton & Olson (76) suggest that this is the result of differences in cultural factors that affected both infant and parent health, including birth spacing, breastfeeding duration, and high numbers of children per family. Due to religious beliefs, time between births and length of breastfeeding period both tended to be shorter in the French-Canadian community. At this time, Quebec had some of the highest fertility rates ever recorded, which may have also contributed to increased infant mortality rates (78). Individuals from the Sainte-Marie and Saint-Antoine cemetery collections would have been mostly French-Canadian, and these shared cultural practices could be another factor contributing to the similar prevalence of scurvy in these two locations.

Pointe-aux-Trembles is an outlier and has a significantly higher scurvy prevalence (59.1%), which is equivalent to famine samples (e.g. Geber & Murphy, 2012 (46)). Pointe-aux-

Trembles was primarily an agricultural village with a majority French-Canadian population, but a road (the *Chemin du Roi*, or King's Road) was built to connect the village to Montréal in 1734, leading to increased trade and migration, including children sent to Pointe-aux-Trembles to be wet-nursed (8,50). In addition to environmental conditions that affected food availability, this practice may have contributed to the high scurvy prevalence at Pointe-aux-Trembles.

In 17th-18th century France, a mortality rate of 40-50% was seen amongst children who were wet-nursed (79), which is similar to the pattern observed at Pointe-aux-Trembles. The vitamin C content of breastmilk typically ranges from 40-100 mg/L, and is affected by maternal intake (80). Children typically receive sufficient vitamin C through breastfeeding, as long as their mother or wet nurse is not severely deficient (81). The high prevalence of scurvy in children could reflect severe vitamin C deficiency in mothers at Pointe-aux-Trembles; typically, only individuals experiencing severe malnutrition will be unable to meet infant vitamin C requirements through breastfeeding (80). However, as evidence for metabolic bone conditions in the adults of Pointe-aux-Trembles was limited (50), it seems more likely that the high prevalence of scurvy was related to child feeding and weaning practices instead. A study using stable isotope analysis by Gutierrez et al. (8) found that most children at Pointe-aux-Trembles were gradually weaned from about six months to two years, with complementary weaning and supplementary foods introduced starting at around six months. Some children (27% of the sample) showed introduction of complementary foods before six months. These foods typically included breadcrumbs soaked in water, oatmeal, and cow's milk mixed with hot water and sugar (8,21), which would have been low in vitamin C, iron, B12, and folate. Children who subsisted mainly on this diet of foods would have been at a high risk of developing scurvy and/or anemia from nutritional deficiencies. The children who were weaned before six months may represent rural children who were weaned earlier due to the influx of urban children sent to Pointe-aux-Trembles; wet nurses in the village may have been unable to support breastfeeding all children (8).

Notably, Pointe-aux-Trembles is also the site of one of the oldest windmills in Quebec (constructed between 1719 and 1721) (82). As such, flour production and grain processing were important industries in the village, and products were eaten as a staple foods throughout the community (83). These foods also would have lacked vitamin C, further contributing to high scurvy prevalence, and therefore higher mortality, in this context.

5.3 Disease clustering and co-occurrence

The current study uses a population-based approach to evaluating co-occurrence, and found that anemia/scurvy co-occurrence developed in 6.5% of individuals across the sample. Since anemia can develop as a direct consequence of scurvy, it is likely that any context where scurvy can be diagnosed will also have cases of co-occurrence. The high scurvy prevalence seen in these samples indicates unusually severe nutritional deficiencies may have contributed to elevated risk of anemia, but the physiological mechanisms behind scurvy/anemia co-occurrence mean that it can develop even when the effects of other nutritional deficiencies are not considered. Systemic investigation of anemia/scurvy co-occurrence in other contexts with known

cases of scurvy should be undertaken to help establish if the co-occurrence prevalence seen here is typical.

Establishing timing of both anemia and scurvy can be challenging, as the association between when the condition is initiated and when skeletal evidence develops or remodels is largely unknown, and is influenced by a wide variety of factors. This can make it difficult to establish co-occurrence on an individual level. Instead, or in addition to the individual-based approach, assessing clustering of these conditions within a sample and on a site-level can be another way to understand the effects of co-occurrence. This population-based approach is used and recommended by Perry and Edwards (50) in their study of multiple metabolic conditions amongst comingled remains from Hisban, Jordan. For scurvy and anemia, the biological relationship means that they are likely to co-occur in any context where scurvy is found, but the prevalence of co-occurrence or clustering of these two conditions and the way it arises (i.e. strictly due to physiological mechanisms, or because of multiple nutritional deficiencies affecting the sample) will differ based on contextual factors. In the current study, metabolic bone disease across all three sites was exacerbated by harsh winters and crop failure, lack of food availability, and cultural practices around weaning and childbirth, and these factors help to explain why the prevalence of scurvy and/or anemia was high amongst all three samples. Studying disease co-occurrence at a broader, site-wide level helps to better understand the pathways and variables that affect disease clustering, and explain why these pathways can differ depending on local factors.

6.0 Conclusion

In this paper, investigating co-occurrence of anemia and scurvy in different but related contexts has enabled a more complete understanding of how metabolic conditions affected childhood health and mortality risk. In the context of 18th-19th century Quebec, environmental and socioeconomic factors likely contributed to an increased risk of anemia and scurvy across urban and rural communities. These variables led to a high rate of scurvy and anemia in all three studied samples, although these effects are most strongly seen at Pointe-aux-Trembles, where cultural factors such as infant feeding and weaning practices such as wet-nursing and the early introduction of complementary foods with low nutritional value were most evident. The representativeness of the sample does affect the strength of these interpretations, and expanding the current sample sizes will help to improve understanding of mortality in these contexts. High prevalence of metabolic bone diseases contributed to high mortality risk amongst young children, and scurvy significantly affected age-at-death. On a broader level, assessing scurvy, anemia, and co-occurrence helps to better understand pathways of disease clustering, and how the outcomes of these interactions can differ based on local variables. Co-occurrence with anemia should be a consideration for other settings characterized by the presence of scurvy, and serves as a point of comparison for understanding health dynamics in other archaeological contexts.

Acknowledgements

Ethics approval granted by the Hamilton Integrated Research Ethics Board. Thank you to Ville de Montréal (François Bélanger) for providing access and information for the Saint-Antoine and

Pointe-aux-Trembles collections. Additional thanks to Conseil de la Fabrique de Sainte-Marie-de-Beauce for access to the Sainte-Marie collection. Thanks to Emilie Dion (Université de Montréal) who did the dental age estimations of the Quebec collections. Thanks also to Dr. Andrew Nelson for facilitating micro-CT imaging, and Dr. Heather Hatch at the Museum of Ontario Archaeology for access to micro-CT facilities. This research was supported by a Social Science and Humanities Research Council (SSHRC) Joseph-Armand Bombardier Canada Graduate Scholarship, the McMaster University Shelley Saunders/Koloshuk Family Scholarship, a SSHRC Insight Grant (File Number: 435-2021-0665), the Canadian Association for Biological Anthropology Shelley R. Saunders Thesis Research Grant, and undertaken, in part, thanks to funding from the Canada Research Chairs program.

Supplemental Data

Table 4-S1: Recording of lesions associated with scurvy for individuals from the Pointe-aux-Trembles collection.

Individual			**7A2-S1**	**7A2-S10**	**7A2-S22**	**7A2-S24**	**7A2-S3**	**7A2-S32**	**7A2-S6**	**7A9-S12**	**7A9-S18**	**7A9-S21**	**7A9-S25**	**7A9-S44**	**7A9-S48**	**7A9-S51**
Sphenoid	Greater Wing	*Left*	1(P)	1(N)	1(N)	0	1(P)	-	1(P)	-	-	1(M)	0	1(N)	-	0
		Right	1(P)	0	1(N)	0	-	-	1(P)	-	-	1(M)	0	1(N)	-	0
	Foramen Rotundum	*Left*	-	0	0	-	0	-	0	-	-	1(P)	0	1(N)	-	0
		Right	0	0	-	0	-	-	1(P)	-	-	1(P)	0	1(N)	-	0
Orbit		*Left*	-	1(N)	1(M)	0	-	1(P)	1(M)	1(P)	-	1(M)	-	1(M)	0	0
		Right	1(P)	1(N)	-	0	-	1(P)	1(M)	1(P)	-	1(P)	1(P)	0	1(M)	0
Maxilla	Infraorbital Foramen	*Left*	0	-	-	-	-	-	-	0	-	-	-	-	-	0
		Right	-	-	-	-	-	0	-	0	-	1(P)	-	-	-	0
	Posterior	*Left*	1(P)	-	-	-	0	-	-	0	-	-	-	-	-	0
		Right	1(P)	0	-	-	0	-	1(P)	0	-	-	-	-	-	0
	Palate	*Left*	1(P)	-	-	-	1(P)	1(P)	-	0	-	0	-	1(P)	-	0
		Right	1(P)	-	-	-	1(P)	1(P)	1(P)	0	-	0	-	0	-	0
	Alveolar Bone	*Left*	0	-	-	-	0	0	-	0	-	0	-	0	0	0
		Right	-	1(P)	-	-	0	0	1(P)	0	-	0	-	0	1(P)	0
Mandible	Mylohyoid Line		0	-	-	-	-	0	-	0	-	0	0	0	0	0
	Coronoid Process		0	-	-	-	-	0	-	0	-	0	-	-	-	0
	Alveolar Bone		0	0	-	-	-	0	-	0	-	0	1(N)	0	1(P)	0
Scapula	Supraspinous Fossa	*Left*	1(P)	1(P)	1(P)	1(P)	1(P)	1(P)	1(P)	1(P)	0	-	-	-	1(M)	0
		Right	1(P)	1(P)	1(P)	0	1(P)	1(P)	0	1(P)	0	1(N)	1(M)	-	-	0
	Infraspinous Fossa	*Left*	0	1(M)	1(P)	0	1(P)	0	1(M)	1(P)	0	0	-	1(N)	0	0
		Right	0	1(M)	1(P)	0	1(P)	0	0	1(P)	0	0	0	1(N)	-	0
Medial Zygomatic		*Left*	-	1(P)	0	0	1(P)	-	-	-	-	1(P)	-	-	0	0
		Right	0	-	1(P)	0	0	-	-	-	-	1(P)	-	0	-	0
Cranial Vault			0	1(N)	0	0	0	1(P,N)	1(P,N)	0	-	1(P, N)	0	1(N)	0	0
Medial Ilium		*Left*	0	1(P)	-	0	0	0	-	-	0	0	1(M)	0	-	0
		Right	0	0	-	0	0	0	-	-	0	0	1(M)	0	-	0
Long Bone Metaphyses			0	1(M)	1(M)	1(M)	1(N)	1(M)	0	1(P)	0	0	1(M)	1(P)	0	0
Scurvy Diagnosis			H	H	H	N	H	H	D	C	N	D	C	D	C	N

Individual			**7A9-S53**	**7A9-S54**	**7A9-S55**	**7A9-S56**	**7A11-S57**	**7A11-S59**	**7A11-S63**
Sphenoid	Greater Wing	*Left*	-	0	0	-	1(M)	0	1(M)
		Right	-	0	-	-	1(M)	0	1(M)
	Foramen Rotundum	*Left*	-	0	-	-	1(M)	0	0
		Right	-	0	-	-	-	0	1(M)
Orbit		*Left*	-	0	1(P)	1(N)	1(M)	1(M)	1(M)
		Right	-	-	-	1(N)	-	1(M)	1(M)
Maxilla	Infraorbital Foramen	*Left*	-	-	-	-	-	-	0
		Right	-	-	-	-	-	-	0
	Posterior	*Left*	-	-	-	1(N)	0	-	0
		Right	-	-	-	-	0	-	0
	Palate	*Left*	-	-	-	-	1(P)	1(P)	0
		Right	1(P)	-	-	1(M)	1(P)	-	0
	Alveolar Bone	*Left*	0	0	-	0	1(P)	-	0
		Right	0	0	-	0	1(P)	0	0
Mandible	Mylohyoid Line		0	-	-	-	0	-	0
	Coronoid Process		1(P)	-	0	-	0	-	0
	Alveolar Bone		0	0	-	1(M)	0	0	0
Scapula	Supraspinous Fossa	*Left*	1(P)	1(M)	-	1(N)	1(M)	1(P)	0
		Right	1(P)	1(M)	-	-	1(M)	1(P)	1(P)
	Infraspinous Fossa	*Left*	0	0	-	1(N)	0	1(P)	0
		Right	0	0	-	-	0	1(P)	0
Medial Zygomatic		*Left*	-	0	-	-	-	-	1(M)
		Right	0	-	-	-	-		0
Cranial Vault			0	0	0	1(N)	0	1(P)	0
Medial Ilium		*Left*	-	-	-	1(N)	-	-	-
		Right	-	-	-	0	-	-	-
Long Bone Metaphyses			0	1(N)	0	1(N)	0	1(M)	0
Scurvy Diagnosis			H	N	N	H	D	H	H

1: Lesion present 0: Lesion absent -: Could not be evaluated
(P): Porosity (N): New bone formation M: Mixed lesion
D: Diagnostic of scurvy H: Highly consistent with scurvy C: Consistent with scurvy N: Not consistent with scurvy
N/A: Could not be evaluated for scurvy

Table 4-S2: Recording of lesions associated with scurvy for individuals from the Sainte-Marie collection.

Individual			2A15	2G3	2G5	2E3	2E5	2E4	2E7	1C2	1G2	1G6	2A1	2A13	2A2	2F3	2G1
Sphenoid	Greater Wing	*Left*	-	-	1(P)	1(M)	1(P)	-	-	-	-	-	-	-	-	-	-
		Right	1(P)	1(P)	-	1(M)	1(P)	-	0	0	0	0	-	0	-	-	-
	Foramen Rotundum	*Left*	0	-	0	0	0	0	0	-	0	0	0	0	-	-	-
		Right	0	0	-	1(P)	0	0	0	0	1(P)	0	-	-	-	-	-
Orbit		*Left*	-	1(M)	1(P)	1(P)	1(N)	1(P)	1(P)	0	1(P)	0	-	-	0	-	0
		Right	-	1(P)	1(P)	1(P)	1(M)	-	0	0	1(P)	0	-	0	0	-	0
Maxilla	Infraorbital Foramen	*Left*	-	-	-	-	0	-	-	-	-	-	-	-	-	-	-
		Right	-	-	-	-	0	-	-	-	-	0	-	-	-	-	-
	Posterior	*Left*	-	-	-	-	0	-	-	-	-	0	-	-	-	-	-
		Right	-	0	-	-	0	-	-	-	-	0	-	-	-	-	-
	Palate	*Left*	-	1(P)	-	-	1(P)	-	-	-	-	0	-	-	-	-	-
		Right	-	1(P)	-	-	1(P)	-	-	-	-	0	-	-	-	-	-
	Alveolar Bone	*Left*	-	0	-	-	1(P)	0	-	0	-	0	-	-	-	-	-
		Right	-	0	-	-	0	-	-	-	-	0	-	-	-	-	-
Mandible	Mylohyoid Line		-	-	-	-	0	-	-	-	0	0	-	-	-	0	-
	Coronoid Process		-	-	-	1(P)	1(P)	-	-	-	0	0	-	-	-	0	-
	Alveolar Bone		-	0	-	-	0	-	-	-	0	0	-	-	-	0	0
Scapula	Supraspinous Fossa	*Left*	-	-	-	0	1(M)	-	0	0	-	0	0	0	-	0	0
		Right	0	-	-	0	1(P)	-	0	1(P)	0	0	0	0	0	0	0
	Infraspinous Fossa	*Left*	-	-	-	0	-	-	-	0	0	0	1(P)	-	0	-	0
		Right	-	-	-	0	-	-	0	0	0	0	0	-	0	-	0
Medial Zygomatic		*Left*	0	-	-	0	1(P)	0	0	0	0	-	0	0	-	-	-
		Right	0	-	-	0	1(P)	-	0	0	0	-	0	-	-	-	-
Cranial Vault			0	1(P)	1(P)	0	0	0	1(P,N)	0	0	0	0	0	0	-	0
Medial Ilium		*Left*	-	0	0	-	0	0	-	0	-	0	-	-	-	0	0
		Right	-	-	-	-	-	-	-	-	-	-	-	-	-	1(P)	-
Long Bone Metaphyses			1(P, N)	0	0	1(N)	1(N)	0	0	0	0	0	0	0	0	0	0
Scurvy Diagnosis			C	C	C	D	D	N	N	N	N	N	N	N	N	N	N

1: Lesion present 0: Lesion absent -: Could not be evaluated
(P): Porosity (N): New bone formation M: Mixed lesion
D: Diagnostic of scurvy H: Highly consistent with scurvy C: Consistent with scurvy N: Not consistent with scurvy

N/A: Could not be evaluated for scurvy

Table 4-S3: Recording of lesions associated with scurvy for individuals from the Saint-Antoine collection.

Individual			**17Z-S2(1)**	**20F-S21**	**20F-S6**	**20Z-S5**	**21U-S6**	**20A-S3**	**20F-S2**	**21N-S3**	**20F-S39**	**21E-S14**	**21E-S4**	**21F-S5**	**21N-S11**
Sphenoid	Greater Wing	*Left*	-	-	0	-	1(P)	1(M)	0	1(M)	0	-	-	0	0
		Right	-	-	-	0	1(P)	1(M)	1(P)	0	0	-	-	0	0
	Foramen Rotundum	*Left*	-	-	-	-	0	1(P)	0	-	0	-	-	0	0
		Right	-	-	-	1(N)	-	0	0	0	0	-	-	0	0
Orbit		*Left*	-	-	1(M)	1(P)	1(P)	1(P)	1(P)	-	1(P)	0	1(P)	-	1(P)
		Right	-	-	-	1(P)	1(P)	-	1(M)	-	0	1(P)	-	0	0
Maxilla	Infraorbital Foramen	*Left*	-	-	-	-	-	-	0	0	-	-	-	-	0
		Right	-	-	-	-	-	-	0	-	-	-	-	-	0
	Posterior	*Left*	-	-	-	-	-	-	0	0	-	-	-	-	0
		Right	-	-	-	-	-	-	0	-	-	-	-	-	0
	Palate	*Left*	-	-	-	-	-	-	1(P)	0	-	-	-	-	0
		Right	-	-	-	-	-	-	1(P)	-	-	-	-	-	0
	Alveolar Bone	*Left*	-	-	1(P)	-	-	-	0	0	-	-	-	-	0
		Right	-	-	-	-	-	-	0	-	-	-	-	-	0
Mandible	Mylohyoid Line		-	-	-	-	-	-	1(P)	-	-	0	-	-	0
	Coronoid Process		-	-	-	-	-	-	0	0	-	0	-	-	0
	Alveolar Bone		-	-	-	-	-	-	0	-	1(P)	0	0	-	0
Scapula	Supraspinous Fossa	*Left*	1(P)	1(P)	1(P)	-	-	1(P)	1(P)	1(P)	-	-	0	-	0
		Right	1(P)	0	-	-	0	-	1(P)	0	-	0	0	-	0
	Infraspinous Fossa	*Left*	1(P)	1(P)	1(P)	-	0	0	0	-	-	-	0	-	0
		Right	1(P)	1(P)	-	-	0	-	0	0	-	0	0	-	0
Medial Zygomatic		*Left*	-	-	1(P)	1(P)	-	-	0	-	-	0	0	-	0
		Right	-	-	-	1(P)	-	-	0	-	-	0	0	-	0
Cranial Vault			-	-	1(P,N)	0	1(P,N)	0	0	0	0	0	0	0	0
Medial Ilium		*Left*	-	0	-	-	0	0	0	-	-	0	0	-	0
		Right	-	0	-	-	1	-	0	-	-	0	0	-	0
Long Bone Metaphyses			1(P)	0	0	-	0	0	0	0	0	0	0	-	0
Scurvy Diagnosis			C	C	C	C	C	D	H	C	N	N	N	N	N

Individual			**21R-S5**	**23E-S11**	**24G-S1**	**25C-S24**	**30R-S7**
Sphenoid	Greater Wing	*Left*	0	0	-	0	0
		Right	0	0	0	0	0
	Foramen Rotundum	*Left*	0	1(P)	0	0	0
		Right	0	-	-	0	-
Orbit		*Left*	1(P)	-	-	-	1(P)
		Right	1(P)	-	1(P)	-	0
Maxilla	Infraorbital Foramen	*Left*	-	-	-	-	-
		Right	-	-	-	-	-
	Posterior	*Left*	-	-	-	-	-
		Right	-	-	-	-	-
	Palate	*Left*	1(P)	-	-	-	-
		Right	-	-	-	-	0
	Alveolar Bone	*Left*	0	-	-	-	-
		Right	-	-	-	-	0
Mandible	Mylohyoid Line		-	-	-	-	0
	Coronoid Process		-	-	-	-	0
	Alveolar Bone		-	-	0	-	0
Scapula	Supraspinous Fossa	*Left*	-	0	0	-	0
		Right	-	0	-	0	0
	Infraspinous Fossa	*Left*	-	0	0	0	0
		Right	-	0	-	0	0
Medial Zygomatic		*Left*	-	-	-	-	0
		Right	-	-	0	0	0
Cranial Vault			0	0	0	0	0
Medial Ilium		*Left*	0	0	0	-	-
		Right	0	0	-	-	-
Long Bone Metaphyses			0	0	0	0	0
Scurvy Diagnosis			N	N	N	N	N

1: Lesion present 0: Lesion absent -: Could not be evaluated
(P): Porosity (N): New bone formation M: Mixed lesion
D: Diagnostic of scurvy H: Highly consistent with scurvy C: Consistent with scurvy N: Not consistent with scurvy
N/A: Could not be evaluated for scurvy

Table 4-S16: Compilation of metric and visual data used as part of anemia assessment.

Skeleton ID	Site	Age (years)*	Cortical Thinning score	Trabecular separation score	Trabecular Thinning score	Frontal Ratio[1]	CtThOL T-score[2]	TbTh T-score[2]	TbSp T-score[3]	Anemia Assessment
7A11-S59	Pointe-aux-Trembles	0.70	2	2	1	----	-0.3	0.2	0.9	N
7A11-S63	Pointe-aux-Trembles	0.75	1	1	1	----	Baseline			N
7A9-S21	Pointe-aux-Trembles	0.75	1	1	1	----	Baseline			N
7A9-S55	Pointe-aux-Trembles	1.75	1	1	1	----	Baseline			N
7A9-S44	Pointe-aux-Trembles	0.25	3	0	1	----	Baseline			N
7A2-S6	Pointe-aux-Trembles	0.38	2	1	1	4.6	-0.8	**-1.2**	0.0	N
7A9-S12	Pointe-aux-Trembles	0.38	3	1	2	----	-0.2	-0.7	-0.9	N
7A2-S10	Pointe-aux-Trembles	0.50	3	1	2	----	-0.3	-0.3	-0.1	N
7A9-S48	Pointe-aux-Trembles	0.50	3	0	0	----	Baseline			N
7A11-S57	Pointe-aux-Trembles	1.00	3	3	3	----	-0.1	-0.7	**1.7**	H
7A2-S22	Pointe-aux-Trembles	1.50	2	2	1	**2.8**	-0.1	1.1	**1.6**	C
7A2-S24	Pointe-aux-Trembles	1.50	2	2	2	----	-0.3	-0.3	**1.2**	H
7A2-S1	Pointe-aux-Trembles	1.50	0	0	0	----	Baseline			N
7A2-S32	Pointe-aux-Trembles	1.58	2	2	1	**4.9**	-0.2	0.2	**1.4**	H
7A9-C6	Pointe-aux-Trembles	5.00	0	0	1	----	Baseline			N
21N-S12	St-Antoine	0.75	2	0	1	----	Baseline			N
20F-S6	St-Antoine	0.75	1	0	0	----	Baseline			N
21R-S5	St-Antoine	7.60	2	3	3	0.6	**-1.1**	**-1.6**	0.8	C
20F-S39	St-Antoine	0.50	2	1	1	2.0	-0.5	-0.7	0.5	N
17L-S4	St-Antoine	1.00	2	2	3	----	0.2	-0.3	**2.0**	C
20F-S9	St-Antoine	1.00	1	1	1	----	Baseline			N
21N-S11	St-Antoine	1.33	1	1	1	----	Baseline			N
21E-S8	St-Antoine	1.40	1	3	1	0.9	0.8	**-1.2**	**1.6**	C
20A-S3	St-Antoine	1.50	2	2	2	----	1.3	0.2	**2.9**	C
20Z-S5	St-Antoine	1.50	0	1	0	----	Baseline			N
8J-S4.2	St-Antoine	1.50	1	0	0	----	Baseline			N
21E-S4	St-Antoine	3.00	0	2	1	----	1.5	-0.5	**1.0**	C
21F-S5	St-Antoine	3.00	1	2	2	----	**-1.2**	-0.3	**1.3**	H
20F-S2	St-Antoine	7.00	2	2	2	**4.0**	**-1.4**	-0.1	0.4	C
21E-S14	St-Antoine	7.00	0	2	1	----	1.1	-0.4	0.8	N
30R-S7	St-Antoine	7.6	2	3	3	**3.5**	0.8	**-1.3**	**3.5**	H
21U-S6	St-Antoine	10.25	2	3	2	----	**-3.0**	-0.1	**1.8**	H
2E5	Ste-Marie	0.25	1	1	1	----	Baseline			N
2E3[4]	Ste-Marie	1.50	1	2	1	----	1.9	1.6	**2.1**	N
1G2	Ste-Marie	1.50	2	1	2	1.4	2.0	0.6	**1.4**	N
2G3	Ste-Marie	2.50	3	2	2	**6.9**	**-1.9**	-0.3	0.9	C
1G6	Ste-Marie	4.00	3	2	3	----	-0.3	-0.4	**1.2**	H

* Midpoint age estimate

[1]Bolded values are over 2.5, which was considered pathological by Panzer et al.,(2023) and Sebes & Diggs (1979), based on radiographic ratios from Reynolds (1962, 1965).

[2]Bolded values ≤ -1, and are considered evidence of cortical or trabecular thinning.

[3] Bolded values are ≥ 1, and are considered evidence of increased trabecular separation.

CtThOL= Average cortical thickness of the orbital lamina

TbSp= Average trabecular separation

TbTh=Average trabecular thickness

D= Diagnostic of H= Highly consistent with C= Consistent with N= Not consistent with

[4] As this individual had significantly positive values for all T-scores, their positive TbSp score is not likely to be indicative of anemia, and may reflect that that their bone microarchitecture was generally more developed for their age group.

Baseline individuals showed no evidence of skeletal manifestations of marrow hyperplasia, and were used as part of T-score calculations.

Table 4-S5: Summary of age estimates and final diagnoses for all assessable individuals in the current study.

Skeleton ID	Site	Midpoint Age Estimate (years)	Anemia Assessment	Scurvy Assessment	Co-Occurrence
7A9-S44	Pointe-aux-Trembles	0.25	N	D	No
7A9-S54	Pointe-aux-Trembles	0.25	----	N	----
7A9-S25	Pointe-aux-Trembles	0.33	----	C	----
7A9-S12	Pointe-aux-Trembles	0.375	N	C	No
7A2-S6	Pointe-aux-Trembles	0.38	N	D	No
7A2-S10	Pointe-aux-Trembles	0.50	N	H	No
7A9-S48	Pointe-aux-Trembles	0.5	N	C	No
7A9-S51	Pointe-aux-Trembles	0.5	----	N	----
7A11-S59	Pointe-aux-Trembles	0.7	N	H	No
7A11-S63	Pointe-aux-Trembles	0.75	N	H	No
7A9-S21	Pointe-aux-Trembles	0.75	N	D	No
7A9-S56	Pointe-aux-Trembles	0.75	----	H	----
7A11-S57	Pointe-aux-Trembles	1	H	D	Yes
7A2-S3	Pointe-aux-Trembles	1.25	----	H	----
7A2-S1	Pointe-aux-Trembles	1.5	N	H	No
7A2-S22	Pointe-aux-Trembles	1.5	C	H	No
7A2-S24	Pointe-aux-Trembles	1.5	H	N	No
7A9-S18	Pointe-aux-Trembles	1.5	----	N	----
7A2-S32	Pointe-aux-Trembles	1.58	H	H	Yes
7A9-S53	Pointe-aux-Trembles	1.75	----	H	----
7A9-S55	Pointe-aux-Trembles	1.75	N	N	No
7A9-C6	Pointe-aux-Trembles	5.00	N	----	----
7A9-S39	Pointe-aux-Trembles	6.50	----	N	----
20F-S39	St-Antoine	0.50	N	N	No
20F-S21	St-Antoine	0.75	----	C	----
21N-S12	St-Antoine	0.75	N	----	----
20F-S6	St-Antoine	0.75	N	C	No
17L-S4	St-Antoine	1.00	C	----	----
20F-S9	St-Antoine	1.00	N	----	----
21N-S11	St-Antoine	1.33	N	N	No
21N-S3	St-Antoine	1.33	----	C	----
21E-S8	St-Antoine	1.40	C	----	----
17Z-S2(1)	St-Antoine	1.50	----	C	----
20Z-S5	St-Antoine	1.50	N	C	No
25C-S24	St-Antoine	1.50	----	N	----
8J-S4.2	St-Antoine	1.50	N	----	----
20A-S3	St-Antoine	1.5	C	D	No
21E-S4	St-Antoine	3.00	C	N	No
21F-S5	St-Antoine	3.00	H	N	No
24G-S1	St-Antoine	4.00	----	N	----
20F-S2	St-Antoine	7.00	C	H	No
21E-S14	St-Antoine	7.00	N	N	No
21R-S5	St-Antoine	7.60	C	N	No
30R-S7	St-Antoine	7.60	H	N	No
23ES-11	St-Antoine	10.00	----	N	----
21U-S6	St-Antoine	10.25	H	C	No
2E5	Ste-Marie	0.25	N	D	No
2E3	Ste-Marie	1.50	N	D	No
2E7	Ste-Marie	1.50	----	N	----
1G2	Ste-Marie	1.50	N	N	No
2G3	Ste-Marie	2.50	C	C	No
2E4	Ste-Marie	4.00	----	N	----
1G6	Ste-Marie	4.00	H	N	No
2A1	Ste-Marie	4.00	----	N	----
2G1	Ste-Marie	4.00	----	N	----
2G5	Ste-Marie	4.00	----	C	----
1C2	Ste-Marie	7.00	----	N	----
2A2	Ste-Marie	7.00	----	N	----
2F3	Ste-Marie	7.00	----	N	----
2A13	Ste-Marie	10.00	----	N	----
2A15	Ste-Marie	10.00	----	C	----

----: Could not be assessed D: Diagnostic of H: Highly consistent with C: Consistent with N: Not consistent with

References

1. Kirkpatrick SI, Tarasuk V. Food insecurity is associated with nutrient inadequacies among Canadian adults and adolescents. J Nutr. 2008;138(3):604-612.
2. Pimentel L. Scurvy: historical review and current diagnostic approach. Am J Emerg Med. 2003;21(4):328-332.
3. Dickinson JA, Young B. A short history of Quebec. Montreal (QC: McGill-Queen's Press; 2008.
4. Crist TA, Sorg MH. Adult scurvy in New France: Samuel de Champlain's “mal de la terre” at Saint Croix Island, 1604–1605. Int J Paleopathol. 2014;5:95-105.
5. Sasseville D. Scurvy: curse and cure in new France. JAMA Dermatol. 2015;151(4):431-431.
6. Brickley MB, Schattmann A, Ingram J. Possible scurvy in the prisoners of Old Quebec: A re-evaluation of evidence in adult skeletal remains. Int J Paleopathol. 2016;15:92-102.
7. Gagnon A, Mazan R. Influences of early life conditions on old age mortality in old Québec. PSC Discussion Papers Series. 2006;20(5):1.
8. Gutierrez E, Ribot I, Hélie JF. Weaning among colonists from Montreal and environs: What can nitrogen isotope analysis on dentine tell us? Bioarchaeol Int. 2021;5(3-4).
9. Singer M, Bulled N, Ostrach B, Mendenhall E. Syndemics and the biosocial conception of health. Lancet. 2017;389(10072):941-950.
10. Brickley M, Mays S, Ives R. The bioarchaeology of metabolic bone disease. 2nd ed. Oxford: Academic Press; 2020.
11. Perry MA, Gowland RL. Compounding vulnerabilities: Syndemics and the social determinants of disease in the past. Int J Paleopathol. 2022;39:35-49.
12. Lopez A, Cacoub P, Macdougall IC, Peyrin-Biroulet L. Iron deficiency anaemia. Lancet. 2016;387(10021):907-916.
13. Trapani S, Rubino C, Indolfi G, Lionetti P. A narrative review on pediatric scurvy: the last twenty years. Nutrients. 2022;14(3):684.
14. Snoddy AME, Halcrow SE, Buckley HR, Standen VG, Arriaza BT. Scurvy at the agricultural transition in the Atacama desert (ca 3600–3200 BP): nutritional stress at the maternal-foetal interface? Int J Paleopathol. 2017;18:108-120.
15. Fyson D. Between the ancien Régime and liberal modernity: law, justice and state formation in colonial Quebec, 1760–1867. Hist Compass. 2014;12(5):412-432.
16. Pelletier F, Légaré J, Bourbeau R. Mortality in Quebec during the nineteenth century: From the state to the cities. Popul Stud. 1997;51(1):93-103.
17. Amorevieta-Gentil M. Les niveaux et les facteurs determinants de la mortalite infantile en Nouvelle-France et au debut du Regime Anglais (1621-1779) [Doctoral thesis]. University of Montreal, Canada; 2010.
18. Duchemin E. L’ancien cimetière Saint-Antoine (1799-1854) et son voisin rural à Pointe-aux-Trembles (1709-1843): Analyse comparative de la mortalité des enfants de deux populations du XIXe siècle sur l’île de Montréal [Master's Thesis]. University of Montreal, Canada; 2024.
19. Thornton P, Olson S. Mortality in late nineteenth-century Montreal: Geographic pathways of contagion. Pop. Stud. 2011;65(2):157-181.

20. Bigué R-A. Palaeoepidemiological analysis of a historical urban population from Montréal: Exploring the interactions between vitamin D deficiency and various palaeopathological skeletal manifestations [Master's Thesis]. University of Montreal, Canada; 2021.
21. Morland F. Nutrition et état de santé: études paléochimique et paléopathologique de la population exhumée du cimetière protestant Saint-Matthew, ville de Québec, Canada (1771-1860) [Master's Thesis]. University of Montreal, Canada; 2010.
22. Ribot I, Morland F, Boisjoli ME, Leach P. La bioarchéologie humaine, à la frontière entre le «social» et le «biologique» Démographie, archéologie et état de santé de populations historiques euroquébécoises. Collection Paléo-Québec. 2010(34):27-54.
23. Houle-Wierzbicki Z. Étude paléopathologique préliminaire à travers l'analyse macroscopique et scanographique: Exemple du cimetière St. Matthew, ville de Québec (1771-1860) [Master's Thesis]. University of Montreal, Canada; 2016.
24. Vigeant J, Ribot I, Hélie JF. Dietary habits in New France during the 17th and 18th centuries: An isotopic perspective. Am J Phys Anthropol. 2017;162(3):462-475.
25. Desloges Y, de Courval M. À table en Nouvelle-France: alimentation populaire, gastronomie et traditions alimentaires dans la vallée laurentienne avant l'avènement des restaurants. Quebec City (QC): Septentrion; 2009.
26. Ouellet F. Economic and social history of Quebec, 1760-1850: structures and conjonctures (Vol. 120). Montreal (QC): McGill-Queen's Press-MQUP; 1980.
27. Rousseau J, Bethune G, Morisset P. Voyage de Pehr Kalm au Canada en 1749. Rosemère, QC: Pierre Tisseyre; 1977.
28. Thornton PA, Olson S. Family contexts of fertility and infant survival in nineteenth-century Montreal. J. Fam. Hist. 1991 Oct;16(4):401-17.
29. Gagnon A. Crises and trends: Mortality in historical perspective. Can Stud Popul. 2012;39(3-4):1-7.
30. Schlueter AK, Johnston CS. Vitamin C: overview and update. J Evid Based Complement Altern Med. 2011;16(1):49-57.
31. Golding PH. Experimental folate deficiency in human subjects: What is the influence of vitamin C status on time taken to develop megaloblastic anaemia? BMC Hematol. 2018;18:1-10.
32. Khalife R, Grieco A, Khamisa K, Tinmouh A, McCudden C, Saidenberg E. Scurvy, an old story in a new time: The hematologist's experience. Blood Cells Mol Dis. 2019;76:40-44.
33. World Health Organization (WHO). Scurvy and its prevention and control in major emergencies. Geneva (CH): World Health Organization. 1999.
34. World Health Organization (WHO). Accelerating anaemia reduction: A comprehensive framework for action. Geneva (CH): World Health Organization. 2023.
35. Rowe S, Carr AC. Global vitamin C status and prevalence of deficiency: A cause for concern? Nutrients. 2020;12(7):2008.
36. Klaus HD. Paleopathological rigor and differential diagnosis: Case studies involving terminology, description, and diagnostic frameworks for scurvy in skeletal remains. Int J Paleopathol. 2017;19:96-110.

37. Aghajanian P, Hall S, Wongworawat MD, Mohan S. The roles and mechanisms of actions of vitamin C in bone: New developments. J Bone Miner Res. 2015;30(11):1945-1955.
38. Ortner DJ, Ericksen MF. Bone changes in the human skull probably resulting from scurvy in infancy and childhood. Int J Osteoarchaeol. 1997;7(3):212-220.
39. Brickley MB, Mays S. Metabolic disease. In: Buikstra J, ed. Ortner's identification of pathological conditions in human skeletal remains. Cambridge (MA): Academic Press; 2019:531-566.
40. Ortner DJ, Butler W, Cafarella J, Milligan L. Evidence of probable scurvy in subadults from archaeological sites in North America. Am J Phys Anthropol. 2001;114(4):343-351.
41. Brickley MB, Morgan B. Assessing diagnostic certainty for scurvy and rickets in human skeletal remains. Am J Biol Anthropol. 2023;181(4):637-645.
42. Hoffbrand V, Steensma DP. Hoffbrand's essential haematology. Hoboken (NJ): John Wiley & Sons; 2019.
43. Jaffe HL. Metabolic, degenerative, and inflammatory diseases of bones and joints. Philadelphia (PA): Lea and Febiger; 1972.
44. Morgan B, Langlois M, Schats R, Waters-Rist A, van der Merwe A, Ribot I, Brickley MB. A framework for anemia diagnosis in paleopathology using metric methods. (Under review).
45. Brickley MB. Cribra orbitalia and porotic hyperostosis: A biological approach to diagnosis. Am J Phys Anthropol. 2018;167(4):896-902.
46. Schattmann A, Bertrand B, Vatteoni S, Brickley M. Approaches to co-occurrence: Scurvy and rickets in infants and young children of 16–18th century Douai, France. Int J Paleopathol. 2016;12:63-75.
47. Gongidi P, Johnson C, Dinan D. Scurvy in an autistic child: MRI findings. Pediatr Radiol. 2013;43(10):1396-1399.
48. Polat AV, Bekci T, Say F, Bolukbas E, Selcuk MB. Osteoskeletal manifestations of scurvy: MRI and ultrasound findings. Skeletal Radiol. 2015;44:1161-1164.
49. Ethnoscop. Site du premier cimetière de Sainte-Marie, CcEs-1. Inventaire et fouilles archéologiques 2003-2004. Internal archaeological report. Ministère des transports du Québec, Direction de Chaudière-Appalaches; 2006.
50. Ethnoscop. Interventions archéologiques dans le cadre du projet de construction de la Maison du citoyen à Pointe-aux-Trembles, 2014, BjFi-17. Internal archaeological report. Rivière-des-Prairies, Pointe-aux-Trembles et Ville de Montréal; 2016.
51. Ethnoscop. Projet de réaménagement de la place du Canada. Site archéologique du cimetière Saint-Antoine (1799–1854), BiFj-37, Montréal. Fouille et supervision archéologique (2014). Internal archaeological report. Ville de Montréal; 2016.
52. Gustafson G, Koch G. Age estimation up to 16 years of age based on dental development. Odontol Revy. 1974;25:297-306.
53. Geber J, Murphy E. Scurvy in the Great Irish Famine: Evidence of vitamin C deficiency from a mid-19th century skeletal population. Am J Phys Anthropol. 2012;148(4):512-524.
54. Mazan R. Delayed measles mortality among exposed children who survived the epidemic of 1714–15 in New France. Can Stud Popul. 2012;39(3-4):9-22.

55. Bruckner TA, Gailey S, Hallman S, Amorevieta-Gentil M, Dillon L, Gagnon A. Epidemic cycles and environmental pressure in colonial Quebec. Am J Hum Biol. 2018;30(5):e23155.
56. Sorg MH, Craig BC. Patterns of infant mortality in the Upper St. John Valley French population: 1791-1838. Hum Biol. 1983;101-113.
57. Pavard S, Gagnon A, Desjardins B, Heyer E. Mother's death and child survival: the case of early Quebec. Journal of Biosocial Science. 2005 Mar;37(2):209-27.
58. Hill G, Johnston G, Campbell S, Birdsell J. The medical and demographic importance of wet-nursing. Can. B. Med. His. 1987 Oct;4(2):183-92.
59. Perry MA, Edwards E. Differential diagnosis of metabolic disease in a commingled sample from 19th century Hisban, Jordan. Int J Paleopath. 2021;33:220-33.
60. Follis Jr RH, Park EA, Jackson D. The prevalence of scurvy at autopsy during the first two years of age. Bull Johns Hopkins Hosp. 1950;87:569-592.
61. Woodruff C. Infantile scurvy: The increasing incidence of scurvy in the Nashville area. JAMA. 1956;161(5):448-456.
62. Bronte-Stewart B. The anaemia of adult scurvy. Q J Med. 1953;22(87):309-29.
63. Zuffo CRK, Osório MM, Taconeli CA, Schmidt ST, Silva BHCD, Almeida CCB. Prevalence and risk factors of anemia in children. J Pediatr. 2016;92:353-360.
64. Li Q, Liang F, Liang W, Shi W, Han Y. Prevalence of anemia and its associated risk factors among 6-months-old infants in Beijing. Front Pediatr. 2019;7:286.
65. Agarwal KN, Dhar N, Shah MM, Bhardwaj OP. Roentgenologic changes in iron deficiency anemia. Am J Roentgenol. 1970;110(3):635-637.
66. Wood JW, Milner GR, Harpending HC, Weiss KM, Cohen MN, Eisenberg LE, et al. The osteological paradox: Problems of inferring prehistoric health from skeletal samples [and comments and reply]. Curr Anthropol. 1992;33(4):343-370.
67. Young BJ. Respectable burial: Montreal's Mount Royal Cemetery. Montreal: McGill-Queen's Press; 2003.
68. Buckley HR, Kinaston R, Halcrow SE, Foster A, Spriggs M, Bedford S. Scurvy in a tropical paradise? Evaluating the possibility of infant and adult vitamin C deficiency in the Lapita skeletal sample of Teouma, Vanuatu, Pacific islands. Int J Paleopathol. 2014;5:72-85.
69. McCallum J. Unequal beginnings: agriculture and economic development in Quebec and Ontario until 1870 (Vol. 244). Peterborough: Ontario Audio Library Service; 1980.
70. Greer A. Peasant, lord, and merchant: Rural society in three Quebec parishes, 1740-1840 (Vol. 39). Toronto (ON): University of Toronto Press; 1985.
71. Mays S. The palaeopathology of scurvy in Europe. Int J Paleopathol. 2014;5:55-62.
72. Newman SL, Gowland RL. Dedicated followers of fashion? Bioarchaeological perspectives on socio-economic status, inequality, and health in urban children from the Industrial Revolution (18th–19th C), England. Int J Osteoarchaeol. 2017;27(2):217-229.
73. Gowland RL, Caffell A, Newman S, Levene A, Holst M. Broken childhoods: Rural and urban nonadult health during the Industrial Revolution in northern England (eighteenth–nineteenth centuries). Bioarchaeol Int. 2018;2(1):44-62.
74. Marsan JC. Montreal in evolution: historical analysis of the development of Montreal's architecture and urban environment. Montreal (QC): McGill-Queen's Press-MQUP; 1990.

75. Gilliland J, Olson S. Residential segregation in the industrializing city: A closer look. Urban Geogr. 2010;31(1):29-58.
76. Thornton P, Olson S. A deadly discrimination among Montreal infants, 1860–1900. Continuity Change. 2001;16(1):95-135.
77. Jamieson HC. Some historical aspects of pernicious anaemia. Can Med Assoc J. 1928;18(2):188.
78. Nault F, Desjardins B, Légaré J. Effects of reproductive behaviour on infant mortality of French-Canadians during the seventeenth and eighteenth centuries. Popul. Stud. 1990 Jul 1;44(2):273-85.
79. Le Hamon C. S'alimenter à Douai de 1598 à 1752, l'exemple des maisons charitables [Doctoral dissertation]. Université d'Artois, France; 2008.
80. Bates CJ, Prentice A. Breast milk as a source of vitamins, essential minerals and trace elements. Pharmacology & Therapeutics. 1994 Jan 1;62(1-2):193-220.
81. Dietetic Products, Nutrition and Allergies Panel (NDA). Scientific opinion on dietary reference values for vitamin C. EFSA J. 2013;11(11):3418.
82. Ville de Montreal. Parc du Vieux-Moulin de Pointe-aux-Trembles. Ville de Montreal. https://montreal.ca/lieux/parc-du-vieux-moulin-de-pointe-aux-trembles. Retrieved on November 10th, 2023.
83. Nguiagain-Launière B. Regards sur la paysannerie pointelière à travers le recensement de 1831. [Master's Thesis]. Université du Québec à Montréal, Canada; 2013.

CHAPTER 5: DISCUSSION AND CONCLUSION

The initial goals of this doctoral research were focused on using skeletal imaging to assess porotic lesions and to attempt to link such lesions to anemia. However, as the research progressed, the limitations to this approach became evident. The differences between external macroscopic appearance and internal microstructure appearance highlighted the issues with relying on porotic lesions for anemia diagnosis. Clearer frameworks on how to approach anemia diagnosis within archaeological collections were needed. In response to these issues, the research direction shifted towards a new approach aimed at integrating the biological approach and clinical data, including investigating metric approaches to anemia diagnoses, resulting in the following research question:

1. How can metric changes in bone be leveraged for anemia diagnosis, and how does this change how we study anemia in archaeological contexts?

Novel approaches to diagnosis allow for exploration of currently unexplored aspects of anemia in past communities, including co-occurrence with other conditions, such as scurvy. The next phase of this research sought to apply these methods to archaeological collections from 18th-19th century Quebec to explore the interaction of anemia and scurvy in this context. This research is framed around the following question:

2. How prevalent are scurvy, anemia, and scurvy/anemia co-occurrence within this context, and what factors influence their development and clustering?

The following sections will explore how the research presented in Chapters 2-4 addresses these guiding questions.

5.1 Anemia Diagnosis and Bone Metric Changes

Previous research on metric changes in anemia based on evaluating clinically diagnosed individuals is limited (e.g. Ebel et al., 1995; Reynolds, 1962;1965; Sebes & Diggs, 1979). These studies confirm that changes to bone dimensions, typically described as thinning of the cortex and widening of the diploic space (Agarwal et al., 1970; Reynolds, 1965), can develop during anemia. Past quantitative research on anemia and bone has generally focused on the cranium. Post-cranial evaluation of anemia in known cases has, to date, been limited to qualitative analysis (e.g. Askoy et al., 1966). The current research (Chapter 2) is the first to demonstrate that metric changes can also develop in the sternum, and suggests that changes in relative cortical bone dimensions in the manubrium and sternal body can be the result of marrow hyperplasia. The sternum is a good candidate for observing metric changes during anemia because it is relatively thin, meaning that cortical bone changes can be more readily observed. It is also subjected to less biomechanical demand compared to other sites of active marrow (e.g. the proximal femur) (Martin & Atkinson, 1977), meaning that changes to trabecular structure are more likely to be tolerated. It is also erythropoetically-active in adults (Burkhardt et al., 1987; Chirsty, 1981). Other post-cranial sites with high amounts of active marrow that could undergo expansion during

anemia include the iliac crest, sacrum, and vertebrae, but it is currently unclear if these sites will show metric differences similarly to the sternum.

Although bone microarchitecture changes were observed in the sample in Chapter 3, and have been evaluated in archaeological human remains (e.g. Morgan, 2014; Thevenon et al., 2023), the presence of quantitative differences in trabecular architecture has not yet been confirmed in clinically-diagnosed cases of anemia. This may be partially due to the limitations of imaging methods for living individuals; high-resolution CT is necessary for visualizing trabecular structures, but carries risk of radiation exposure (Saers et al., 2021; Van Dessell et al., 2013), and should therefore be avoided in cases where other investigations are available, sensitive, and specific (e.g. blood tests of hemoglobin levels). Imaging of autopsied individuals, such as the samples used by O'Donnell et al. (2020, 2023) and Anderson et al. (2021), may provide an alternative method for obtaining high-resolution images of the marrow space, although imaging at autopsy is typically done using regular-resolution clinical imaging equipment. Significant changes in microarchitecture measurement T-scores were observed between individuals in Chapter 3, but rarely were all three expected metric differences observed in the same individual (cortical/trabecular thinning, increased trabecular separation), which brings up questions on the order in which microarchitecture changes develop. Increased trabecular separation and trabecular thinning were expected to occur in tandem, and to precede cortical thinning, but many individuals did not show significantly different trabecular thickness measurements. This could be due to anemia severity, duration, the timing of anemia onset, or the overall lack of variation in trabecular thickness, which was observed in the current study and has been documented in other areas of the skeleton. For example, in the tibia, Ding & Hvid (2000) found that trabecular thickness only differed by approximately 0.03 mm on average between individuals in their young and old age categories (age range of sample between 16-85 years). Linking microarchitecture changes to known cases of anemia and establishing the order in which these changes develop would allow for greater diagnostic certainty when using these changes as part of anemia diagnosis.

Metric changes during anemia are likely influenced by a wide variety of factors, including age, age-at-onset of anemia, individual bone remodelling rates, severity of anemia, and type of anemia (i.e. genetic or acquired). Age-related bone loss is a major confounding factor; trabecular architecture and cortical thickness, both key features of skeletal manifestations of marrow hyperplasia, are negatively affected by age (Jang & Kim, 2010), and differentiating between the two processes in archaeological individuals will require incorporating other lines of evidence, such as methods of accounting for decreases in bone quality or quantity in skeletal remains (see Van Spelde et al., 2021: Figure 1), into diagnosis. For example, differentiating between skeletal changes caused by marrow hyperplasia and those caused by osteoporosis will require taking age and bone mineral density into account; if abnormally low amounts of bone are present at key skeletal areas such as the proximal femur or vertebrae for an archaeological individual of a certain age, osteopenia or osteoporosis may be affecting bone microarchitecture for that individual. Methods of differentiating between age-related bone loss and skeletal manifestations of marrow hyperplasia are complicated by the difficulties in establishing accurate age-at-death estimates for older individuals (Boldsen et al., 2022), and skeletal collections with

known ages may be the best way forward for establishing parameters on differentiating between anemia and osteoporosis/osteopenia.

Nutrition is another important confounding factor to metric diagnosis of anemia, particularly when thinking about co-occurrence of anemia with other metabolic bone diseases that may affect bone formation or resorption. When metabolic conditions co-occur, as discussed in Chapter 4, the effects on bone microarchitecture may be exacerbated. For example, Swan et al. (2023) found that children under two years with active rickets displayed enlarged femoral medullary areas and reduced cortical bone. They hypothesized that the mechanism behind this observation was that bone resorption along the endosteal border was increased, in order to release calcium from the pre-existing cortical bone to help correct deficiencies. For individuals with both active rickets and anemia, this effect may be even more exaggerated, and measurements of the medullary space could be even more enlarged. These factors reduce specificity of cortical bone and relative cortical bone analysis for anemia diagnosis, as changes may be caused by factors other than anemia and marrow hyperplasia.

Cortical thickness is a complex product of growth patterns, nutrition, pathology, mechanical loading, body mass, and activity (Cowgill et al., 2023), and untangling the effects of anemia specifically can be challenging. The range of cortical bone across different ages can also be highly variable and the wide variety of factors that can affect cortical thickness means that our ability to establish a 'normal' range of variation currently limited (Cowgill et al., 2023). Malnutrition has been found to specifically affect cortical area and cortical thickness (Cowgill et al., 2023; Gan et al., 1969), and metabolic conditions can also significantly affect cortical bone by disrupting normal growth patterns (Swan et al., 2023). It is important to note that most studies on cortical bone and nutrition have focused on cross sectional analysis of long bones, and how the amount that areas most affected by skeletal manifestations of marrow hyperplasia (i.e. the cranium) might display similar changes in bone microarchitecture in response to stress is unknown. However, the knowledge that other factors may affect cortical thickness, and exacerbate or mimic the skeletal manifestations of marrow hyperplasia, demonstrates the importance of considering contextual information and whole-skeleton pathology even when using quantitative methods as a part of diagnosis. The most significant limitation to the use of metric changes to evaluate anemia currently is that there are many unanswered questions on how these changes develop and the factors that affect them, but confirming that they do occur is a good proof-of-concept for further research that seeks to address these limitations.

5.2 Changes to Anemia Diagnosis

Paleopathological studies that investigate metric changes associated with porous cranial lesions have been done (e.g. Morgan, 2014; Rivera & Lahr, 2017; Stuart-Macadam, 1987; Zuckerman et al., 2014), but leveraging this data as part of anemia diagnosis is not common throughout paleopathological research. Many of the previously used methods require complex measurements taken at a wide variety of points, which may not always be feasible for researchers. Importantly, all of the currently published research on quantitative methods for anemia diagnosis have used the presence of porotic lesions as a basis for differentiating between

non-pathological and control groups. As analysis of porotic sternal lesions in Chapter 2 and visual evaluation of microarchitecture changes in Chapter 3 demonstrate, not all individuals who display porotic lesions have underlying accompanying indicators of marrow hyperplasia. Many of the earlier studies on quantitative methods have not found definitive correlations between presence of porotic lesions and changes to vault thickness or bone microarchitecture, and the presence of individuals with porotic lesions that developed due to a different etiology is likely to be a confounding factor in these analyses. In addition, many individuals in the sample from Chapter 3 did not display porotic lesions, but did show internal evidence of skeletal manifestations of marrow hyperplasia. For example, individual 17L-S4 displays no macroscopic porotic orbital lesions, but shows evidence of enlarged trabecular spacing and trabecular/cortical thinning through examination of the internal orbit, in additional to statistically significant widened trabecular separation (Figure 5-1). This individual was under two years old at time of death, and was likely deceased before porotic lesions as a result of marrow space changes could fully develop. Inclusion of similar individuals as part of non-pathological control groups in quantitative studies may have further skewed results, leading to inconclusive findings.

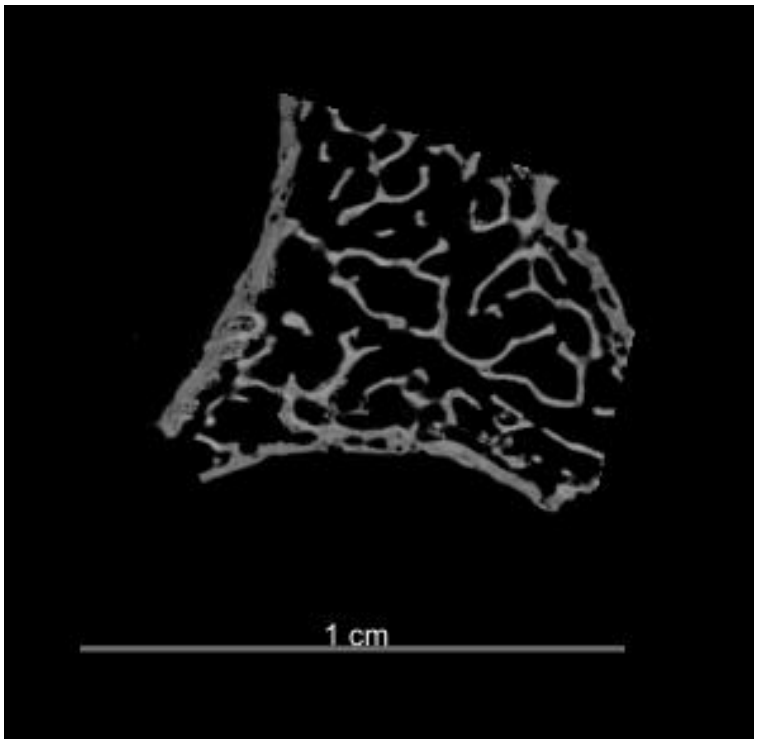

Figure 5-1: Individual 17L-S4, with evidence of cortical/trabecular thinning and widened trabecular spacing, which is consistent throughout the entire 3D orbit reconstruction. No evidence of porotic lesions were visible macroscopically (although some can be seen on the micro-CT reconstruction) despite these changes.

Incorporating metric analysis into anemia diagnosis can be used to reduce reliance on porous cranial lesions as part of anemia analysis in skeletal remains. It emphasizes the importance of using internal marrow space changes and deprioritizes CO and PH (Brickley, 2018). Throughout the current work, it has become increasingly clear that evaluating marrow hyperplasia, and therefore diagnosing anemia, is not necessarily possible through evaluation of

porous lesions alone. In Chapter 2, part of the initial research design was similar to the earlier research described above; the aim was to use macroscopic assessment to establish groups of individuals with no evidence of porous lesions that could then be used to establish baseline orbital measurements. However, visual evaluation of the micro-CT orbit reconstructions revealed that absence of macroscopically-observable lesions did not necessarily mean there were no internal microarchitecture changes indicative of marrow hyperplasia (see Figure 5), and that this method was not appropriate. For many individuals in the current research, a priori division into non-anemic vs anemic groups based on macroscopic assessment of lesions directly contradicted the metric data and/or the results of the visual assessment, further emphasizing that caution is needed for interpreting the etiology of porous orbital lesions using macroscopic evaluation alone. The result of this new approach is that initial diagnoses are conservative, but they could be adjusted in the future with the addition of new baseline data or additional clinical research, and can be built upon as part of moving away from directly correlating porosity with anemia in skeletal remains.

While porotic lesions may develop because of skeletal manifestations of marrow hyperplasia, they should not be the most important part of anemia diagnosis in skeletal remains. Marrow hyperplasia originates with the internal marrow space, and this should be the aspect of bone that is evaluated in studies of anemia. Quantitative microarchitecture analysis and bone ratio measurements specifically prioritize evaluation of the internal marrow space over scoring of external lesion appearance, ensuring that the biological mechanisms that cause skeletal changes in anemia are more consistently considered as part of diagnosis. When/if porotic lesions can be linked to underlying skeletal manifestations of marrow hyperplasia, they can play a role in anemia diagnosis, but should not be considered conclusive indicators on their own.

In recent years, interobserver error studies of porous lesion scoring have demonstrated subjectivity and low concordance in evaluation and recording of porous lesions (Anderson, 2023; Buckberry et al., 2023; Morgan et al., 2023; Santos et al., 2023). Although various recording and scoring systems for external lesion evaluation have been proposed, Anderson (2023) found observer disagreement and lack of consistency in data collection across four of the most used recording rubrics, indicating that lack of agreement is a universal problem for external lesion evaluation, and is not tied to the use of one specific scoring system. Furthermore, the use of different rubrics by different researchers can cause further confusion and inconsistency when comparing data across contexts (Anderson, 2023). If researchers cannot agree on how to describe the same lesion, agreement on lesion etiology is likely to be similarly inconsistent (Biehler-Gomez et al., 2020). Quantitative analysis is a less subjective method of evaluating skeletal indicators of marrow hyperplasia (Anderson et al., 2021; Brickley, 2024), and while it is still necessary to consider underlying factors that could be contributing to any observed metric differences, it can help to ensure greater consistency in diagnosis between different researchers. There can still be error associated with metric evaluation, but reproducibility tends to be improved overall.

In addition to having low rates of observer agreement, most scoring rubrics for porous lesions do not actually include categories for evaluating the cause of lesions, and therefore are

not necessarily useful for assessing anemia in a robust, consistent fashion. As discussed by Brickley (2024), evaluation of anemia in skeletal remains was originally based on the biological approach, and the underlying physiological mechanisms for porous lesion development were considered as part of anemia diagnosis. This process shifted towards more of a comparative approach (as defined by Mays, 2018) at best; rubrics are used to describe lesions, but the scored features of porosity (i.e. severity) are not necessarily tied to assessing lesion etiology (Brickley, 2024). As Anderson (2023) notes on current descriptive scoring methods, "morphological categories are only meaningful if they correspond to differences in the causes, outcomes, or individual experiences of lesion-causing processes" (p.70). Without internal evaluation of the marrow space, it is difficult to differentiate skeletal manifestations of marrow hyperplasia from other lesion-causing processes. Quantitative analysis helps to bring diagnosis back to a biological approach and adds a measurable diagnostic parameter as another method of anemia diagnosis (Brickley, 2024). Using metric methods, such as the ones described throughout this thesis, inherently evaluates changes that can be directly tied to skeletal manifestations of marrow hyperplasia, improving the level of certainty researchers can have in their diagnoses.

Chapters 2 and 3 demonstrate two possible metric methods of evaluating anemia: relative cortical bone ratios and microarchitecture measurements. These methods can be used in archaeological contexts where imaging analysis is possible, and incorporated into anemia diagnosis following the recommendations set out in Chapter 3. Micro-CT imaging will be necessary for visualization of microarchitecture changes, but radiography and CT imaging, which are more accessible, can be used for ratio assessment. In cases where the individual cannot undergo imaging, and the internal marrow space is not visible, anemia cannot be evaluated, and porotic cranial lesions like CO and PH can be used as general indicators of health or stress only.

The ability to evaluate anemia in archaeological individuals improves specificity of diagnosis, allowing researchers to present more precise or detailed interpretations of health in past contexts. Porotic lesions such as CO and PH are often used in conjunction with mortality data and survivorship analysis (e.g. Betsinger et al., 2020; McFadden & Oxenham, 2020), which is effective for paleoepidemiological analysis of frailty/resilience, or as a proxy for assessing non-specific stress level within a population or demographic group. These types of analyses do not typically include specific anemia diagnoses, likely due to the inherent constraints of diagnosing anemia based on the evaluation of porous lesions. Anemia has known effects on health, including weakened immune system functioning, fatigue, and impaired mental cognition and is a good proxy for overall population health (WHO, 2023). It also interacts and is influenced by a wide variety of environmental, structural, and social variables (see Chapter 1, Figure 1). Research that specifically assesses anemia within a sample (instead of lesions) can access these aspects of health and well-being, and better understand the factors that contributed to anemia (instead of non-specific stress) within a context.

The incorporation of post-cranial elements into studies of anemia (e.g. Chapter 2) can expand who can be evaluated for anemia, and better determine when the individual experienced anemia. Without post-cranial indicators, in cases where the cranium is poorly preserved, or even absent, investigation of anemia would be impossible, but use of the sternum would allow for a

potential diagnosis. In contrast to common sites of marrow hyperplasia, such as the cranium, the sternum maintains active or mixed bone marrow into adulthood (Brickley, 2018), and could be used as an indicator of anemia that was initiated past childhood, which cannot currently be evaluated through cranial indicators. McFadden and Oxenham (2020) discuss the differences between interpretations of CO in adults and nonadults, and that analysis of CO in adults gives insight into frailty and resilience, instead of prevalence of health conditions. Post-cranial elements that can be linked to episodes of anemia that did not start in childhood could allow for calculation of anemia prevalence in older individuals, and interpretations of how active health conditions affected adult lived experience.

5.3 Anemia and Scurvy Co-Occurrence

Demographic data demonstrates high rates of early childhood mortality in Colonial Quebec (Bruckner et al., 2018; Gagnon & Mazan, 2006; Mazan, 2012). Perceptions at the time were that children in urban cities were more at risk, as epidemics were frequent, and poor sanitary infrastructure, overcrowding, and poverty were prevalent, particularly for lower socioeconomic status communities (Pelletier et al., 1997; Thorton & Olson, 2011). The inclusion of an urban (Saint-Antoine), rural (Sainte-Marie), and suburban (Pointe-aux-Trembles) site in the current research allowed for investigation of this idea, although sample composition does limit the certainty of the conclusions that can be drawn, and is a consideration when interpreting observed trends.

The scurvy/anemia prevalence data from Chapter 4 does not support the hypothesis that rural children were better off than urban ones in 18th-19th century Quebec, which is a main finding of this research. Urban and rural comparisons in bioarcheological collections are common, particularly when studying the health of past communities. In their comprehensive analysis of the study of urbanization in bioarchaeology, Betsinger & DeWitte (2022) found 50 English-language publications that compared some aspect of health in urban versus rural populations. Of these studies, seven focus on metabolic disease and/or vitamin deficiencies, and most of these (5/7) did also not find any difference between urban and rural contexts. The results from Chapter 4, in conjunction with the results of these other publications, suggest that determinants of health are more complicated than a strict urban/rural dichotomy. The negative factors of urban environments that are often thought to contribute to worse health (e.g. overcrowding, spread of infectious disease) do not affect all individuals equally as those of higher socioeconomic status tend to be less affected by many of these factors (Betsinger & DeWitte, 2022; Gowland et al., 2018). In this context, shared environmental stressors and cultural practices around weaning and childbirth between the French-Canadian samples from Saint-Antoine and Sainte-Marie are likely to have played more of a role in metabolic disease prevalence than differences in urban versus rural living.

Total anemia prevalence in the Quebec samples (approximately 29%) is high, and the age-at-death distribution for anemia peaking in the 1-2.9 year age category speaks to the challenges facing mothers and their children in these samples. However, as this research is the first to investigate anemia prevalence in an archaeological context through imaging and analysis

of the internal marrow space, comparisons of crude anemia prevalence from these sites to other contemporary communities are difficult. The prevalence of anemia in this study was lower than has been reported in other archaeological contexts (e.g. >50%, Hens et al., 2019), but previous methods have tended to rely on macroscopic examination of porous lesions, rather than evaluation of internal skeletal manifestations of marrow hyperplasia. Correlation of crude CO or PH prevalence with anemia prevalence is likely to overrepresent the number of cases of anemia in a skeletal sample, and may mean that other causes of porous cranial lesions, including metabolic disease like scurvy, are underrepresented. Further research using the framework presented in Chapter 3 will be necessary to generate comparative data so that stronger interpretations about anemia prevalence in these communities can be made.

The site of Pointe-aux-Trembles was notably different from both Saint-Antoine and Sainte-Marie in terms of mean age-at-death and scurvy prevalence. As discussed in Chapter 4, Pointe-aux-Trembles was a suburban village just outside of Montreal, which enjoyed increased trade and migration with the city after 1734. Due to perceptions about differences in health between urban and rural environments, children were sent away from Montreal to be wet-nursed by women in Pointe-aux-Trembles; over 60 children were sent to the village of Pointe-aux-Trembles in a 50-year span (Ethnoscop, 2016a). The increased number of children in the village may bias the sample towards younger individuals, and this limitation does affect interpretation of mortality trends. However, Pointe-aux-Trembles had a notably higher prevalence of scurvy (59.1%) compared to both Saint-Antoine and Sainte-Marie, as well as most other contemporary sites. Geber & Murphy (2012), who examined a mass grave collection from the Great Famine in Ireland, found a similar prevalence (66-68%) in nonadults when including probable, possible, and definite categories of scurvy diagnosis, demonstrating how severe the levels of nutritional deficiency at Pointe-aux-Trembles were. Pointe-aux-Trembles also had a significantly lower mean age-at-death than the other two sites, and many of the individuals estimated to be under one year were diagnosed with scurvy. Adequate vitamin C is generally provided to children through breastfeeding, unless their mother or wet nurse is severely malnourished and deficient in vitamin C (NDA, 2013). The high prevalence of scurvy in infants at Pointe-aux-Trembles could reflect severe vitamin C deficiencies in breastfeeding women, or it could also be a product of wet-nursing practices, with local women unable to support feeding of all children. The site of Pointe-aux-Trembles demonstrates the effect of scurvy on mortality risk for young children, and the impact of early childhood feeding on overall health.

The mean age-at-death for individuals from Pointe-aux-Trembles was 1.3 years, and the high prevalence of very young individuals in this collection particularly raises the issue of paleopathological diagnosis in very young children. Porosity is a typical feature of growth and development (Lewis, 2017a, b), and clinical studies have also identified periosteal new bone in healthy infants (e.g. Shopfner 1966). Therefore, ruling out normal, growth-related porosity and new bone from possible pathology can be challenging, particularly for children under one year old (Lewis, 2017a, b). In the current research, lesion location and expression were key parts of differentiating between changes related to growth and development and those related to scurvy. In scurvy, lesions typically develop at locations where blood vessels are most likely to rupture, such as those near commonly-used muscles (Klaus, 2017). Bilateral lesions of the greater wing

of the sphenoid, for example, are thought to be associated with blood vessel rupture caused by chewing or mouth movements (Klaus, 2017). Porosity and SPNB at sites that do not meet this criterion are less likely to be associated with scurvy-induced inflammation. Lesions were also evaluated microscopically to clarify scoring, diagnostic certainty assignments reflected cases across all three collections where growth and development could not be excluded as a potential factor contributing to lesion appearance.

Applying novel diagnostic frameworks for anemia to collections from 18th-19th century Quebec allowed for a more holistic analysis of health and multimorbidity in this context. Previous paleopathological analysis and historical documentation have demonstrated that access to nutrition and food insecurity were problems in Colonial Quebec, but examining anemia/scurvy co-occurrence in three related, but unique communities, helped to specifically explore the pathways that led to such challenges. The high prevalence of scurvy and anemia across urban, rural, and suburban communities is linked to the unique cultural, environmental, and structural variables that operated within these contexts, including harsh winters, famine, differential access to resources and culturally mediated infant feeding, weaning and maternal practices. Although the prevalence of individuals diagnosed with both anemia and scurvy was low (6.5%), and the sample size was too small to conclude that co-occurrence significantly affected age-at-death, these factors all likely contributed to clustering of both conditions within all three contexts.

As discussed in Chapter 1, paleopathological literature on anemia and scurvy co-occurrence is rare. Paleopathological studies that do discuss it usually mention co-occurrence as a factor to consider during differential diagnosis (e.g. Byrnes & Muller, 2022). The question of whether anemia *or* scurvy contributed to possible changes may be asked (e.g. Zuckerman et al., 2014), but rarely is co-occurrence seriously investigated on a wider scale (exceptions include Perry & Edwards, 2021). The investigation of co-occurrence in Chapter 4 did identify multiple individuals who displayed skeletal indicators of both conditions, even with a conservative approach to anemia diagnosis. This finding suggests that the possibility for scurvy/anemia co-occurrence should not be thought of as a rare paleopathological incident. Instead of asking whether anemia *or* scurvy has contributed to observed skeletal lesions or changes, researchers should also consider whether both conditions could have occurred in the same individual, and evaluate what the presence of co-occurrence might mean for the sample as a whole.

The ability to specifically assess anemia in this research allows for greater confidence in identifying cases of co-occurrence and therefore in interpreting paleopathological trends. For example, if the research in Chapter 4 had examined prevalence of CO and PH instead of anemia and scurvy specifically, assessing potential differences between how each condition contributed to mortality risk would not have been possible. Improved certainty and reproducibility in anemia diagnosis and reporting will allow researchers to investigate anemia co-occurrence more consistently throughout the archaeological record. This allows for further investigation of how/if anemia has exacerbated the effects of other diseases or contributed to elevated mortality risk in different archaeological contexts. Perry & Edwards (2021) discuss how a population-based approach to studying co-occurrence falls under the umbrella of syndemic theory. In the current study, a synergistic relationship between anemia and scurvy cannot be inferred with available

data. However, this does not mean that co-occurrence of scurvy and anemia will not negatively affect age-at-death in other contexts. Social, cultural, political, and environmental variables can have different effects on the same disease depending on context (Mendenhall, 2016), and scurvy/anemia co-occurrence at other sites will help to further investigate their potential for syndemic interaction in the past.

5.4 Future Research Directions

A limitation that affected all three papers of this thesis was sample size. The clinical sample of anemia patients in Chapter 2 that fit the chosen criteria was small, the sample of older nonadults in Chapter 3 was limited, and only 31 individuals could be assessed for co-occurrence of anemia and scurvy in Chapter 4, meaning that only a subset could be used to explore the relationship between co-occurrence and mortality trends. Limitations imposed on fieldwork by COVID-19 and changes in the overall direction of this research meant that expanding on sample sizes was challenging. For all these projects, expanding sample size is a key part of future research, and will help to establish greater confidence in the interpretations that have been made.

The observations made about orbital microstructure in Chapter 3 raise questions about the process of how skeletal manifestations of marrow hyperplasia arise that could be explored in future research. It is expected that increased trabecular separation as a result of marrow hyperplasia is directly related to trabecular thinning/atrophy, as more space is needed for the increased amount of bone marrow (Brickley, 2018). However, many of the nonadult orbits in Chapter 3 displayed evidence of increased trabecular separation with no concurrent evidence of trabecular thinning. One hypothesis is that young individuals with developing orbits who are undergoing orbital marrow hyperplasia do not develop the same type of trabecular structure as those who are not, and instead develop trabeculae with a large degree of separation for marrow to exist within. This would mean that enlarged trabecular separation for these individuals is not due to trabeculae that have developed and then been resorbed, but that the trabecular network did not develop fully in the first place due to the increased demand for active marrow. The limited remodelling of the orbit means that this structure would then persist in older individuals (McFadden & Oxenham, 2020; Mendelson & Wong, 2012). Further investigation of patterns of bone microarchitecture growth and development in a large sample of nonadults spanning various age categories would help to clarify the timing of these processes.

As evidenced from the difficulty in directly comparing micro-CT and CT images in Chapter 2, there are challenges to comparing results from different imaging sources. Panzer et al. (2023) and Anderson et al. (2021) both describe difficulties in visualizing orbital porosity due to the limitations of the imaging methods that were used; similar issues in visualizing sternal porosity using CT imaging was found in the current research. As discussed in Chapter 3, the original cranial ratios were measured using radiographs (Reynolds 1962, 1965; Sebes & Digg, 1979), and the use of different imaging techniques, especially more precise methods like micro-CT, will affect measurement comparisons and skew ratios, making use of these threshold values less reliable. Therefore, developing different standards for different imaging methods, or developing methods that allow for comparison of measurements from different imaging sources

(e.g. Saers et al., 2021), will be necessary for the broader incorporation of metric methods that rely on imaging into anemia diagnosis. Comparing ratio and microarchitecture measurements in the same bone utilizing different imaging methods will help to better understand how much measurements can differ, and if there are underlying structural properties that can skew the appearance of bone across the different techniques.

In addition to future technical research, the study of co-occurrence in Colonial Quebec specifically has raised biocultural questions that could be addressed by also evaluating co-occurrence in different contexts. For example, in a community where different local factors were at play, would anemia or scurvy/anemia co-occurrence significantly affect age-at-death? In a context where more individuals tend to live past childhood episodes of scurvy, would co-occurrence prevalence be different? These questions require comparative data to answer, and routine consideration of scurvy/anemia co-occurrence in other archaeological contexts would help to generate such data.

5.5 Conclusions

Paleopathologists are interested in a wide variety of different aspects of anemia in the archaeological record. Questions surrounding the relationship between anemia and mortality, how common anemia was, if it relates to diet and nutrition, and how it might have interacted with or influenced the progression of other diseases have been asked since the connection between anemia and porous lesions was originally made. These lines of research will continue to be of interest to paleopathologists, and can provide key information on different aspects of health and disease in the past. However, since current methods for assessing anemia can be problematic, the development of novel methods for identifying and diagnosing anemia is a critical part of answering these questions.

My research has found that there are skeletal changes to relative bone ratios in known cases of anemia, and suggests that bone microarchitecture changes evaluated through micro-CT analysis can be a useful tool for identifying baseline differences that represent pathology. Recognizing relative differences in sternal cortical bone is a novel method for anemia investigation in skeletal remains, and Chapter 2 represents the only research to date that incorporates both hematological and paleopathological data. Additional metric methods, such as relative cortical bone ratios in the frontal bone and bone microarchitecture T-scores (a method commonly used in clinical osteoporosis diagnosis), also have utility for anemia diagnosis in skeletal remains (Chapter 3). The use of multiple methods in conjunction with a consideration of the other factors that affect skeletal manifestations of marrow hyperplasia, such as age and other pathology, helps to improve anemia diagnostic certainty. This research sets a precedent for future quantitative methods of evaluating anemia, and provides a general framework that researchers can follow as part of their own investigations into anemia in past contexts.

I have also demonstrated that porotic lesions, both in the sternum and the orbital roof, are not necessarily associated with skeletal manifestations of marrow hyperplasia, and that assessment of the internal marrow space is crucial for differentiating between different sources

of porosity (Chapter 2, 3). This is a main takeaway of this research, and future paleopathological work that seeks to assess anemia in archaeological contexts must move away from strict external assessment of porosity (e.g. Chapter 4), and should incorporate the underlying biological and physiological mechanisms that contribute to skeletal changes in the assessment of skeletal pathology. Visual and metric assessment of orbits with and without porous lesions demonstrated that there are often underlying microarchitecture changes that cannot be visualized externally, and that caution is needed when interpreting lesions if no method of analyzing the marrow space is possible.

By applying these methodological frameworks to an archaeological context, I was able to conduct a broader study on scurvy and anemia co-occurrence (Chapter 4), which is a new direction for anemia research in paleopathology. All three urban and rural sites had a high prevalence of scurvy and anemia amongst individuals under 15 years, and scurvy likely contributed to higher mortality risk and younger age-at-death. This is the first population-based study of scurvy and anemia co-occurrence specifically, and it demonstrates that clustering of these conditions is not uncommon in contexts experiencing significant nutritional and environmental stress. It also demonstrates that urban and rural lifestyles were not the most important factor in determining prevalence of scurvy/anemia or age-at-death, as expected, but that the weaning and child feeding practices at Pointe-aux-Trembles had the most influence on metabolic disease prevalence instead.

Anemia is a complex condition, and is equally complex to assess in skeletal remains. It can develop due to a wide variety of factors, it can co-occur with other conditions, and the skeletal changes it causes can overlap with other conditions. The methods presented here, including internal evaluation of the marrow space and metric assessments, offer new avenues for pursing anemia diagnosis in skeletal remains. This research provides a starting point for future research into anemia diagnosis in paleopathology, and a proof of concept for metric methods as part of anemia diagnosis. It highlights the importance of analyzing bone microarchitecture changes when evaluating skeletal changes related to anemia, and emphasizes the importance of moving away from porous lesions for anemia analysis in past contexts.

REFERENCES

Agarwal, K. N., Drar, N., Shah, M. M., & Bhardwaj, O. P. (1970). Roentgenologic changes in iron deficiency anemia. *American Journal of Roentgenology, 110*(3), 635-637.

Aksoy, M., Çamli, N., & Erdem, S. (1966). Roentgenographic bone changes in chronic iron deficiency anemia: A study in twelve patients. *Blood, 27*(5), 677-686.

Anderson, A. S. (2023). Observer agreement on the morphology of porous cranial lesions: Results from a workshop at the 2019 meeting of the Paleopathology Association. *International Journal of Paleopathology, 43,* 68-71.

Anderson, A. S., Sutherland, M. L., O'Donnell, L., Hill, E. C., Hunt, D. R., Blackwell, A. D., & Gurven, M. D. (2021). Do computed tomography findings agree with traditional osteological examination? The case of porous cranial lesions. *International Journal of Paleopathology, 33,* 209-219.

Angel, J. L. (1954). Human biology, health and history in Greece from the first settlement until now. *Yearbook of the American Philosophical Society, 98,* 168-174.

Angel, J. L. (1966). Porotic hyperostosis, anemias, malarias, and marshes in the prehistoric eastern Mediterranean. *Science, 153*(3737), 760-763.

Angel, J.L. (1950). Skeletons. *Archaeology, 3,* 233-241.

Balarajan, Y., Ramakrishnan, U., Özaltin, E., Shankar, A. H., & Subramanian, S. V. (2011). Anaemia in low-income and middle-income countries. *The Lancet, 378*(9809), 2123-2135.

Berger, A. J., & Kahn, D. (2012). Growth and development of the orbit. *Oral and Maxillofacial Surgery Clinics, 24*(4): 545-555.

Betsinger, T. K., & DeWitte, S. N. (2021). Toward a bioarchaeology of urbanization: Demography, health, and behavior in cities in the past. *American Journal of Physical Anthropology, 175,* 79-118.

Betsinger, T. K., DeWitte, S. N., Justus, H. M., & Agnew, A. M. (2020). Frailty, survivorship, and stress in medieval Poland: A comparison of urban and rural populations. In T.K. Betsinger and S.N. Dewitte (Eds.) *The bioarchaeology of urbanization: The biological, demographic, and social consequences of living in* cities (pp. 223-243). Springer.

Biehler-Gomez, L., Indra, L., Martino, F., Campobasso, C. P., & Cattaneo, C. (2020). Observer error in bone disease description: A cautionary note. *International Journal of Osteoarchaeology, 30*(5), 607-615.

Blebea, J. S., Houseni, M., Torigian, D. A., Fan, C., Mavi, A., Zhuge, Y., Iwanaga, T., Mishra, S., Udupa, J., Zhuang, J., Gopal, R., & Alavi, A. (2007). Structural and functional imaging of normal bone marrow and evaluation of its age-related changes. *Seminars in Nuclear Medicine, 37*(3), 185-194).

Boldsen, J. L., Milner, G. R., & Ousley, S. D. (2022). Paleodemography: From archaeology and skeletal age estimation to life in the past. *American Journal of Biological Anthropology*, *178*, 115-150.

Brickley, M. B. (2018). Cribra orbitalia and porotic hyperostosis: A biological approach to diagnosis. *American Journal of Physical Anthropology*, 167(4), 896-902.

Brickley, M. B. (2024). Perspectives on anemia: Factors confounding understanding of past occurrence. *International Journal of Paleopathology*, *44*, 90-104.

Brickley, M. B., & Morgan, B. (2022). Metabolic and endocrine diseases. In A.L. Grauer (Ed) *The Routledge handbook of paleopathology* (pp. 338-359). Routledge.

Britton, H. A., Canby, J. P., & Kohler, C. M. (1960). Iron deficiency anemia producing evidence of marrow hyperplasia in the calvarium. *Pediatrics*, *25*, 621-628.

Bruckner, T. A., Gailey, S., Hallman, S., Amorevieta-Gentil, M., Dillon, L., & Gagnon, A. (2018). Epidemic cycles and environmental pressure in colonial Quebec. *American Journal of Human Biology*, *30*(5), e23155.

Buckberry, J., Ali, A., Hebda, M., Evans, A., Sparrow, T., Koon, H., & Wilson, A. (2023). Visualizing cribra orbitalia using modern imaging techniques [conference presentation]. In Monge Calleja, A. M., Santos, A. L., & Gomes, R.A.M.P. (Coord.). (2023). *International Meeting on Porous Skeletal Lesions: Achievements and future directions. Program and Abstract Book*. University of Coimbra, Research Centre in Anthropology and Health (CIAS). http://hdl.handle.net/10316/108791.

Buikstra, J. E., & Prevedorou, E. (2012). John Lawrence Angel (1915–1986). In J.E. Buiksta & C. Roberts (Eds.), *The global history of paleopathology: Pioneers and prospects* (pp.13-33). Oxford University Press.

Burkhardt, R., Kettner, G., Böhm, W., Schmidmeier, M., Schlag, R., Frisch, B., Mallman, B., Eisenmenger, W., & Gilg, T. H. (1987). Changes in trabecular bone, hematopoiesis and bone marrow vessels in aplastic anemia, primary osteoporosis, and old age: a comparative histomorphometric study. *Bone*, *8*(3), 157-164.

Byrnes, J. F., & Muller, J. L. (2022). A child left behind: Malnutrition and chronic illness of a child from the Erie County Poorhouse Cemetery. *International Journal of Osteoarchaeology*, *32*(5), 1035-1048.

Cascio, M. J., & DeLoughery, T. G. (2017). Anemia: evaluation and diagnostic tests. *Medical Clinics*, *101*(2), 263-284.

Chaparro, C. M., & Suchdev, P. S. (2019). Anemia epidemiology, pathophysiology, and etiology in low-and middle-income countries. *Annals of the New York Academy of Sciences*, *1450*(1), 15-31.

Clynes, M. A., Harvey, N. C., Curtis, E. M., Fuggle, N. R., Dennison, E. M., & Cooper, C. (2020). The epidemiology of osteoporosis. *British Medical Bulletin*, *133*(1), 105-117.
Cowgill, L., Harrington, L., MacKinnon, M., & Kurki, H. K. (2023). Gains in relative cortical area during growth and their relationship to nutrition, body size, and physical activity. *American Journal of Biological Anthropology*, *182*(2), 177-193.

Ding, M., & Hvid, I. (2000). Quantification of age-related changes in the structure model type and trabecular thickness of human tibial cancellous bone. *Bone*, *26*(3), 291-295.

Ebel, K. D., Richter, E., & Willich, E. (1995). Differential diagnose in der Pädiatrischen Radiologie Band I. Thieme-Verlag.

El-Najjar, M. Y., Ryan, D. J., Turner, C. G., & Lozoff, B. (1976). The etiology of porotic hyperostosis among the prehistoric and historic Anasazi Indians of southwestern United States. *American Journal of Physical Anthropology*, *44*(3), 477-487.

Erslev, A. J. (1991). Erythropoietin. *New England Journal of Medicine*, *324*(19), 1339-1344.

Ethnoscop. (2016). Interventions archéologiques dans le cadre du projet de construction de la Maison du citoyen à Pointe-aux-Trembles, 2014, BjFi-17. Internal archaeological report. Rivière-des-Prairies, Pointe-aux-Trembles et Ville de Montréal.

Fairgrieve, S. I., & Molto, J. E. (2000). Cribra orbitalia in two temporally disjunct population samples from the Dakhleh Oasis, Egypt. *American Journal of Physical Anthropology*, *111*(3), 319-331.

Fischer, N. C., Shamah-Levy, T., Mundo-Rosas, V., Méndez-Gómez-Humarán, I., & Pérez-Escamilla, R. (2014). Household food insecurity is associated with anemia in adult Mexican women of reproductive age. *The Journal of Nutrition*, *144*(12), 2066-2072.

Gagnon, A., & Mazan, R. (2006). Influences of early life conditions on old age mortality in old Québec. *PSC Discussion Papers Series*, *20*(5), 1.

Garn, S. M., Guzmán, M. A., & Wagner, B. (1969). Subperiosteal gain and endosteal loss in protein-calorie malnutrition. *American Journal of Physical Anthropology*, *30*(1), 153-155.

Grauer, A. L. (2019). Circulatory, reticuloendothelial, and hematopoietic disorders. In J.E. Buikstra (Ed.) *Ortner's identification of pathological conditions in human skeletal remains* (pp. 491-529). Academic Press.

Guillerman, R. P. (2013). Marrow: red, yellow, and bad. *Pediatric Radiology*, *43*, 181-192.

Hiram-Bab, S., Liron, T., Deshet-Unger, N., Mittelman, M., Gassmann, M., Rauner, M., Franke, K., Wielockx, B., Neumann, D., & Gabet, Y. (2015). Erythropoietin directly stimulates osteoclast precursors and induces bone loss. *The FASEB Journal*, *29*(5), 1890-1900.

Hoffbrand, V., & Steensma, D. P. (2019). *Hoffbrand's essential haematology*. John Wiley & Sons.

Hollar, M. A. (2001). The hair-on-end sign. *Radiology*, *221*(2), 347-348.

Hooten, E. A. (1930). *Indians of Pecos Pueblo*. The Yale University Press.

Jaffe, H. L. (1972). *Metabolic, degenerative, and inflammatory diseases of bones and joints*. Lea and Febeiger.

Jang, I. G., & Kim, I. Y. (2010). Computational simulation of simultaneous cortical and trabecular bone change in human proximal femur during bone remodeling. *Journal of Biomechanics*, *43*(2), 294-301.

Kassebaum, N. J., & GBD 2013 Anemia Collaborators. (2016). The global burden of anemia. *Hematology/Oncology Clinics of North America*, *30*(2), 247-308.

Klaus, H. D. (2017). Paleopathological rigor and differential diagnosis: Case studies involving terminology, description, and diagnostic frameworks for scurvy in skeletal remains. *International Journal of Paleopathology*, *19*, 96-110.

Klein, L., Li, Q. X., Donovan, C. A., & Powell, A. E. (1990). Variation of resorption rates in vivo of various bones in immature rats. *Bone and Mineral*, *8*(2), 169-175.

Lewis, M. E. (2017a). Fetal paleopathology: an impossible discipline. In S. Han, T. K. Betsinger, & A. B. Scott (Eds.), *The anthropology of the fetus: Biology, Culture, and Society* (pp.112-145). Berghahn.

Lewis, M. E. (2017b). Paleopathology of children: Identification of pathological conditions in the human skeletal remains of non-adults. Academic Press.

Lovasz, G., Schultz, M., Goedde, J., Bereczki, Z., Pálfi, G., Marcsik, A., & Molnar, E. (2013). Skeletal manifestations of infantile scurvy in a late medieval anthropological series from Hungary. *Anthropological Science*, *121*(3), 173-185.

Lucca, U., Tettamanti, M., Mosconi, P., Apolone, G., Gandini, F., Nobili, A., Tallone, M. V., Detoma, P., Giacomin, A., Clerico, M., Tempia, P., Guala, A., Fasolo, G., & Riva, E. (2008). Association of mild anemia with cognitive, functional, mood and quality of life outcomes in the elderly: the "Health and Anemia" study. *PloS One*, *3*(4), e1920.

Ludwig, H., & Strasser, K. (2001). Symptomatology of anemia. *Seminars in Oncology*, *28*, 7-14.

Marsan, J. C. (1990). *Montreal in evolution: historical analysis of the development of Montreal's architecture and urban environment*. McGill-Queen's Press-MQUP.

Martin, R. B., & Atkinson, P. J. (1977). Age and sex-related changes in the structure and strength of the human femoral shaft. *Journal of Biomechanics*, *10*(4), 223-231.

Mays, S. (2018). How should we diagnose disease in palaeopathology? Some epistemological considerations. *International Journal of Paleopathology*, *20*, 12-19.

Mazan, R. (2012). Delayed measles mortality among exposed children who survived the epidemic of 1714–15 in New France. *Canadian Studies in Population*, *39*(3-4), 9-22.

McFadden, C., & Oxenham, M. F. (2020). A paleoepidemiological approach to the osteological paradox: Investigating stress, frailty, and resilience through cribra orbitalia. *American Journal of Physical Anthropology*, *173*(2), 205-217.

McIlvaine, B. K. (2015). Implications of reappraising the iron-deficiency anemia hypothesis. *International Journal of Osteoarchaeology*, *25*(6), 997-1000.

Mendelson, B., & Wong, C. H. (2012). Changes in the facial skeleton with aging: Implications and clinical applications in facial rejuvenation. *Aesthetic Plastic Surgery*, *44*(4), 1151-1158.

Mendenhall, E. (2016). Beyond comorbidity: a critical perspective of syndemic depression and diabetes in cross-cultural contexts. *Medical Anthropology Quarterly*, *30*(4), 462-478.

Mendenhall, E. (2017). Syndemics: a new path for global health research. *The Lancet*, *389*(10072), 889-891.

Mensforth, R. P., Lovejoy, C. O., Lallo, J. W., & Armelagos, G. J. (1978). Part two: The role of constitutional factors, diet, and infectious disease in the etiology of porotic hyperostosis and periosteal reactions in prehistoric infants and children. *Medical Anthropology*, *2*(1), 1-59.

Morgan, B., Schats, R., Ribot, I., & Brickley, M.B. (2023). Quantifying the accuracy of anemia diagnosis using porous orbital lesions [conference presentation]. In Monge Calleja, A. M., Santos, A. L., & Gomes, R.A.M.P. (Coord.). (2023). *International Meeting on Porous Skeletal Lesions: Achievements and future directions. Program and Abstract Book*. University of Coimbra, Research Centre in Anthropology and Health (CIAS). http://hdl.handle.net/10316/108791.

Morgan, J. A. (2014). *The methodological and diagnostic applications of micro-CT to palaeopathology: a quantitative study of porotic hyperostosis* [Doctoral thesis]. The University of Western Ontario (Canada).

Moseley, J. E. (1965). The paleopathologic riddle of" symmetrical osteoporosis". *American Journal of Roentgenology*, *95*(1), 135-142.

Naveed, H., Abed, S. F., Davagnanam, I., Uddin, J. M., & Adds, P. J. (2012). Lessons from the past: Cribra orbitalia, an orbital roof pathology. *Orbit*, *31*(6), 394-399.

Dietetic Products, Nutrition and Allergies Panel (NDA). Scientific opinion on dietary reference values for vitamin C. EFSA J. 2013;11(11):3418.

O'Donnell, L., Buikstra, J. E., Hill, E. C., Anderson, A. S., & O'Donnell Jr, M. J. (2023). Skeletal manifestations of disease experience: Length of illness and porous cranial lesion formation in a contemporary juvenile mortality sample. *American Journal of Human Biology*, e23896.

O'Donnell, L., Hill, E. C., Anderson, A. S. A., & Edgar, H. J. (2020). Cribra orbitalia and porotic hyperostosis are associated with respiratory infections in a contemporary mortality sample from New Mexico. *American Journal of Physical Anthropology*, *173*(4), 721-733.

O'Neal, M. L., Dwornik, J. J., Ganey, T. M., & Ogden, J. A. (1998). Postnatal development of the human sternum. *Journal of Pediatric Orthopaedics*, *18*(3), 398-405.

Ortner, D. J., Butler, W., Cafarella, J., & Milligan, L. (2001). Evidence of probable scurvy in subadults from archeological sites in North America. *American Journal of Physical Anthropology*, *114*(4), 343-351.

Oxenham, M. F., & Cavill, I. (2010). Porotic hyperostosis and cribra orbitalia: The erythropoietic response to iron-deficiency anaemia. *Anthropological Science*, *118*(3), 199-200.

Palkovich, A. M. (1987). Endemic disease patterns in paleopathology: Porotic hyperostosis. *American Journal of Physical Anthropology*, *74*(4), 527-537.

Panzer, S., Schneider, K. O., Zesch, S., Rosendahl, W., Thompson, R. C., & Zink, A. R. (2023). Anemias in ancient Egyptian child mummies: Computed tomography investigations in European museums. *International Journal of Osteoarchaeology*, *33*(3), 532-545.

Pechenkina, E. A., & Delgado, M. (2006). Dimensions of health and social structure in the early intermediate period cemetery at Villa El Salvador, Peru. *American Journal of Physical Anthropology*, *131*(2), 218-235.

Pelletier, F., Légaré, J., & Bourbeau, R. (1997). Mortality in Quebec during the nineteenth century: From the state to the cities. *Population Studies*, *51*(1), 93-103.

Perini, T. A., Oliveira, G. L. D., Ornellas, J. D. S., & Oliveira, F. P. D. (2005). Technical error of measurement in anthropometry. *Revista Brasileira de Medicina do Esporte*, *11*, 81-85.

Perry, M. A., & Edwards, E. (2021). Differential diagnosis of metabolic disease in a commingled sample from 19th century Hisban, Jordan. *International Journal of Paleopathology*, *33*, 220-233.

Perry, M. A., & Gowland, R. L. (2022). Compounding vulnerabilities: Syndemics and the social determinants of disease in the past. *International Journal of Paleopathology*, *39*, 35-49.

Piperata, B. A., Hubbe, M., & Schmeer, K. K. (2014). Intra-population variation in anemia status and its relationship to economic status and self-perceived health in the Mexican family life survey: Implications for bioarchaeology. *American Journal of Physical Anthropology*, *155*(2), 210-220.

Reynolds, J. (1962). An evaluation of some roentgenographic signs in sickle cell anemia and its variants. *Southern Medical Journal*, *55*(11), 1123-8.

Reynolds, J. (1965). *The roentgenological features of sickle cell disease and related hemoglobinopathies.* Charles C Thomas Publisher.

Rivera, F., & Mirazón Lahr, M. (2017). New evidence suggesting a dissociated etiology for cribra orbitalia and porotic hyperostosis. *American Journal of Physical Anthropology*, *164*(1), 76-96.

Rowe, S., & Carr, A. C. (2020). Global vitamin C status and prevalence of deficiency: a cause for concern?. *Nutrients*, *12*(7), 2008.

Saers, J. P., DeMars, L. J., Stephens, N. B., Jashashvili, T., Carlson, K. J., Gordon, A. D., Ryan, T. M., & Stock, J. T. (2021). Automated resolution independent method for comparing in vivo and dry trabecular bone. *American Journal of Physical Anthropology*, *174*(4), 822-831.

Saint-Martin, P., Dedouit, F., Rérolle, C., Guilbeau-Frugier, C., Dabernat, H., Rougé, D., Telmon, D., Crubézy, E. (2015). Diagnostic value of high-resolution peripheral quantitative computed tomography (HR-pQCT) in the qualitative assessment of cribra orbitalia–A preliminary study. *Homo*, *66*(1), 38-43.

Santos, A.L., Gomes, R., & Monge, A. (2023, August 9-11). *Lesiones Esqueléticas porosas: Tiempos de parar, sopesar y reiniciar* [conference presentation]. 9th Annual PAMinSA Meeting, Bolivia.

Scaffidi, B. K. (2020). Spatial paleopathology: A geographic approach to the etiology of cribrotic lesions in the prehistoric Andes. *International Journal of Paleopathology*, *29*, 102-116.

Schaefer, M., Black, S. M., Schaefer, M. C., & Scheuer, L. (2009). *Juvenile osteology*. Academic Press.

Sebes, J. I., & Diggs, L. W. (1979). Radiographic changes of the skull in sickle cell anemia. *American Journal of Roentgenology*, *132*(3), 373-377.

Shahidi, N. T., & Diamond, L. K. (1960). Skull changes in infants with chronic iron-deficiency anemia. *New England Journal of Medicine*, *262*(3), 137-139.

Shiozawa, Y., Jung, Y., Ziegler, A. M., Pedersen, E. A., Wang, J., Wang, Z., Song, J., Wang, J., Lee, C. H., Sud, S., Pienta, K. J., Krebsbach, P. H., & Taichman, R. S. (2010). Erythropoietin couples hematopoiesis with bone formation. *PloS one*, *5*(5), e10853.

Shopfner, C. E. (1966). Periosteal bone growth in normal infants: A preliminary report. *American Journal of Roentgenology*, *97*(1), 154-163.

Sifakis, S., & Pharmakides, G. (2000). Anemia in pregnancy. *Annals of the New York Academy of Sciences*, *900*(1), 125-136.

Singer, M. (1994). AIDS and the health crisis of the US urban poor; The perspective of critical medical anthropology. *Social Science and Medicine*, *39*(7), 931-948.

Singer, M., Bulled, N., Ostrach, B., & Mendenhall, E. (2017). Syndemics and the biosocial conception of health. *The Lancet*, *389*(10072), 941-950.

Stuart-Macadam, P. (1985). Porotic hyperostosis: Representative of a childhood condition. *American Journal of Physical Anthropology*, *66*(4), 391-398.

Stuart-Macadam, P. (1987). A radiographic study of porotic hyperostosis. *American Journal of Physical Anthropology*, *74*(4), 511-520.

Stuart-Macadam, P. (1989). Porotic hyperostosis: Relationship between orbital and vault lesions. *American Journal of Physical Anthropology*, *80*(2), 187-193.

Sullivan, A. (2005). Prevalence and etiology of acquired anemia in Medieval York, England. *American Journal of Physical Anthropology*, *128*(2), 252-272.

Thevenon, F., Dutailly, B., Dutour, O., Coqueugnoit, H. (2023). *Cribra sunt e pluribus unum***:** 3D-µCT and thickness mapping confirms that more than one process can cause cribra orbitalia [conference presentation]. In Monge Calleja, A. M., Santos, A. L., & Gomes, R.A.M.P. (Coord.). (2023). *International Meeting on Porous Skeletal Lesions: Achievements and future directions. Program and Abstract Book*. University of Coimbra, Research Centre in Anthropology and Health (CIAS). http://hdl.handle.net/10316/108791.

Thornton, P., & Olson, S. (2011). Mortality in late nineteenth-century Montreal: Geographic pathways of contagion. *Population Studies*, *65*(2), 157-181.

Tsai, A. C. (2018). Syndemics: a theory in search of data or data in search of a theory? *Social Science & Medicine*, *206*, 117-122.

Van Dessel, J., Huang, Y., Depypere, M., Rubira-Bullen, I., Maes, F., & Jacobs, R. (2013). A comparative evaluation of cone beam CT and micro-CT on trabecular bone structures in the human mandible. *Dentomaxillofacial Radiology*, *42*(8), 20130145.

Van Spelde, A. M., Schroeder, H., Kjellström, A., & Lidén, K. (2021). Approaches to osteoporosis in paleopathology: How did methodology shape bone loss research? *International Journal of Paleopathology*, *33*, 245-257.

Von Endt, D. W., & Ortner, D. J. (1982). Amino acid analysis of bone from a possible case of prehistoric iron deficiency anemia from the American Southwest. *American Journal of Physical Anthropology*, *59*(4), 377-385.

Walker, P. L., Bathurst, R. R., Richman, R., Gjerdrum, T., & Andrushko, V. A. (2009). The causes of porotic hyperostosis and cribra orbitalia: A reappraisal of the iron-deficiency-anemia hypothesis. *American Journal of Physical Anthropology*, *139*(2), 109-125.

Wapler, U., Crubézy, E., & Schultz, M. (2004). Is cribra orbitalia synonymous with anemia? Analysis and interpretation of cranial pathology in Sudan. *American Journal of Physical Anthropology*, *123*(4), 333-339.

Williams, H. U. 1929 Human paleopathology, with some observations on symmetrical osteo-porosis of the skull. *Archives of Pathology, 7*; 839-902.

World Health Organization (WHO). (2023). *Accelerating anaemia reduction: A comprehensive framework for action.* World Health Organization.

World Health Organization. (1999). *Scurvy and its prevention and control in major emergencies* (No. WHO/NHD/99.11). World Health Organization.

World Health Organization. (2011). *Haemoglobin concentrations for the diagnosis of anaemia and assessment of severity*. World Health Organization.

Yaussy, S. L., DeWitte, S. N., & Redfern, R. C. (2016). Frailty and famine: Patterns of mortality and physiological stress among victims of famine in medieval London. *American Journal of Physical Anthropology*, *160*(2), 272-283.

Yildirim, T., Agildere, A. M., Oguzkurt, L., Barutcu, O., Kizilkilic, O., Kocak, R., & Niron, E. A. (2005). MRI evaluation of cranial bone marrow signal intensity and thickness in chronic anemia. *European Journal of Radiology*, *53*(1), 125-130.

Zuckerman, M. K., Garofalo, E. M., Frohlich, B., & Ortner, D. J. (2014). Anemia or scurvy: A pilot study on differential diagnosis of porous and hyperostotic lesions using differential cranial vault thickness in subadult humans. *International Journal of Paleopathology*, *5*, 27-33.

APPENDIX 1

Visual Scoring Criteria for Manubrium Microarchitecture Changes

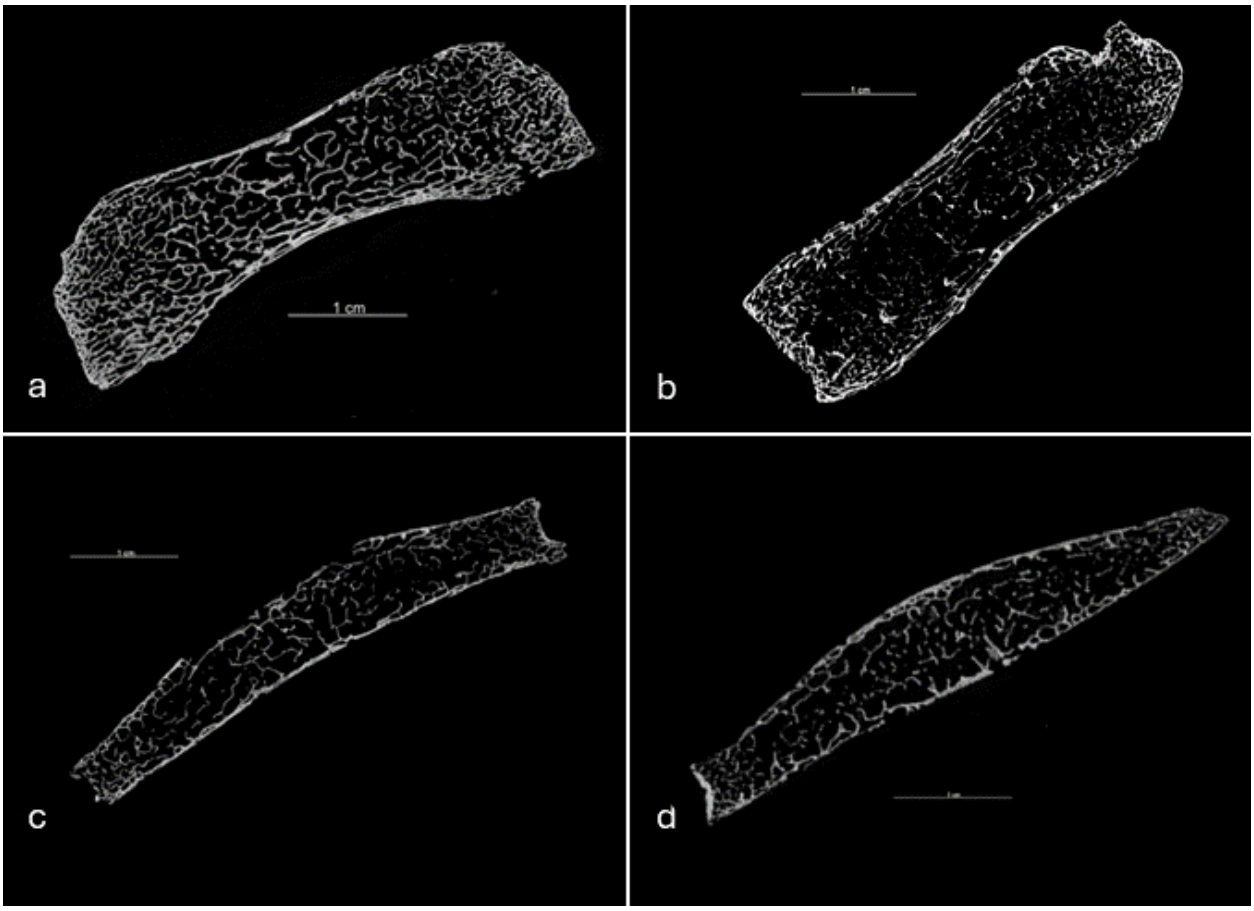

Figure A-1: Examples and description of cortical thinning for each scoring category, using a transverse view through the manubrium. Anterior is towards the top of the image, and posterior is towards the bottom. a) Cortical thinning score of 0. b) Cortical thinning score of 1, with small patches of thinned cortex. c) Cortical thinning score of 2. The cortex has worn away in places, and is as thin/thinner than trabeculae in section of the anterior cortex (top of image). However, the posterior cortex (bottom of image) is thicker. d) Cortical thinning score of 3. The cortex has worn away in places, and is as thin/thinner than trabeculae in places. This is consistent throughout the entire 3D reconstruction.

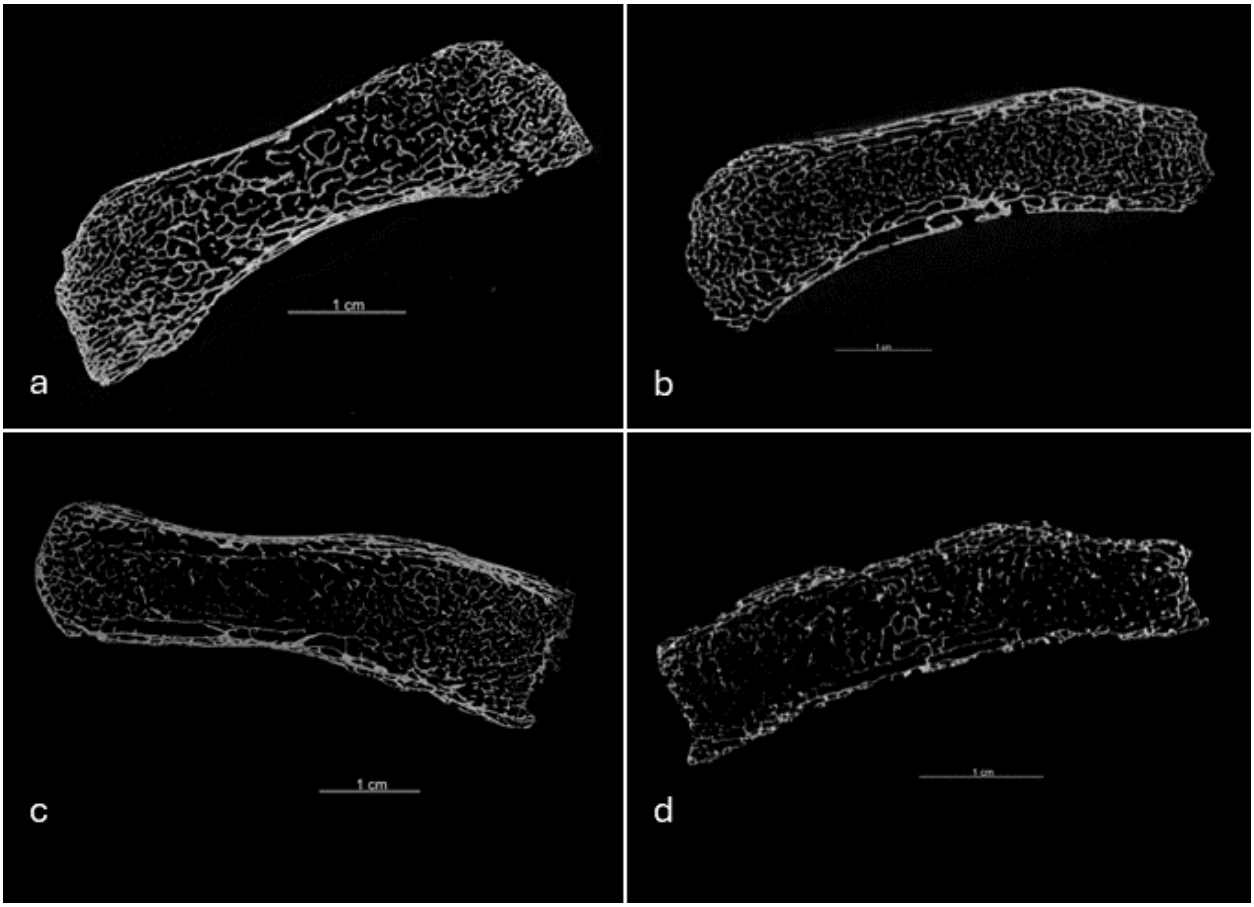

Figure A-2: Examples and description of increased trabecular separation for each scoring category, using a transverse view through the manubrium. Anterior is towards the top of the image, and posterior is towards the bottom. a) Increased trabecular separation score of 0. b) Increased trabecular separation score of 1. c) Increased trabecular separation score of 2. Increased spacing in present, but not throughout the entire bone. d) Increased trabecular separation score of 3, with many empty spaces throughout the entirety of the bone.

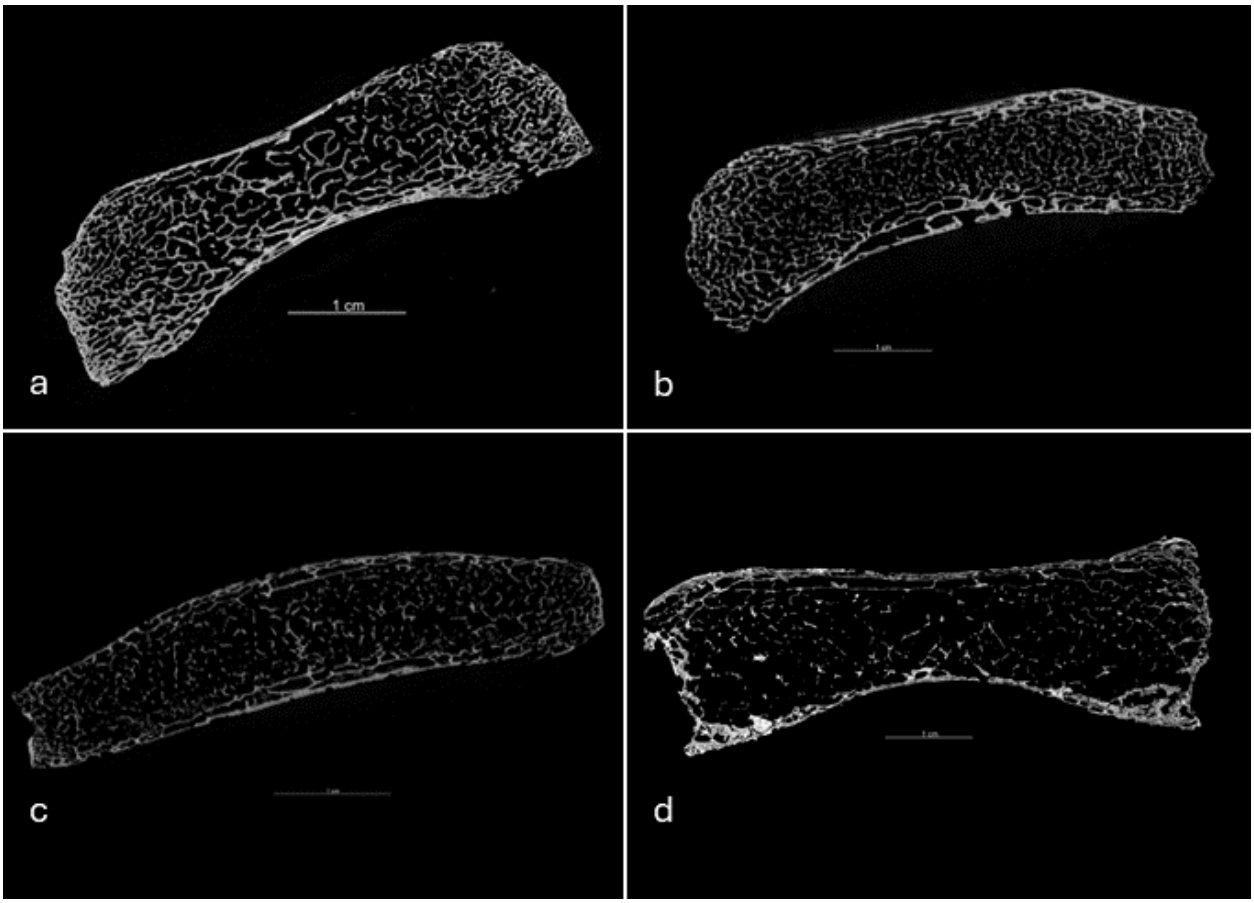

Figure A-3: Examples and description of trabecular thinning for each scoring category, using a transverse view through the manubrium. Anterior is towards the top of the image, and posterior is towards the bottom. a) Thinned trabeculae score of 0. b) Trabecular thinning score of 1. c) Trabecular thinning score of 2. Throughout the bone, trabeculae are consistently thinner than the cortex. d) Trabecular thinning score of 3. Trabeculae are markedly thinner compared to the cortex.